

23. H. K. D. H. Bhadeshia and A. R. Waugh: *Acta Metall.*, 1982, vol. 30, p. 775.
24. R. C. Reed and H. K. D. H. Bhadeshia: *Unpublished research* based on the method of J. S. Kirkaldy, B. A. Thomson and E. Baganis, "Hardenability Concepts with Applications to Steel", Ed. D. V. Doane and J. S. Kirkaldy, Pub. ASM, Warrendale, U. S. A., 1977, p. 82.

Chapter 7

ALLOTRIOMORPHIC FERRITE FORMATION IN A HETEROGENEOUS STEEL

7.1 Introduction

Allotriomorphic ferrite is the first phase to form by the reconstructive transformation of austenite in low alloy steels, when the austenite is cooled below the A_{e3} temperature^[1,2]. It nucleates at the austenite grain boundaries and in low alloy steels can eventually form continuous polycrystalline layers decorating the grain surfaces. Subsequent growth then essentially involves the one dimensional thickening of these layers into the remaining austenite. During the growth of the ferrite, the carbon partitions into the residual austenite ahead of austenite/ferrite interface so that the driving force for $\gamma \rightarrow \alpha$ transformation is decreased. Eventually, when the equilibrium volume fraction is achieved, the driving force is reduced to zero and interface motion ceases. The fundamental aspects of allotriomorphic ferrite have recently been reviewed^[3].

Variations in alloy content lead to differences in the driving force for transformation, which may have a strong effect on nucleation and the subsequent growth of allotriomorphic ferrite. This has important consequences in the prediction of microstructure. The work presented here is an investigation of the paraequilibrium formation of ferrite in a heterogeneous alloy of average composition Fe-0.2C-1.37Mn-0.35Si wt. %.

7.2 Theoretical Analysis

The lever rule suggests that the maximum volume fraction of ferrite that can form at any given temperature should vary linearly with the average carbon content of the steel concerned. However, it has been reported^[4] that this relation does not hold for chemically heterogeneous steels. Bhadeshia^[5] presented a model for ferrite formation in heterogeneous dual-phase steels which explained these data, and suggested that the effect of segregation should vary with undercooling. This model was discussed in terms of a ternary alloy, *e.g.*, Fe-Mn-C, of average Mn concentration \overline{Mn} , but with local variations ranging between the limits Mn_{min} and Mn_{max} . In his simplified model, the transformation was considered to take place by the motion of a planar γ/α interface

is normal to the isoconcentration planes, as illustrated in Fig. 7.1. The position of this interface, with respect to Z, at any instant thus defines the volume fraction V of ferrite, *i.e.*, $V \equiv Z$, reaching its maximum value of unity when the interface reaches the position where $Mn = Mn_{max}$.

At relatively high temperatures (above the A_{e3} of the homogeneous alloy), the interface is expected to stop at a point where $Mn < \overline{Mn}$ as shown in Fig. 7.2a. There will then be some transformation in the heterogeneous sample but none in the homogeneous alloy. This situation will continue until the interface reaches a stage where $Mn = \overline{Mn}$ (Fig. 7.2b) *i.e.*, the temperature falls to below the A_{e3} temperature of the homogeneous alloy. The model then suggests that transformation will occur to an identical extent, in both the heterogeneous and homogeneous samples. Beyond this point (Figs. 7.2c and 7.2d) it is expected that there should be more transformation in the homogeneous sample relative to that in the segregated sample.

7.2.1 Computer Simulation of the Published Model^[5]

As will be seen later, circumstances may arise where the transformation front does not necessarily advance in a direction normal to the isoconcentration surfaces. The problem is here investigated by developing a computer model, whose performance is first checked against Bhadeshia's analytical approach.

The computer program was designed to simulate the development of ferrite formation in chemically heterogeneous steels. In this model, consistent with the previous work^[5], the substitutional solute was assumed to vary linearly with distance as illustrated in Fig. 7.3 although the program is able to adopt any arbitrary composition profiles. The heterogeneous steel was represented as a composite of N slices of equal thickness (Fig. 7.4). Each slice, identified by a subscript i , was assigned a different chemical composition within the range of experimental measurements of the minimum and maximum alloy content (Fig. 7.5). Microanalysis experiments were carried out using energy dispersive X-ray analysis (interaction volume approximately $4.5 \mu m^3$) on a scanning electron microscope. The composition within each slice was set to be uniform. The mean composition of all the slices was set to be identical to the mean composition of the as-received steel.

The calculation begins with the complete transformation of the first slice in the solute-depleted region (*i.e.*, $i=1$), given that its A_{e3} temperature ($T_{A_{e3}}^i$) is higher than

the isothermal transformation temperature T and at the same time $x_\gamma = \bar{x}$ is also less than its $x_{A_{e3}}$, which is the maximum carbon that can be tolerated by the austenite transforming under paraequilibrium conditions. x_γ and \bar{x} are the carbon concentrations of the residual austenite and of the average carbon content of the alloy respectively. This transformation changes the carbon concentration of the residual austenite x_γ according to the following simple mass balance equation.

$$x_\gamma = \bar{x} + \frac{\frac{i}{N}(\bar{x} - x_\alpha)}{(1 - \frac{i}{N})} \quad (7.1)$$

Where, $\frac{i}{N} = V$ is the total volume fraction of ferrite when i number of slices are able to transform. x_α is the amount of carbon which is left in the ferrite assumed to be 0.03 wt. %.

The growth of allotriomorphic ferrite in dilute steels generally occurs without the bulk partitioning of substitutional alloying elements^[6], especially when the growth rates involved are large^[7]. Only carbon then partitions during growth. In such circumstances, ferrite growth can occur at a rate controlled by the diffusion of carbon in the austenite ahead of the interface. In these calculations it was, therefore, assumed that α growth occurs by a carbon diffusion paraequilibrium^[8-12] mechanism so that substitutional alloying elements do not partition at all between the phases; carbon then partitions to an extent which allows its chemical potential to be identical in all phases.

Hence, transformation is only allowed to continue in the next slice i if for that slice $x_\gamma < x_{A_{e3}}^i$. The calculation is stopped at a slice i when $x_\gamma = x_{A_{e3}}^i$ as illustrated in Fig. 7.4.

7.2.2 Results and Discussion

The results obtained from the simulation of the Bhadeshia model^[5] are shown in Fig. 7.6. At low undercoolings a greater volume fraction of ferrite was obtained in the heterogeneous alloy compared with the homogeneous alloy. Both volume fractions increased on decreasing temperature but their difference decreased until a crossover point after which the situation is reversed. It can be seen from Fig. 7.7 that the number of transforming slices decreased with an increase in the isothermal transformation temperature. During the course of transformation at any specified temperature, the amount of carbon that can be tolerated by the austenite decreases while at the same

time, the carbon content of the residual austenite goes on increasing. The point where these two curves meet gives the limiting volume fraction of ferrite. These results are in good agreement with the predictions forwarded by Bhadeshia^[5].

Although the model is a good representation of transformation in a heterogeneous sample during continuous cooling, it might not be applicable under isothermal transformation conditions. If the driving force for transformation is large, the initial nucleation and growth of ferrite may not be restricted to the solute-depleted region. The nucleation and growth of ferrite can start at more than one place in case of isothermal transformation at large undercoolings. In these circumstances it is no longer reasonable to expect the transformation front to proceed from the solute-depleted to the solute-enriched regions, but reaction may occur everywhere.

To study this, the computer model was arranged to permit the motion of the γ/α interface to occur parallel to the isoconcentration planes as shown in Fig. 7.8. The calculation was carried out in incremental stages (Fig. 7.9), with each stage identified by the subscript j . It should be noted that each incremental step of transformation now happens in a direction normal to the isoconcentration planes, so that several slices could be reacting at any instant. The computation begins with all the slices being fully austenitic. For the first step ($j = 1$) A_{e3} temperatures are calculated for all the slices. If for any slice, $T_{A_{e3}}^i < T$ then that slice remains untransformed throughout the experiment. For slices which are below their $T_{A_{e3}}^i$ temperatures, a small amount of ferrite is permitted to form, giving a volume fraction increment of ΔV . This increment of transformation changes the carbon concentration in the unreacted regions of the slices according to a simple mass balance equation

$$x_{\gamma}^{ij} = \bar{x} + \frac{V_{ij}(\bar{x} - x_{\alpha})}{(1 - V_{ij})} \quad (7.2)$$

where V_{ij} and x_{γ}^{ij} are, respectively, the total volume fraction of ferrite, and the total carbon concentration of the residual austenite in slice i at stage j of the calculation.

Hence, for $j > 1$, an increment of transformation is only allowed in any given slice if for that slice $x_{\gamma}^{ij} < x_{A_{e3}}^i$. $x_{A_{e3}}$ is the carbon that can be tolerated by the austenite transforming under paraequilibrium conditions. The mean volume fraction of transformation in the alloy as a whole at stage j is given by:

$$\bar{V}_j = \sum_i V_{ij}/N. \quad (7.3)$$

The calculation is stopped when all slices cease to transform; $x_{\gamma}^{ij} = x_{A_{e3}}^i$ for all i .

We consider first the case where the slices transform independently of each other, *i.e.*, without any homogenisation of carbon between the slices. The results thus obtained are shown in Fig. 7.10 which illustrate that as long as the alloy is transformed below the A_{e3} temperature of the homogeneous alloy, there is no difference of volume fractions between the homogeneous and heterogeneous samples. This might be due to the fact that the composition variations detected here are not large enough to produce a remarkable difference in volume fractions of allotriomorphic ferrite in homogeneous and heterogeneous samples. Moreover, due to the small slope of the A_{e3} curve, the effect of chemical heterogeneity in shifting the A_{e3} temperature is less as compared to that on B_s while considering the slope of T_0 curve.

On the other hand, if transformation was induced at temperatures above the A_{e3} temperature of the homogeneous alloy, ferrite formation obviously does not occur in the homogeneous sample, but some slices are able to transform in the heterogeneous sample.

At higher undercoolings, the nucleation and growth of ferrite is restricted to the solute depleted regions of the heterogeneous alloy, with relatively rapid reaction in those regions compared with the homogeneous alloy. The reaction in the segregated alloy will always be faster than the homogenised alloy. Limited transformation in the solute-enriched regions appears to be compensated by the ease of transformation in the solute-depleted regions.

At still higher undercoolings, nucleation and growth becomes possible everywhere in both the homogeneous and heterogeneous samples, *i.e.*, at these temperatures all the slices are able to transform to ferrite to a greater or lesser extent. Growth is then expected to be limited by the carbon enrichment of the residual austenite. For the case considered here, where it is assumed that excess carbon cannot redistribute between slices, the untransformed regions of the heterogeneous sample which are rich in substitutional alloy content, are unable to act as sinks for the excess carbon, so as to allow further transformation in the substitutional solute-depleted regions. When compared with bainite, the allotriomorphic ferrite carbon diffusion field in the austenite will be relatively large partly due to the higher transformation temperatures involved and partly because of the large size and less convoluted morphology of the growing

phase. The significance of this effect can be examined theoretically using the computer model with the additional condition that after every increment ΔV of transformation, the carbon is allowed to redistribute and homogenise between the slices. This should permit the solute-enriched regions to act as sinks for any excess carbon, thereby facilitating further transformation in the solute-depleted regions. The results (Fig. 7.10) show that if carbon is permitted to homogenise in the residual austenite after every increment of transformation, the volume fraction of transformation in the heterogeneous samples should always exceed that in the homogenised samples. The difference between the two cases decreases with an increase in undercooling.

7.3 Dilatometry

Dilatometric experiments were carried out to compare the experimental results with the predictions made by the models described above. The specimens were austenitised at 1000 °C for 10 minutes before helium gas quenching to a variety of isothermal transformation temperatures within the range where the reconstructive growth of ferrite alone is expected. The length change during the isothermal reaction was measured and the corresponding relative length change versus time data plotted as in Fig. 7.11. The optical micrographs in Fig. 7.12 give a comparison of the extent of transformation in the homogeneous and heterogeneous samples. The relative length change corresponding to a volume fraction of ferrite transformed V_b is given by:

$$\frac{\Delta l}{l} = \frac{2V_b a_\alpha^3 + (1 - V_b)a_\gamma^3 - \bar{a}_\gamma^3}{3\bar{a}_\gamma^3} \quad (7.4)$$

where a_α is the lattice parameter of ferrite at the transformation temperature, given by:

$$a_\alpha = a_\alpha^o [1 + e_\alpha(T - 25)] \quad (7.5)$$

and \bar{a}_γ , which is the lattice parameter of austenite of the alloy composition at the transformation temperature, is given by:

$$\bar{a}_\gamma = (a_o^\gamma + \sum c_i x_i)[1 + e_\gamma(T - 25)]. \quad (7.6)$$

In these equations, e_α and e_γ represent the linear thermal expansivities of ferrite and austenite respectively, a_o is the lattice parameter of austenite in pure iron at 25 °C, x_i

is the concentration of alloying element i and $c_i x_i$ represents the change in a_o due to the addition of the alloying elements to pure iron. T is the temperature in °C.

The ferrite linear expansion coefficient was determined by first tempering a specimen at 600 °C for 10 minutes to decompose any retained austenite and then recording the length change during very slow cooling. The measurements do not therefore account for the presence of any carbide, whose volume fraction is in any case expected to be negligibly small for the present purposes.

The graph of relative length versus temperature is plotted in Fig. 7.13, from which the linear expansion coefficient of ferrite was found to be $e_\alpha = 9.847 \times 10^{-6} \text{ K}^{-1}$. The expansion coefficient of austenite was measured while specimen was in the single-phase field, as shown in Fig. 7.14 ($e_\gamma = 2.122 \times 10^{-5} \text{ K}^{-1}$). The ferrite lattice parameter (a_α^o) at ambient temperature was measured using a Debye-Scherrer technique. The test specimen was annealed at 600 °C for half an hour, and then machined to the form of 0.5mm × 0.5mm × 15mm wire. It was then immersed in an aqueous solution made up of 5% HF and 45% H₂O₂ (by volume) for two minutes to remove the deformation layer before testing. The specimens were irradiated with Mo K_α radiations using a standard Debye-Scherrer camera. A value of lattice parameter was calculated for each reflection from the resulting photograph and plotted against the Nelson-Riley function^[13] of Bragg angle θ . Linear regression technique was used to extrapolate a best-fit line back to $\theta = 90^\circ$, to find the intercept and the standard error in the intercept (Fig. 7.15). The resulting value of lattice parameter was found to be as $2.8675 \pm 0.0015 \text{ \AA}$ which is in good agreement with the value calculated to be 2.8667 \AA using data from Leslie^[14]. With these measured values and making the appropriate substitutions in equation 7.4, the volume fractions of ferrite transformed could be deduced using a computer program.

7.3.1 Results and Discussion

The carbon content of residual austenite when isothermal transformation ceases is very useful in understanding the transformation mechanism. The maximum relative length change was converted into the volume fraction of ferrite transformed, from which the carbon content of the residual austenite can be calculated using equation 7.1. It should be noted that no carbide precipitation was observed even at the lowest isothermal transformation temperature considered here which is 700 °C. That is evident from the transmission electron micrograph shown in Fig. 7.16 of the sample isothermally

transformed at 700 °C. Isothermal transformation experiments were carried out over the temperature range 700-760 °C. The data thus obtained are plotted on a phase diagram as shown in Fig. 7.17. It is clear that for the short time heat treatments studied here, the reaction becomes imperceptibly slow before the austenite reaches its equilibrium composition. Hence, the assumption involved in the slice model, that the growth of α occurs under paraequilibrium conditions, seems reasonable.

The experimental data provided in Fig. 7.17 are not sufficiently extensive to confirm how the volume fraction of ferrite in a heterogeneous alloy should differ from a homogeneous alloy but the comparison available at two temperatures (*i.e.*, 700 and 740 °C) shows that more transformation is obtained in heterogeneous sample. This is supported by the results obtained from the slice model, provided the carbon is allowed to homogenise among the slices. The data obtained at 730 °C are not consistent with the rest of the experiments as it shows lesser transformation than that observed at 740 °C. No obvious reasons could be found for this discrepancy, which is tentatively assigned to experimental error.

7.4 Conclusions

Allotriomorphic ferrite formation in a heterogeneous alloy has been modelled for situations equivalent to “continuous cooling” and isothermal transformation. In the first case, the γ/α transformation front was considered to move normal to the isoconcentration planes, *i.e.*, from solute-depleted region to solute-enriched region. The results support the published predictions^[5] that below the volume fraction of 0.5, there will be more transformation in a heterogeneous alloy than the homogeneous alloy while above the volume fraction of 0.5 the situation is reversed.

For isothermal transformation, the motion of γ/α transformation front was considered to be parallel to the isoconcentration planes. At any undercooling below A_{e3} temperature of the homogeneous alloy, limited nucleation (in the areas whose alloy content is either equal or below the average alloy content) in the heterogeneous alloy can be compensated by the faster growth in the solute depleted regions. Moreover, due to higher transformation temperatures involved, carbon can distribute evenly throughout the residual austenite to facilitate still more transformation. It is found that the extent

of transformation is always larger for the heterogeneous samples when compared with the homogenised samples.

The model is based on the hypothesis that the growth of α occurs under paraequilibrium conditions. The experimental results presented here support this hypothesis, and provide a new way of deducing the paraequilibrium mode of transformation.

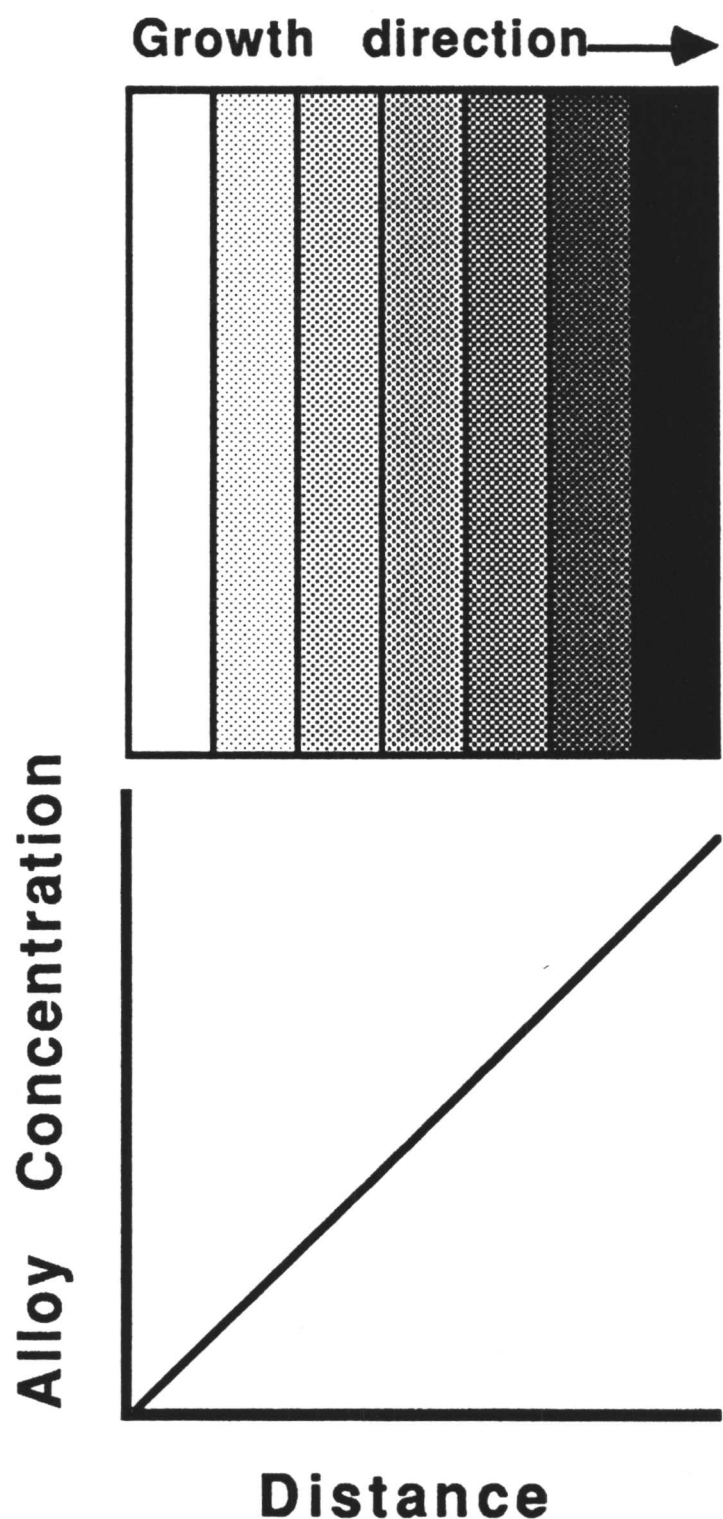


Fig. 7.1: In the model for allotriomorphic ferrite in heterogeneous steels^[5], the growth direction of the ferrite is considered to be normal to the isoconcentration planes.

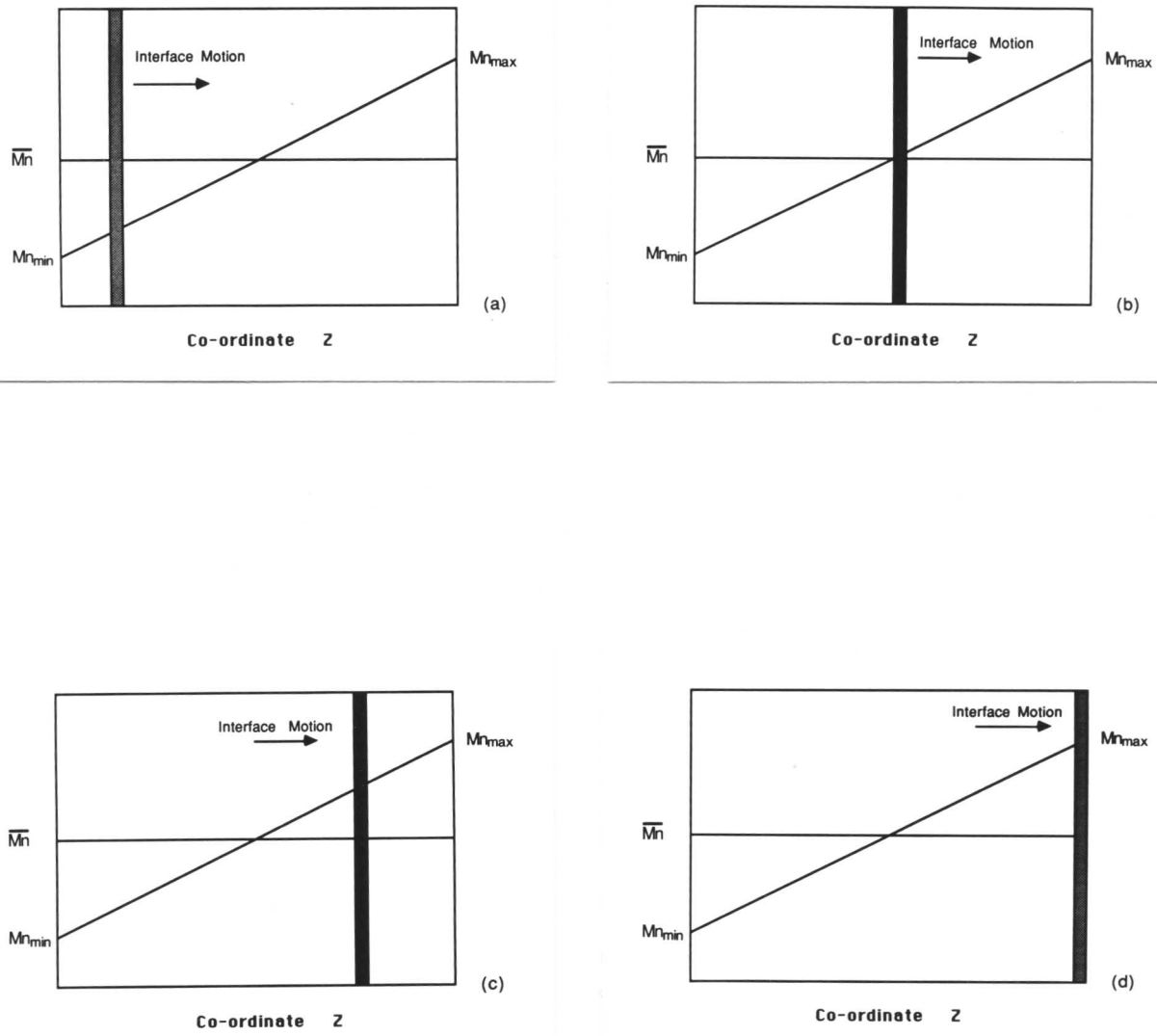


Fig. 7.2: Schematic representation of the position of the γ/α interface in a heterogeneous alloy. The coordinate 'Z' is defined to be normal to the planes of constant composition and is normalised with respect to the specimen length in the Z-direction. Four different positions of the interface are shown:

- when $Mn < \bar{Mn}$,
- when $Mn = \bar{Mn}$,
- when $Mn > \bar{Mn}$,
- when $Mn = Mn_{max}$.

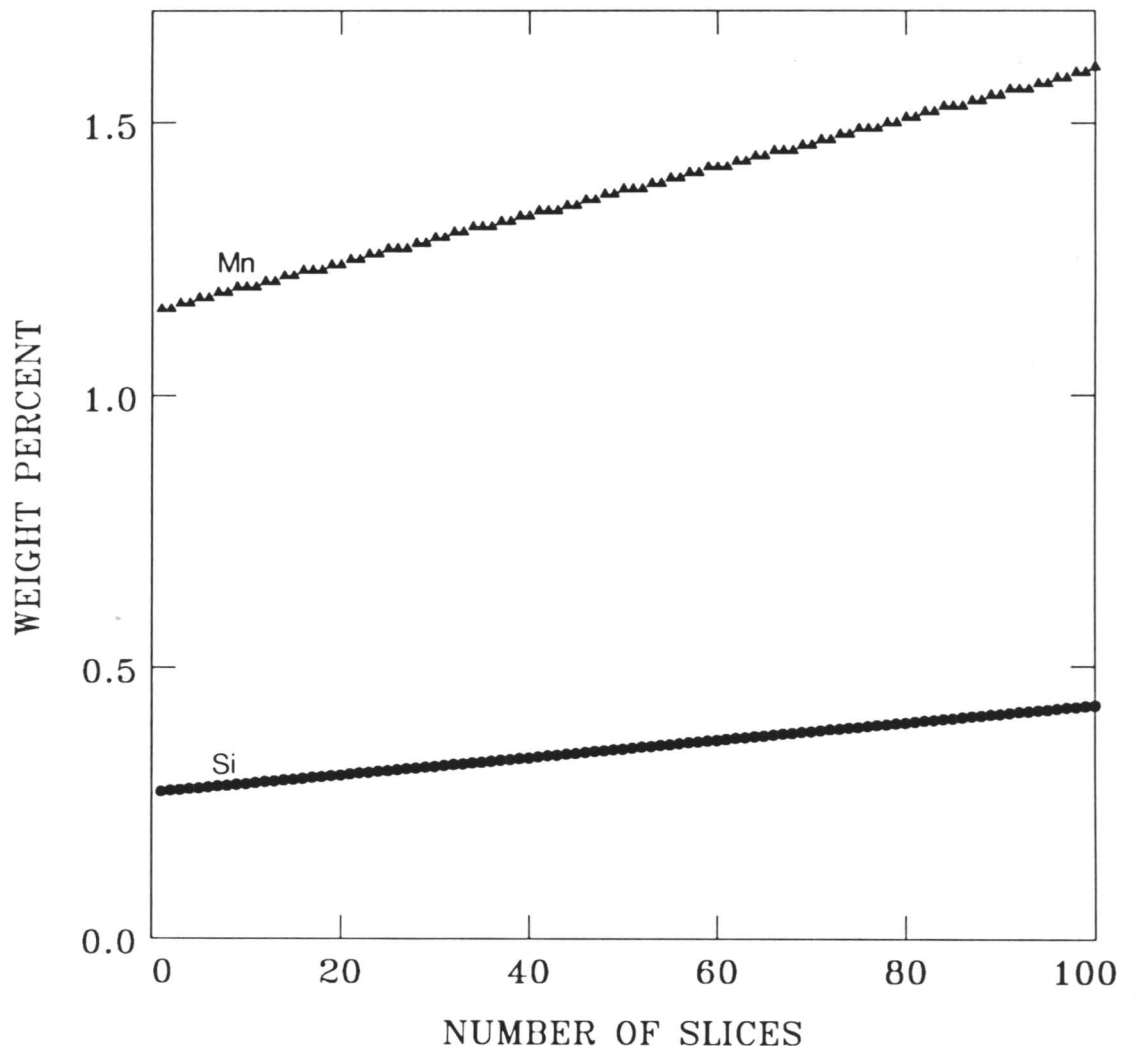


Fig. 7.3: Graph showing the linear variation of Mn and Si concentrations as a function of distance (slice number) as utilised in the slice model presented in the text.

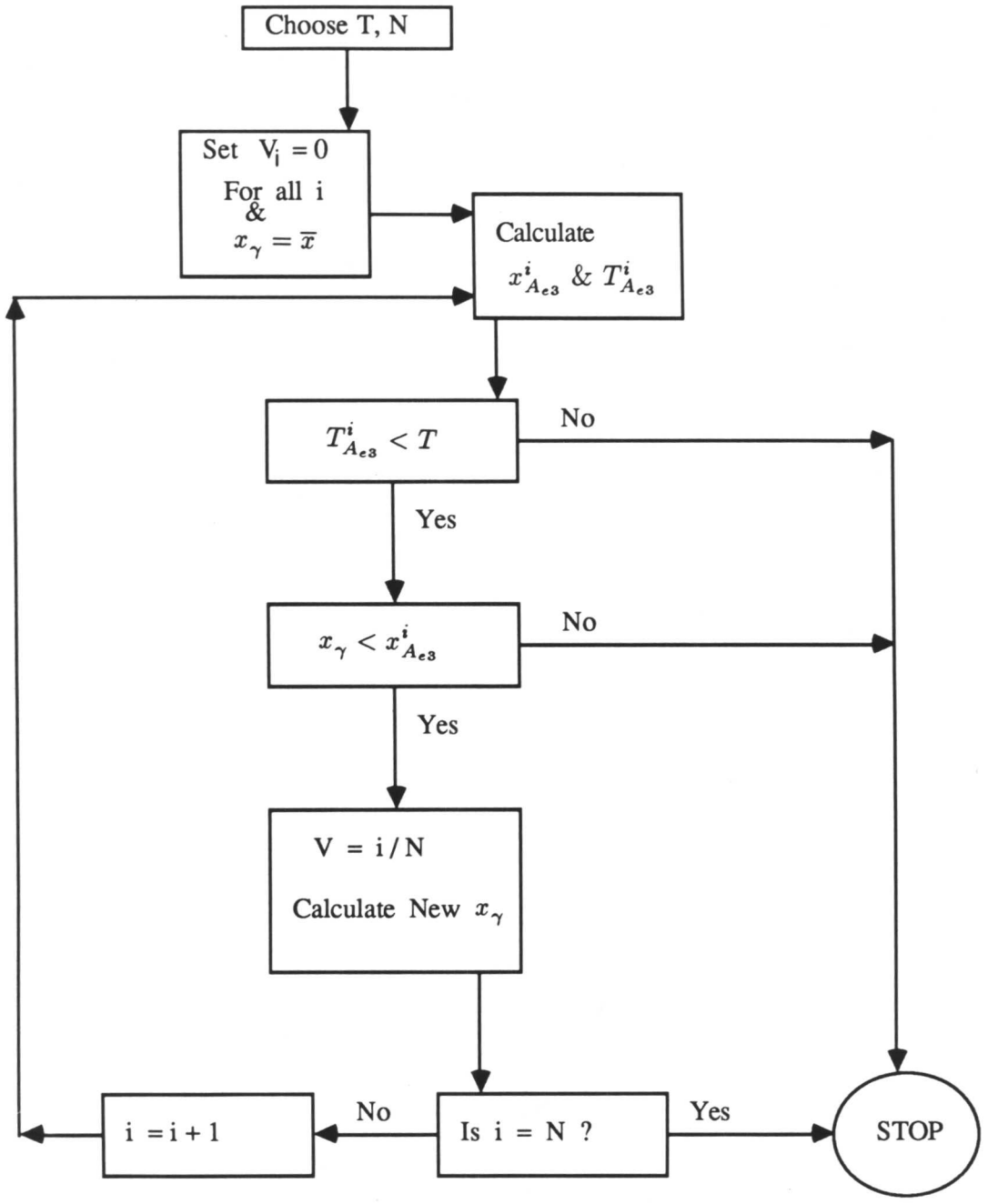


Fig. 7.4: Flow chart illustrating the calculation procedure used to simulate the development of transformation in a heterogeneous steel while the γ/α interface moves normal to the isoconcentration planes in accordance with the Bhadeshia model^[5].

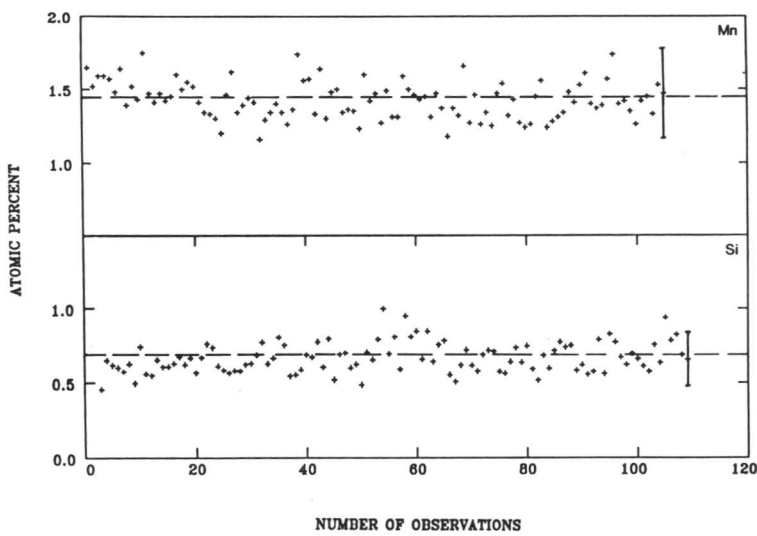


Fig. 7.5: Microanalysis data from heterogeneous sample of Fe-0.17C-0.35Si-1.38Mn wt. % steel which was austenitised at 1000 °C and then transformed isothermally at 700 °C for 60 minutes. The error bars indicate the typical 95% confidence statistical error and the average composition is in each case indicated by the dashed horizontal line.

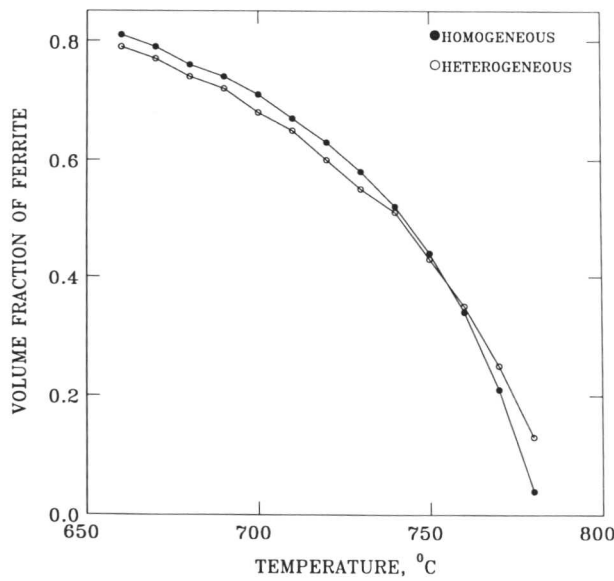


Fig. 7.6: Calculated ferrite volume fraction as a function of isothermal transformation temperature in a heterogeneous alloy as the growth direction of the γ/α interface was considered to be normal to the isoconcentration planes.

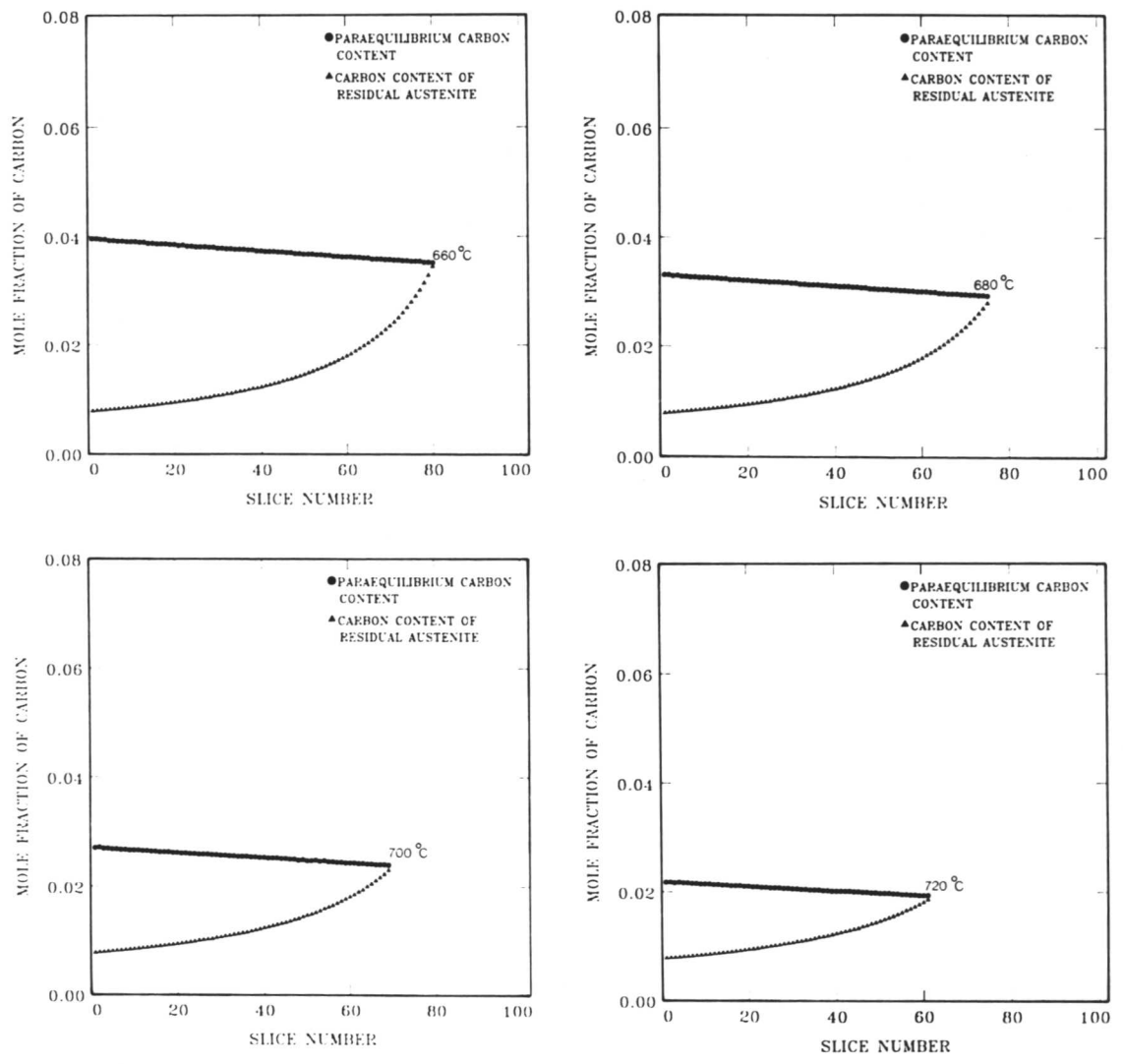


Fig. 7.7: Illustration of how the paraequilibrium carbon concentration and the actual carbon concentration of the residual austenite converge as the transformation front advances into solute-enriched regions.

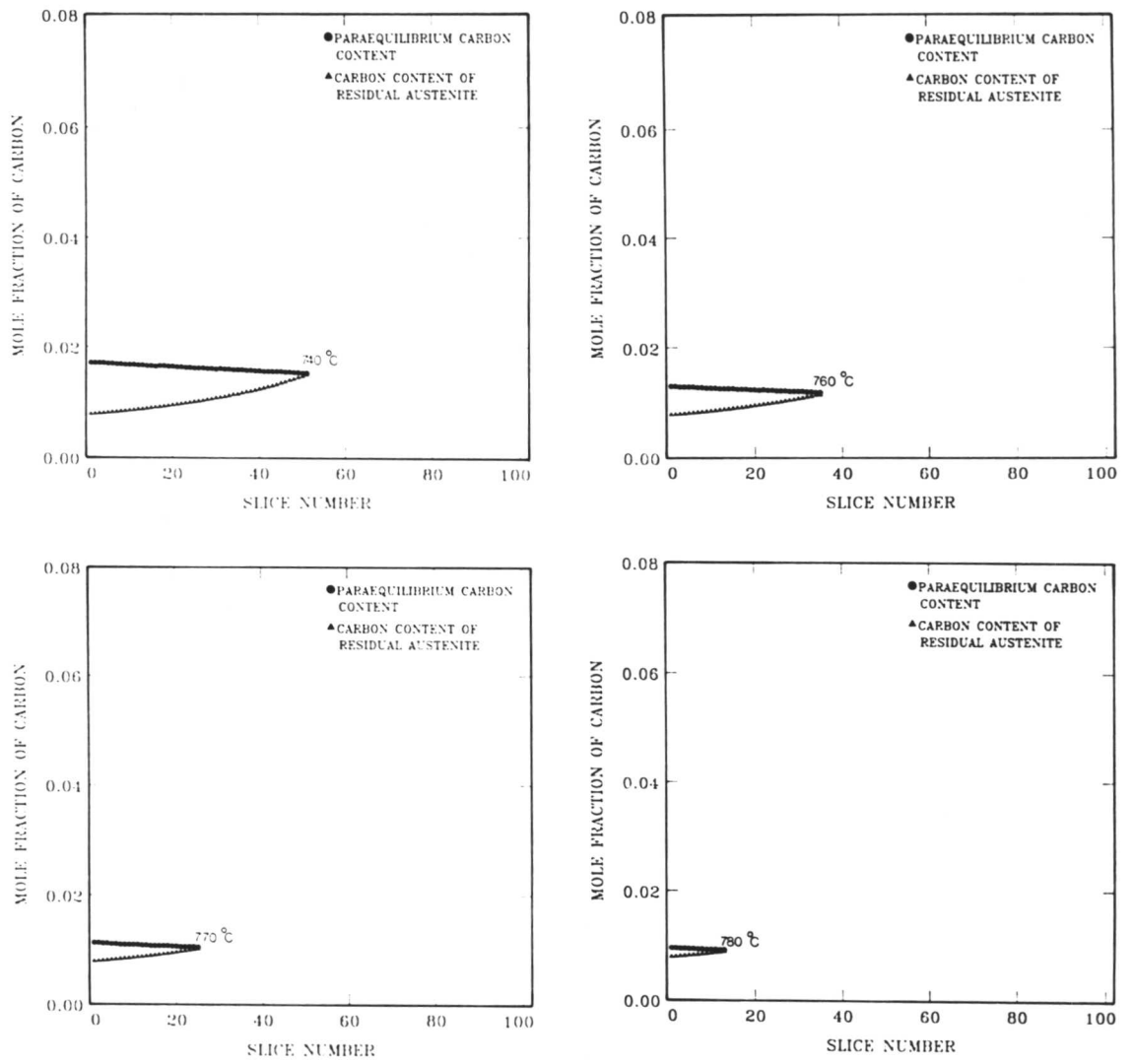


Fig. 7.7: (continued)

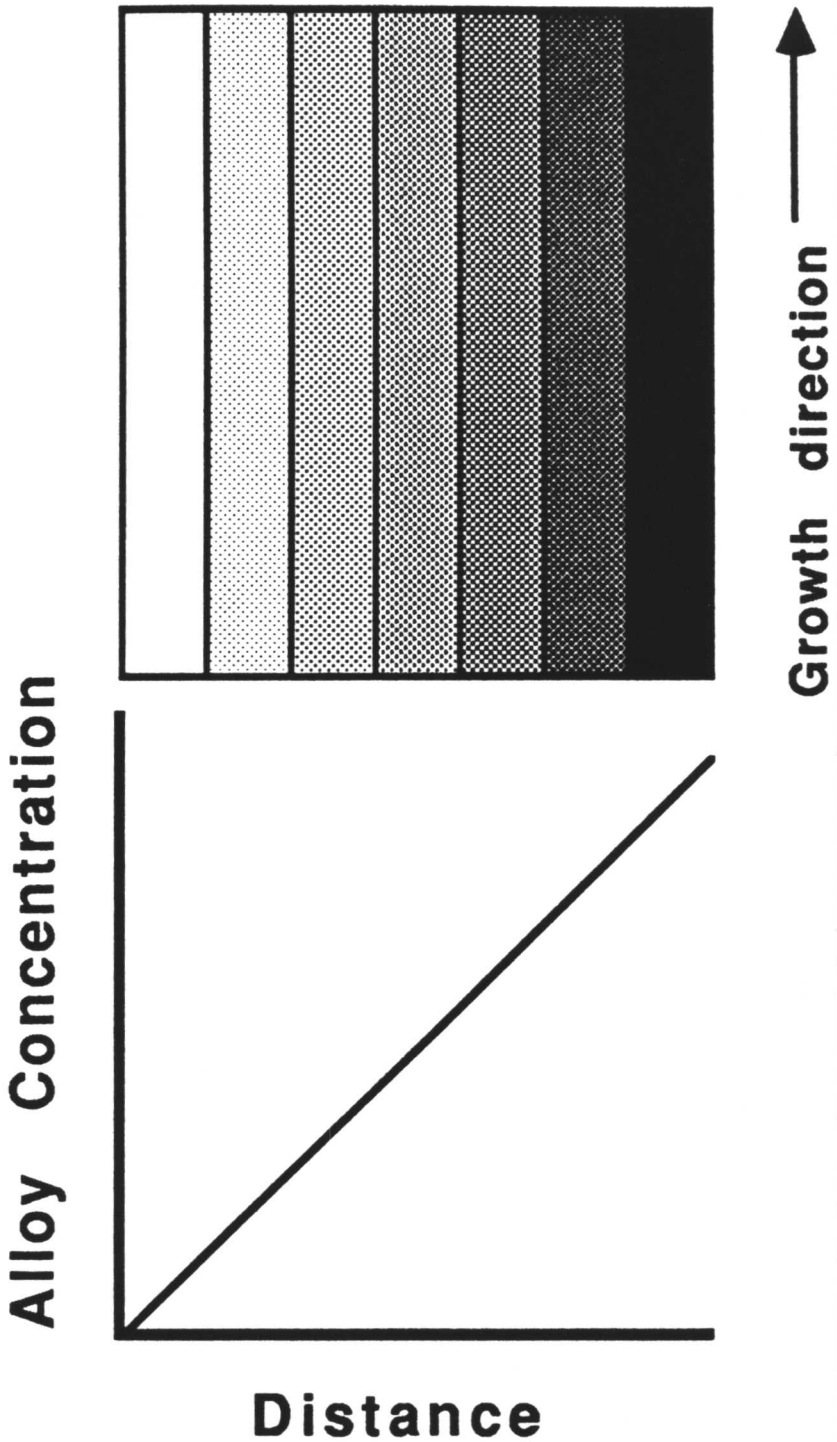


Fig. 7.8: In another model for allotriomorphic ferrite in heterogeneous steels, the growth direction of the ferrite can be considered to be parallel to the isoconcentration planes.

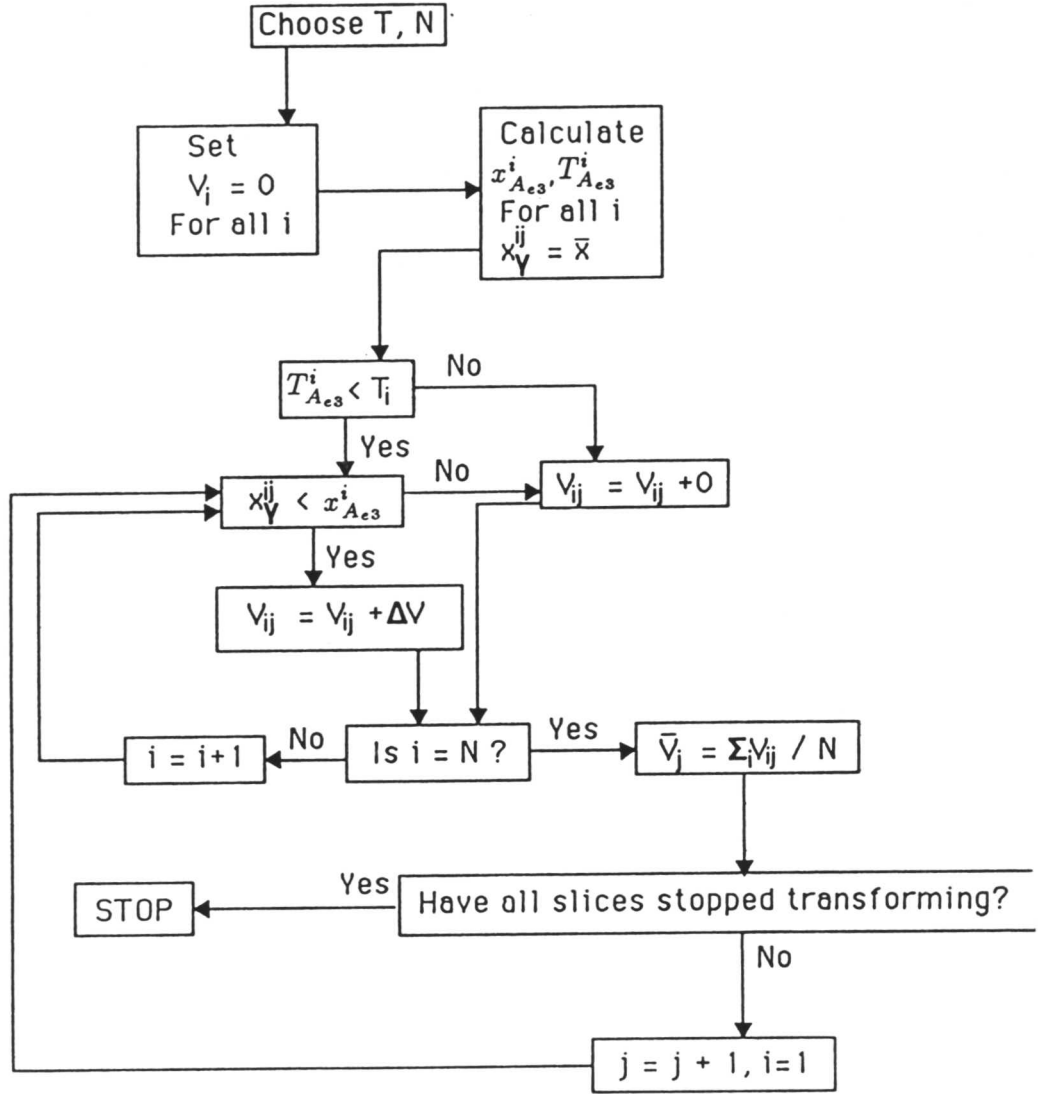


Fig. 7.9: Flow chart illustrating the calculation procedure used to simulate the development of transformation in a heterogeneous steel. T_i represents the isothermal transformation temperature and the subscript i identifies the slice number and composition; the total number of slices is N . The calculation is carried out in stages, with each stage identified by the subscript j . For each value of j (i.e., at each stage of the calculation), the volume fraction V_{ij} of ferrite in each slice is incremented by a small fraction ΔV if transformation is feasible in that slice. The total volume fraction of ferrite at stage j is thus given by $\sum_i V_{ij}/N$.

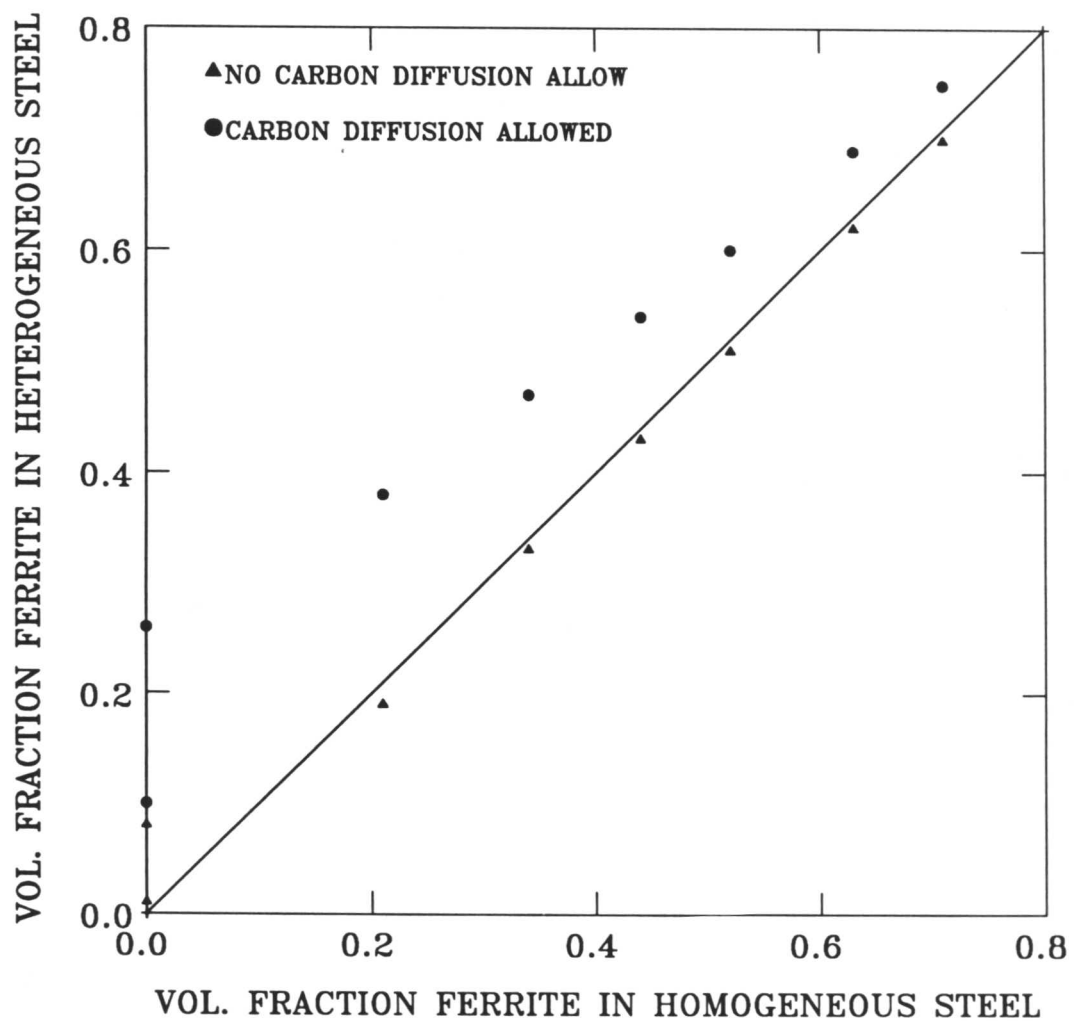


Fig. 7.10: Comparison of maximum volume fraction transformed in homogeneous and heterogeneous samples as calculated by the slice model in which γ/α interface was assumed to move in a direction parallel to the isoconcentration planes. The line has a slope of unity, and serves to show that except above the A_{e3} of the homogeneous sample (where the degree of transformation is larger in case of heterogeneous sample) there is no significant difference between the two, provided the slices are allowed to transform independent of each other. But if an opportunity is provided for carbon to distribute evenly throughout the residual austenite, the extent of transformation is always larger in the heterogeneous samples.

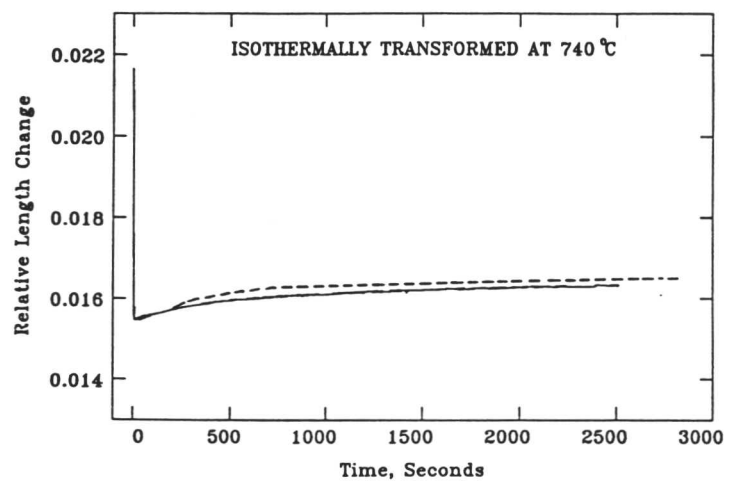
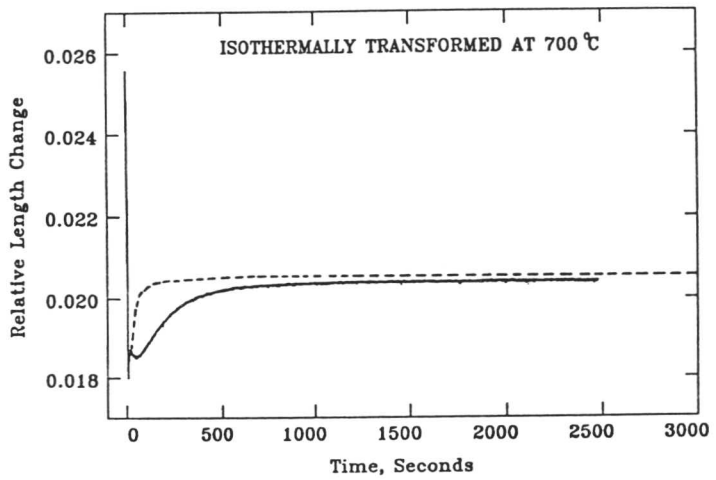


Fig. 7.11a: Dilatometric curves for Fe-0.17C-0.35Si-1.38Mn wt. % steel isothermally transformed at the temperatures indicated. The continuous curves are for the homogenised samples and the dashed curves for the heterogeneous samples.

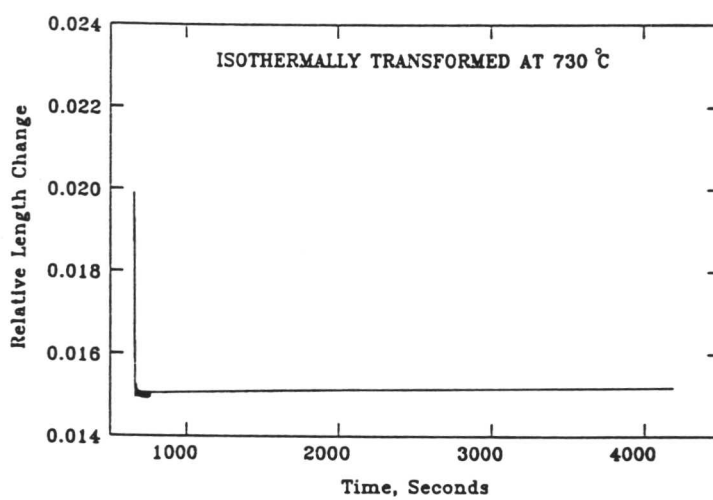
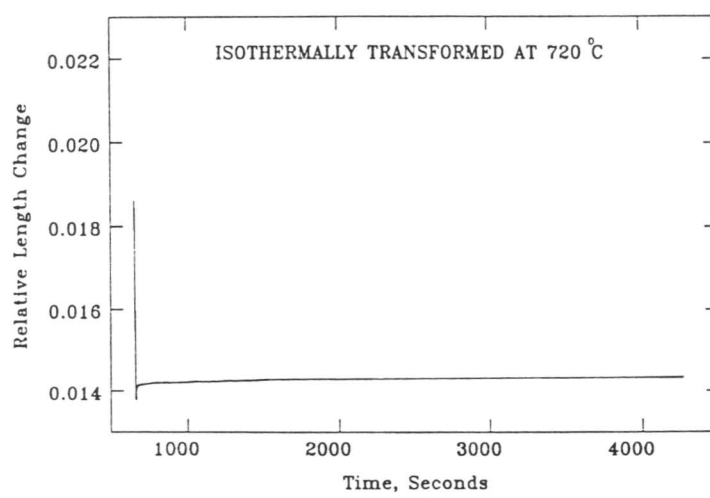


Fig. 7.11b: Dilatometric curves for the homogenised Fe-0.17C-0.35Si-1.38Mn wt. % steel isothermally transformed at the temperatures indicated.

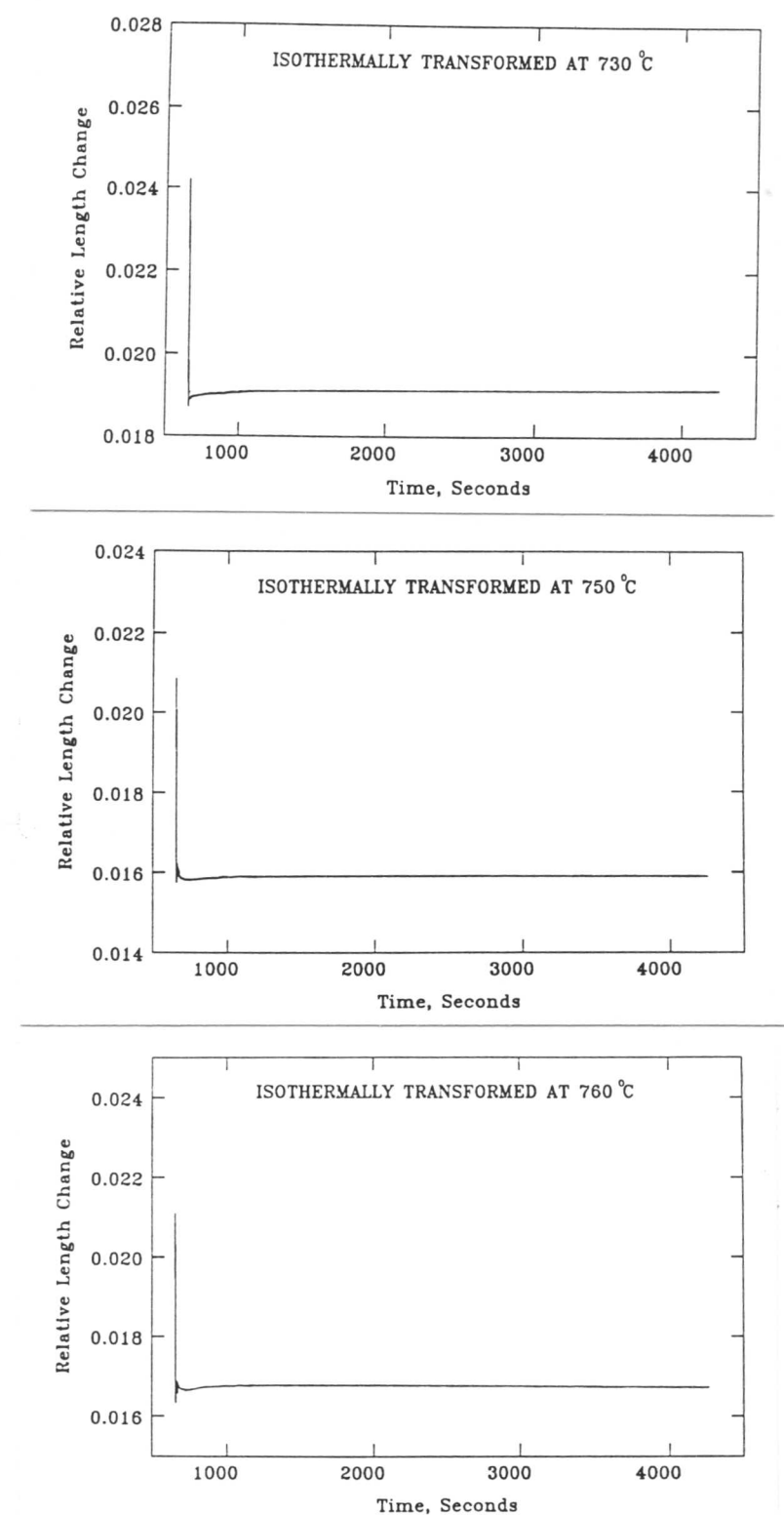


Fig. 7.11c: Dilatometric curves for the heterogeneous Fe-0.17C-0.35Si-1.38Mn wt. % steel isothermally transformed at the temperatures indicated.

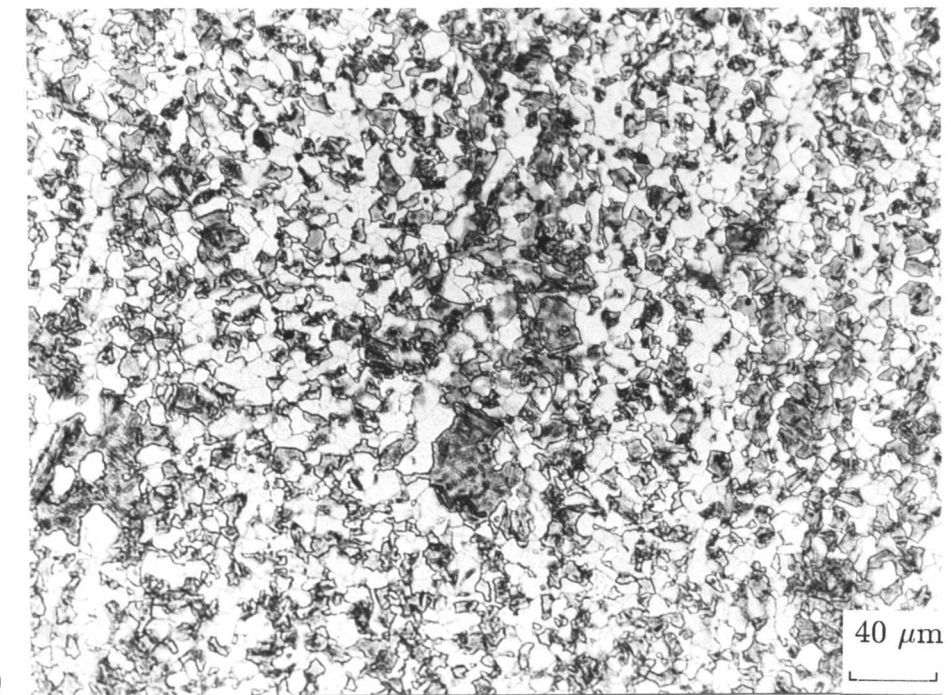
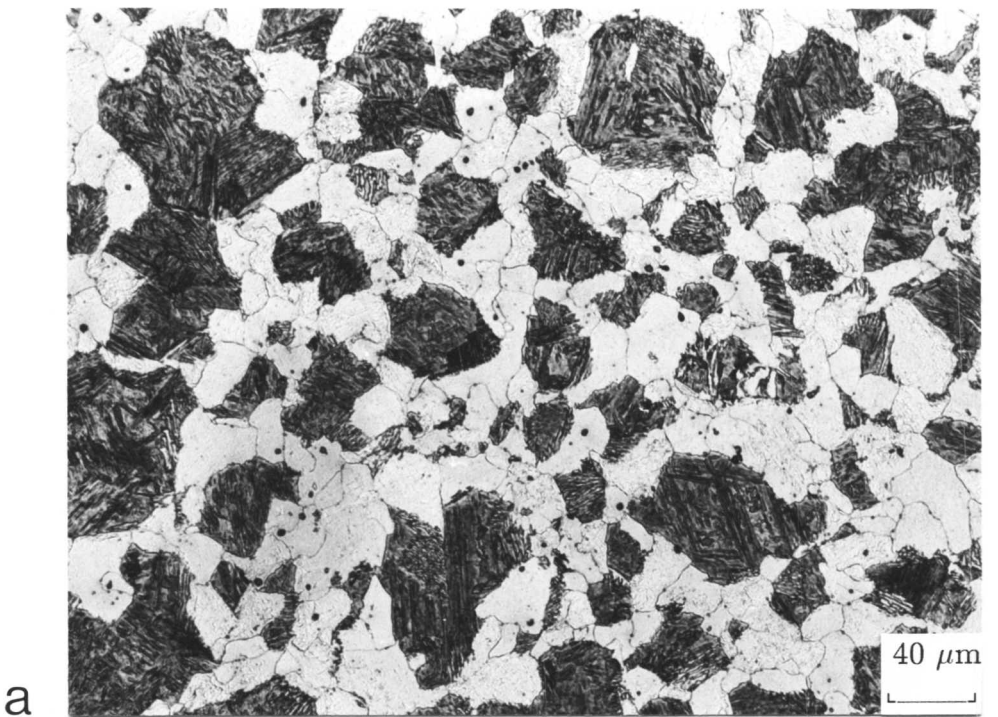


Fig. 7.12: Metallographic confirmation of the curves shown in Fig. 7.9a.

- (a) Optical micrograph of the homogeneous specimen isothermally transformed at 700 °C.
- (b) Optical micrograph of the heterogeneous specimen isothermally transformed at 700 °C.

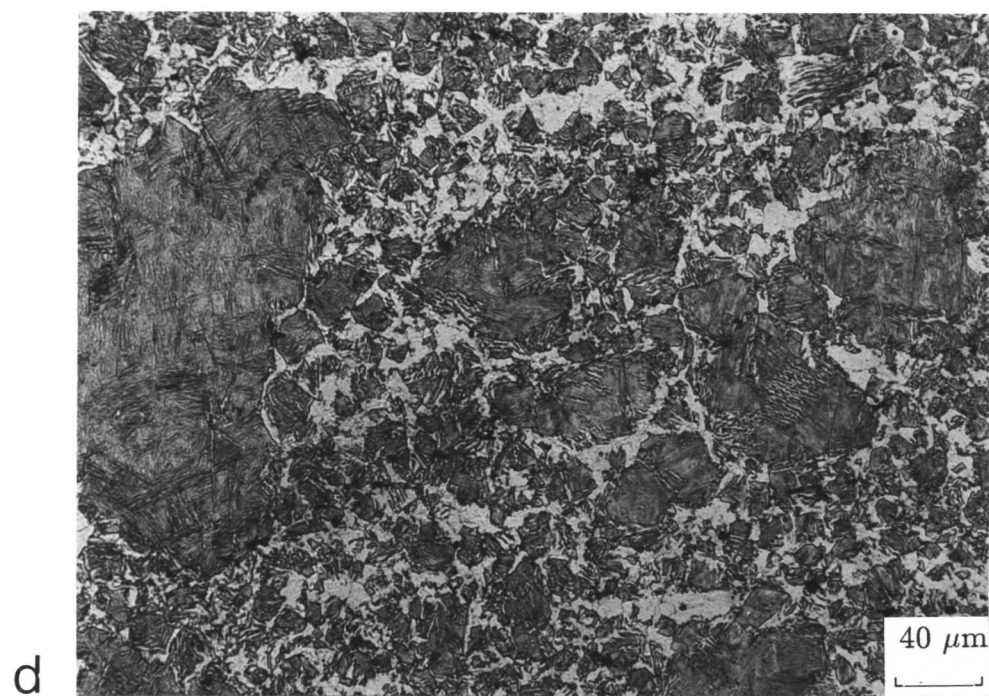
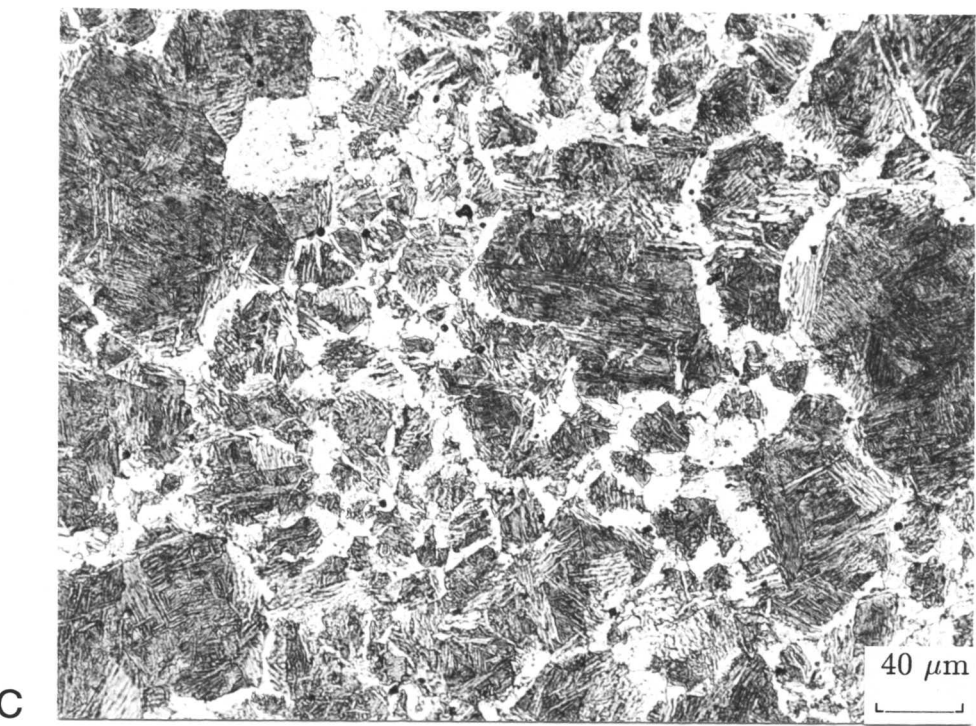


Fig. 7.12: (continued)

(c) Optical micrograph of the homogeneous specimen isothermally transformed at 740 °C.

(d) Optical micrograph of the heterogeneous specimen isothermally transformed at 740 °C.

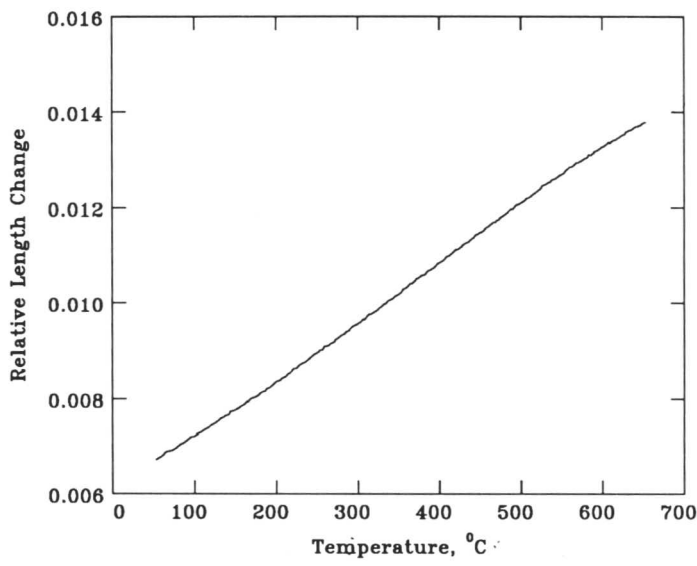


Fig. 7.13: Graph of relative length change versus temperature, from which the linear expansion coefficient of ferrite is obtained.

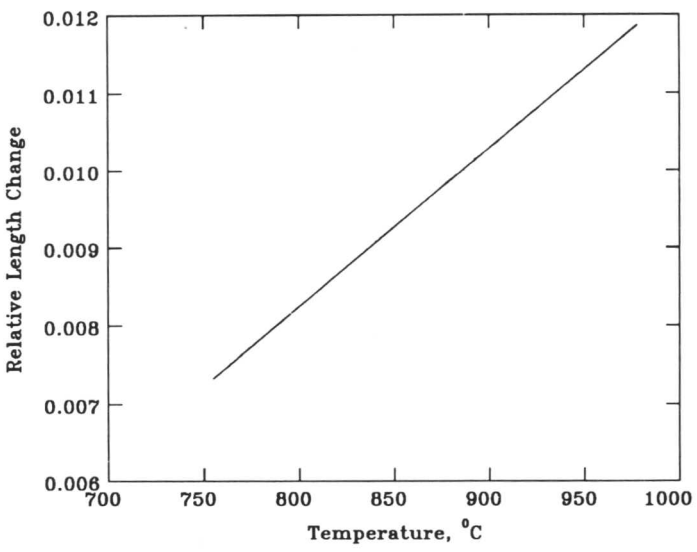


Fig. 7.14: Graph of relative length change versus temperature, from which the linear expansion coefficient of austenite is obtained.

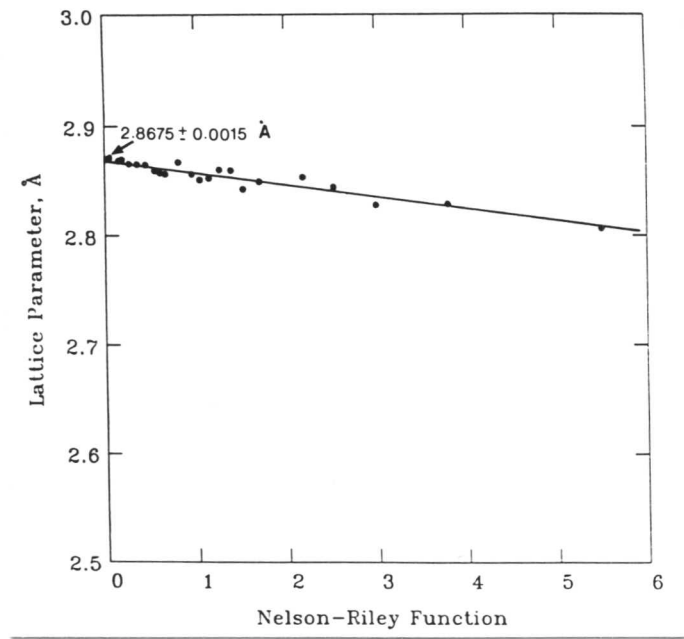


Fig. 7.15: Extrapolation of measured lattice parameter against Nelson-Riley function (i.e., $\frac{\cos^2\theta}{\sin\theta} + \frac{\cos^2\theta}{\theta}$). θ is the diffraction angle.



Fig. 7.16: Bright field transmission electron micrograph from a heterogeneous sample of Fe-0.17C-0.35Si-1.38Mn wt. % steel, transformed isothermally to allotriomorphic ferrite at 700 °C for 60 minutes before quenching to ambient temperature. Shows allotriomorphic ferrite and residual austenite.

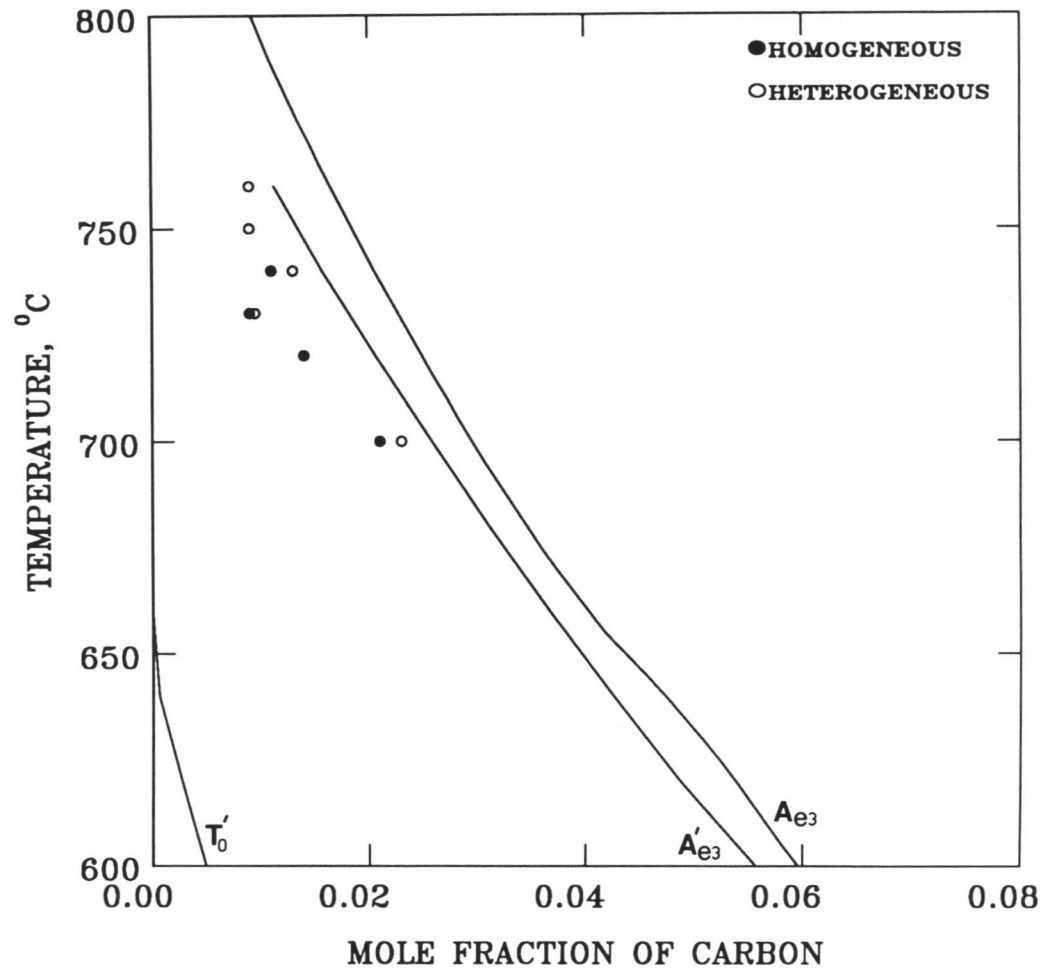


Fig. 7.17: Calculated T'_0 , A'_e3 and A_e3 phase boundaries for Fe-0.17C-0.35Si-1.38Mn wt. % steel. The experimental data are for samples transformed isothermally to allotriomorphic ferrite.

REFERENCES

1. E. Levine and D. C. Hill: *Metall. Trans.*, 1977, vol. 8A, p. 1453.
2. C. L. Choi and D. C. Hill: *Weld. J. Res. Supp.*, 1978, vol. 57-8, p. 23.
3. H. K. D. H. Bhadeshia: *Progress in Materials Science*, 1985, vol. 29, p. 321.
4. G. R. Speich and R. L. Miller: *Mechanical Properties of Dual Phase Steels*, eds. R. A. Kot and J. W. Morris, *Trans. Metall. Soc. AIME*, New Orleans, 1979, p. 145.
5. H. K. D. H. Bhadeshia: *Scripta Metall.*, 1983, vol. 17, p. 857.
6. H. I. Aaronson and H. Domain: *TMS-AIME*, 1966, vol. 236, p. 781.
7. D. E. Coates: *Metall. Trans.*, 1973, vol. 4, p. 2313.
8. H. K. D. H. Bhadeshia, L.-E. Svensson and B. Gretoft: *J. Mater. Sci. Letters*, 1985, vol. 4, p. 305.
9. H. K. D. H. Bhadeshia: *Progress in Materials Science*, 1985, vol. 29, p. 321.
10. A. Hultgren: *Jernkontorets Ann.*, 1951, vol. 135, p. 403.
11. M. Hillert: *Jernkontorets Ann.*, 1952, vol. 136, p. 25.
12. E. Runberg: *Jernkontorets Ann.*, 1952, vol. 136, p. 91.
13. B. D. Cullity: *Elements of X-ray Diffraction*, Addison-Wesley, Reading, N.Y., 1956.
14. W. C. Leslie: *The Physical Metallurgy of Steels*, p. 289, McGraw-Hill Int. Book Company, New York, 1982.

Chapter 8

COMPLETE CALCULATION OF MICROSTRUCTURAL EVOLUTION IN HETEROGENEOUS AUTOMOBILE STEELS

8.1 Introduction

In the previous chapters, various aspects of the transformation of austenite to allotriomorphic ferrite, bainite and martensite in a heterogeneous alloy were discussed. Moreover, some models were presented to help predict the volume fractions and other characteristics of these transformation products both for homogeneous and for chemically segregated steels. The purpose of the work presented in this chapter was to use to apply the models to some new steels which are being developed at Inland Steel (USA) for automobile crash reinforcement bars. The steels are at an early stage of development and could benefit from fundamental alloy design. Cars manufactured in the old days had door panels which were very thick (~20 cm), and consequently could be reinforced against sidewise impact using relatively low strength steel in the form of zig-zag concertina type rectangular rods incorporated within the doors. Modern cars however have thinner panels which are reinforced by high-strength steel bar (the present steels are candidate alloys) running across the panels, in a way which transmits any impact into the structural frame, thereby ensuring the passenger safety. The steels 'US83' and 'US24' are of average compositions Fe-0.20C-0.63Si-2.80Mn-0.04Ni-0.01Mo-1.10Cr wt. % and Fe-0.18C-0.75Si-1.98Mn-0.02Ni-0.01Mo-1.33Cr wt. % respectively. The interesting feature of the alloys is their relatively high silicon concentration, and their bainite microstructure, of the type discussed earlier.

8.2 Dilatometry

Dilatometry was used to study the development of transformation. The specimens were austenitised at 1000 °C for 10 minutes before helium gas quenching to a variety of isothermal transformation temperatures within the bainite transformation range (Fig. 8.1). The length change during the isothermal reaction was measured and the corresponding relative length change versus time data plotted as in Figs. 8.2 and 8.3. The interesting feature of these sigmoidal curves is once again, that the maximum

extent of transformation (*i.e.*, the maximum value of relative length change) at any temperature decreases with increasing isothermal transformation temperature and this is expected from the slope of the T_0 curve as discussed earlier. These results are supported by optical microscopy as seen in Figs. 8.4 and 8.5 which also gives a visual comparison of the extent of reaction in the homogeneous and heterogeneous samples. Banding is always apparent in the as-received alloy, although it seems to become less obvious at high degrees of transformation (*i.e.*, at low transformation temperatures).

Figure 8.6 shows a typical dilatometric curve of the relative length change as a function of temperature for the two steels during cooling from the austenitising temperature to the lowest isothermal transformation temperature used in the present experiments. The linearity of the plot proves the absence of any transformation during the quench to the isothermal transformation temperature, so that the equipment used is clearly capable of permitting isothermal transformation experiments.

To reveal further information from the dilatometric experiments, the data were analysed as in previous chapters. The relative length change corresponding to a volume fraction of bainitic ferrite V_b that grows from austenite, is given by:

$$\frac{\Delta l}{l} = \frac{2V_b a_\alpha^3 + (1 - V_b)a_\gamma^3 - \bar{a}_\gamma^3}{3\bar{a}_\gamma^3} \quad (8.1)$$

where a_α is the lattice parameter of ferrite at the transformation temperature, given by:

$$a_\alpha = a_\alpha^o [1 + e_\alpha(T - 25)] \quad (8.2)$$

and \bar{a}_γ , which is the lattice parameter of austenite of the alloy composition at the transformation temperature, is give by:

$$\bar{a}_\gamma = (a_o^\gamma + \sum c_i x_i)[1 + e_\gamma(T - 25)]. \quad (8.3)$$

In these equations, e_α and e_γ represent the linear thermal expansivities of ferrite and austenite respectively, a_o is the lattice parameter of austenite in pure iron at 25 °C, x_i is the concentration of alloying element i and $c_i x_i$ represents the change in a_o due to the addition of the alloying element to pure iron. T is the temperature in °C. The ferrite linear expansion coefficient was determined by first tempering a specimen at 600 °C for 10 minutes to decompose any retained austenite and then recording the length

change during very slow cooling. The measurements do not therefore account for the presence of any carbide whose volume fraction is in any case expected to be negligibly small for the present purposes. The graphs of relative length versus temperature are plotted in Fig. 8.7, from which the linear expansion coefficients of ferrite were obtained for the two steels ($\epsilon_{\alpha} = 1.022 \times 10^{-5} \text{K}^{-1}$ and $\epsilon_{\alpha} = 1.430 \times 10^{-5} \text{K}^{-1}$ for 'US83' and 'US24' steels respectively). The expansion coefficients of austenite were measured while specimens were in the single-phase field, as shown in Fig. 8.8 ($\epsilon_{\gamma} = 2.030 \times 10^{-5} \text{K}^{-1}$ and $\epsilon_{\gamma} = 2.230 \times 10^{-5} \text{K}^{-1}$ for 'US83' and 'US24' steels respectively).

The ferrite lattice parameter (a_{α}^o) at ambient temperature was measured using a Debye-Scherrer technique. The test specimen was annealed at 600 °C for half an hour, and then machined in the form of 0.5mm × 0.5mm × 15mm wire. Finally the specimen was immersed in an aqueous solution made up of 5% HF and 45% H₂O₂ (by volume) for two minutes to remove the deformation layer before testing. The specimens were irradiated with Mo K_α radiations using a standard Debye-Scherrer camera. A value of lattice parameter was calculated for each reflection from the resulting photograph and plotted against the Nelson-Riley function^[1] of Bragg angle θ . The linear regression technique was used to extrapolate a best-fit line back to $\theta = 90^\circ$, to find the intercept and the standard error in the intercept (Fig. 8.9). The resulting values of lattice parameter came out as $2.8692 \pm 0.0012 \text{ \AA}$ for 'US83' and $2.8670 \pm 0.002 \text{ \AA}$ for 'US24' which are in agreement with the respective values calculated to be 2.8679 \AA and 2.8675 \AA using data from Leslie^[2] but the steel has Mo, which is not included in the data from Leslie.

Using these measured values and making the appropriate substitutions in equation 8.1, the volume fractions of bainitic ferrite transformed were obtained using a computer program and the results thus obtained are shown in Figs. 8.10 and 8.11.

The range of concentration variation was found (Fig. 8.12 and 8.13) to be approximately 0.53-0.73Si, 2.48-3.12Mn, 1.03-1.17Cr wt. % for 'US83' steel and 0.60-0.90Si, 1.65-2.31Mn, 1.15-1.51Cr wt. % for 'US24' steel. Ni, Mo and V concentrations were too low to detect the corresponding small variations using microanalysis.

8.3 Transformation to Bainitic Ferrite

More transformation to bainite was observed in the homogenized samples as compared with the heterogeneous sample, at high undercoolings below the B_s temperature of the homogeneous sample (*i.e.*, 465 °C) for both ‘US83’ and ‘US24’ steels. At low undercoolings, the extent of isothermal transformation is found to be larger in the heterogeneous samples. Typical microstructures, as characterised using transmission electron microscopy are illustrated in figures 8.14 and 8.15. Carbide-free upper bainite was obtained even at the lowest temperatures shown in these figures. The carbon content of residual austenite was calculated using following mass balance equation^[3].

$$x_\gamma = \bar{x} + \frac{V_b(\bar{x} - x_\alpha)}{(1 - V_b)} \quad (8.4)$$

where, V_b is the volume fraction of bainitic ferrite. x_α is the amount of carbon which is left in the ferrite assumed to be 0.03 wt.%. \bar{x} is the actual carbon content of the alloy.

In this way, the carbon concentration in the austenite at the point where isothermal transformation ceases can be calculated, and a comparison of such data for upper bainite, with the T_0 , T'_0 and A'_{e3} curves, calculated^[3,4] from the chemical composition of the homogeneous alloy, is presented in Figs. 8.16 and 8.17. The experimental results are more consistent with the T'_0 curve relative to T_0 curve. It is evident from these figures that the experimental data support the conclusion that the growth of bainite is diffusionless, with the carbon being partitioned subsequently into the residual austenite. The results show that both of these steels accurately exhibit the incomplete reaction phenomenon, which can be used to estimate theoretically the degree of transformation expected as a function of isothermal transformation temperature or in terms of the alloy chemistry.

8.3.1 Theoretical Analysis

The transformation behaviour of these steels was also studied theoretically using the slice model fully described in chapter 4 and compared with the experimental data in figures 8.18 and 8.19. In these calculations, The heterogeneous steel was represented as a composite of many slices of equal thickness but of different chemical composition consistent with the experimentally measured composition range. The γ/α interface is

considered to move parallel to the isoconcentration planes as the microstructure shows banding.

In one case, the slices transform independently of each other, which is the more likely circumstance because of the sheaf morphology of bainite, where carbon trapped in the residual austenite remains isolated from one another.

The reasonable agreement is found in predicting the different behaviours of the as-received and homogenised samples. For most of the data, both theory and experiment show a higher degree of transformation in the homogenised samples, and both show a reversal of this trend as the transformation temperature approaches the B_s temperature of the homogenised alloy. However, the difference in the calculated volume fraction of bainite in the homogeneous and heterogeneous "US24" steel samples was found to be negligible above the B_s temperature of the homogeneous alloy. It should be noted that the "US24" steel not only has lower carbon content but Mn is also less than that in the "US83" steel which is affecting the transformation behaviour of the two steels. To make this point more clear, calculations were carried out for different compositions with varying average Mn content and also for different Mn variation ranges for the "US24" steel. In one case the average Mn content was varied keeping the Mn range constant as shown in Fig. 8.20a. The results were not very different as still the maximum Mn content considered (2.83 wt. %) was just the same as the average Mn concentration (2.80 wt. %) of the "US83" steel. So in another set of calculations the maximum Mn concentration of the heterogeneous "US24" steel was varied (up to 3.35 wt. %) while the minimum concentration was kept constant (*i.e.*, 1.65 wt. %). Fig. 8.20b illustrates that as we increase the Mn content, the austenite can tolerate less and less carbon and the difference in the homogeneous and heterogeneous samples becomes more significant.

In another case of the slice model, carbon is allowed to distribute evenly throughout the residual austenite (*i.e.*, among the slices) during the development of bainitic microstructure. The fact that the carbon does not homogenise during transformation is emphasized by the results shown in Figs. 8.18 and 8.19, where the calculated data (assuming that carbon homogenises between the slices) are seen to overestimate the volume fraction of bainite.

8.4 Martensitic Transformation in ‘US83’ Steel

The dilatometric specimens from the ‘US83’ steel of average composition Fe-0.20C-0.63Si-2.80Mn-0.04Ni-0.01Mo-1.10Cr wt. % were quenched to ambient temperature after an appropriate time of isothermal holding at different temperatures (T_b) in the bainite range. Dilatometric curves of relative length change versus temperature are shown in Fig. 8.21. These data were converted into the volume fraction of martensite (f) using the following relationship:

$$f = \frac{3\Delta La_\gamma^3}{V_\gamma L(2a_\alpha^2 c_\alpha - a_\gamma^3)} \quad (8.5)$$

where a_γ is the lattice parameter of the the carbon-enriched residual austenite, a_α and c_α are the lattice parameters of tetragonal martensite, and V_γ is the volume fraction of austenite present in the sample prior to martensitic transformation. The absolute volume fraction of martensite ($V_{\alpha'}$) can be obtained by multiplying the fraction of austenite transformed to martensite (f) with the actual volume fraction of austenite (V_γ) initially present at T_B , i.e.,

$$V_{\alpha'} = fV_\gamma \quad (8.6)$$

A computer program was written and used for these calculations which takes full account of the changes in lattice parameters as a function of alloy composition and temperature, as described elsewhere [5,6].

Another very useful information obtained from these dilatometric curves was the experimental measurement of the martensitic start temperature (M_s) as the point where the curve deviates from straight line during cooling. A good agreement between the calculated[7,8] and measured M_s temperature of can be seen from the Fig. 8.22. All these data were further used in the theoretical study of the progress of the athermal martensitic transformation as described empirically by the following equation:

$$1 - f = \exp\{-C_1(M_S - T_Q)\} \quad (8.7)$$

where f is the volume fraction of martensite divided by the volume fraction of austenite prior to the formation of martensite, T_Q is a temperature to which the sample is cooled below M_S ; C_1 is a constant obtained originally [9] by fitting to experimental data. The comparison of the experimental and calculated volume fraction of martensite using the

above equation is shown in Fig. 8.23. As mentioned previously in chapter 5, the above empirical equation cannot predict the kinetics of martensite formation at all stages of the reaction. A new model, as described in chapter 5, was then used to study the development of martensitic transformation as a function of undercooling below the M_S temperature. This model includes the effects of autocatalysis^[10-12] and can be described by the following equation:

$$-\frac{\ln\{1-f\}}{f} = 1 + \bar{V}C_6(M_S - T_Q) \quad (8.8)$$

or

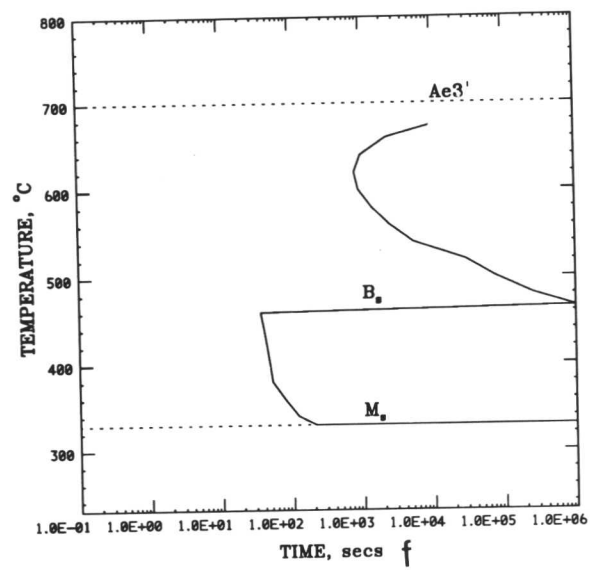
$$-\frac{\ln\{1-f\}}{f} = 1 + C_7(M_S - T_Q) \quad (8.9)$$

where $C_7 = \bar{V}C_6$. \bar{V} is the average volume per newly formed martensite plate assumed to be constant for the course of these calculations.

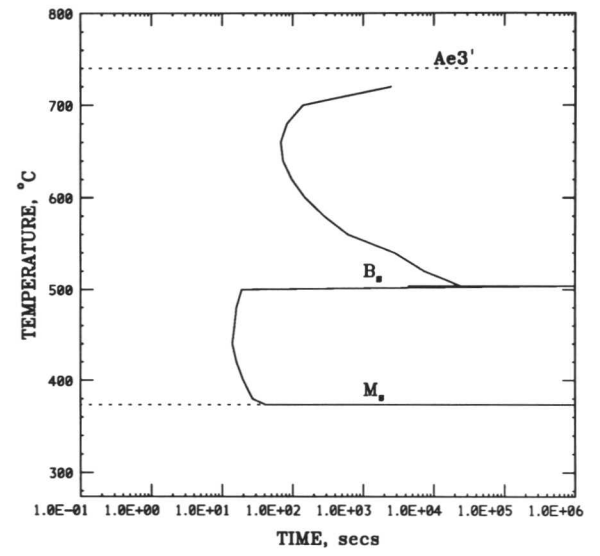
Figure 8.24 shows that the new model can better predict the kinetics of the martensite reaction at all stages.

8.5 Conclusions

All the experimental and theoretical work presented in the previous chapters was tried and tested for two more heterogeneous steels. Figure 8.25 shows the cumulative results of the complete calculation of microstructure in the homogeneous and heterogeneous “US83” steel samples. As expected, more transformation to martensite was obtained with a decrease in the bainitic ferrite volume fraction. The results confirm that the models illustrated previously are valid for other steels also.



a



b

Fig. 8.1: Calculated^[4,13] time-temperature-transformation (TTT) diagrams.

- (a) "US83" steel of average composition Fe-0.20C-0.63Si-2.80Mn-0.04Ni-0.01Mo-1.10Cr wt. %.
- (b) "US24" steel of average composition Fe-0.18C-0.75Si-1.98Mn-0.02Ni-0.01Mo-1.33Cr wt. %.

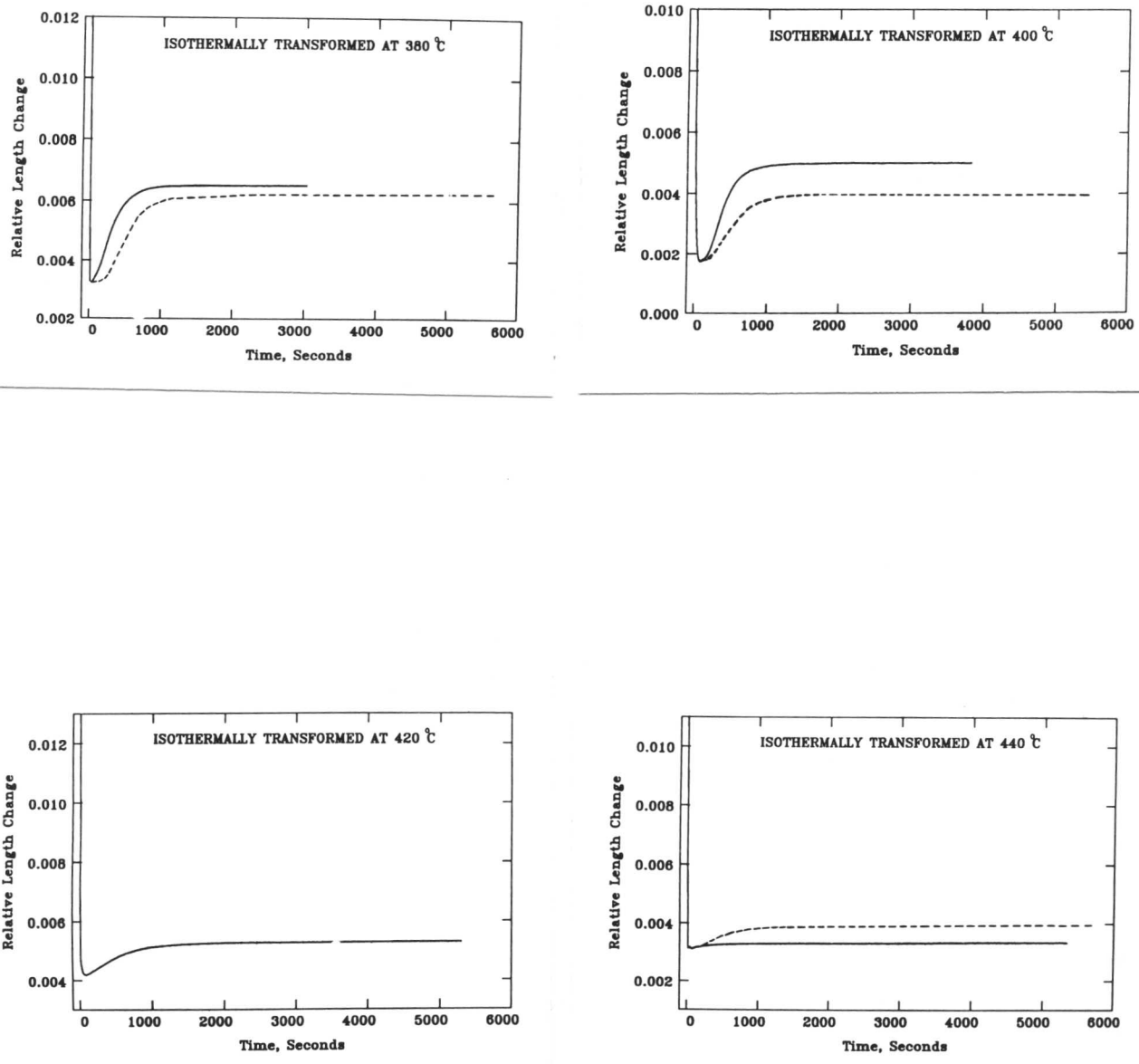


Fig. 8.2: Dilatometric curves for samples of 'US83' steel isothermally transformed at the temperatures indicated. The continuous curves are for the homogenised samples and the dashed curves for the heterogeneous samples.

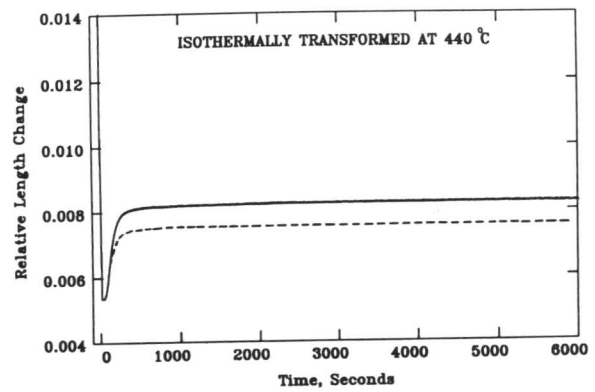
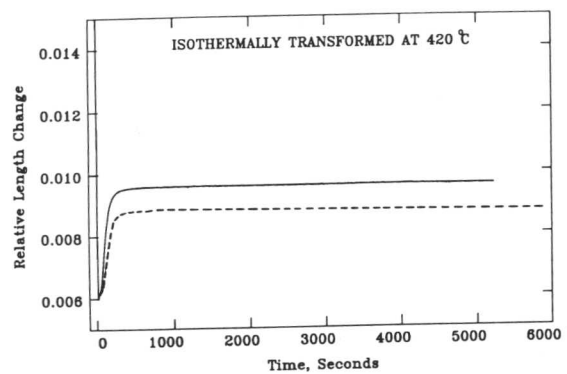
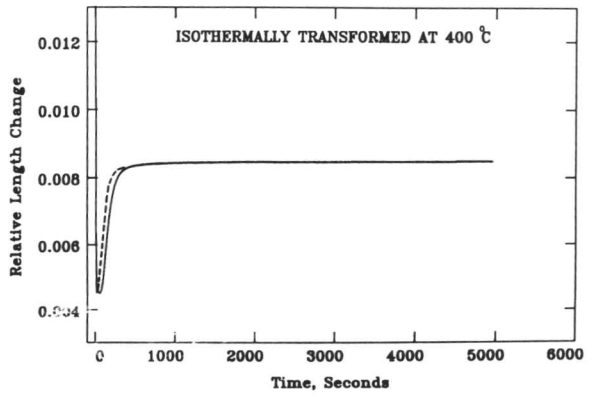
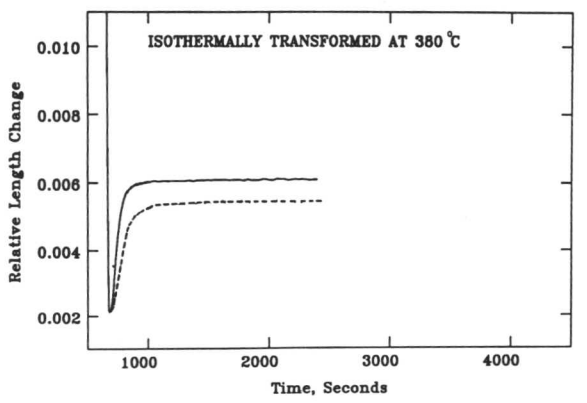


Fig. 8.3: Dilatometric curves for samples of 'US24' steel isothermally transformed at the temperatures indicated. The continuous curves are for the homogenised samples and the dashed curves for the heterogeneous samples.

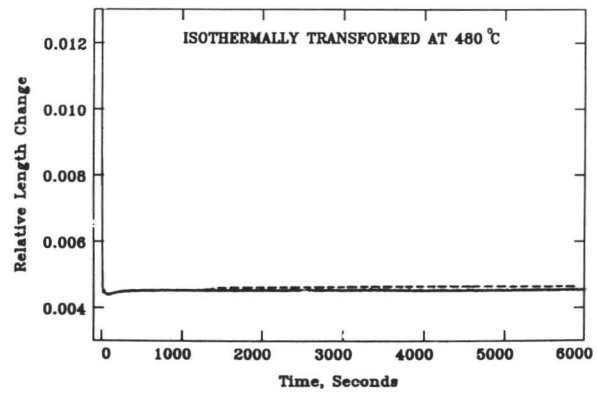
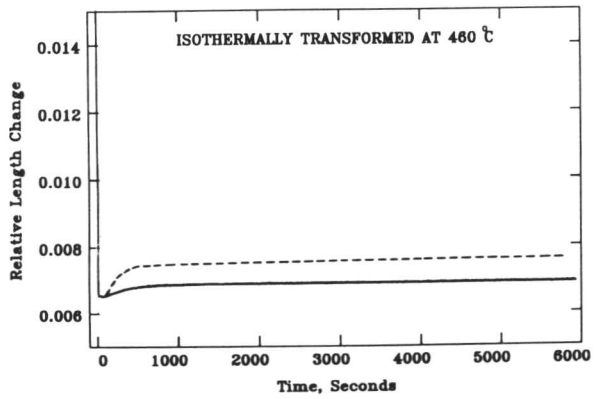


Fig. 8.3:(continued)

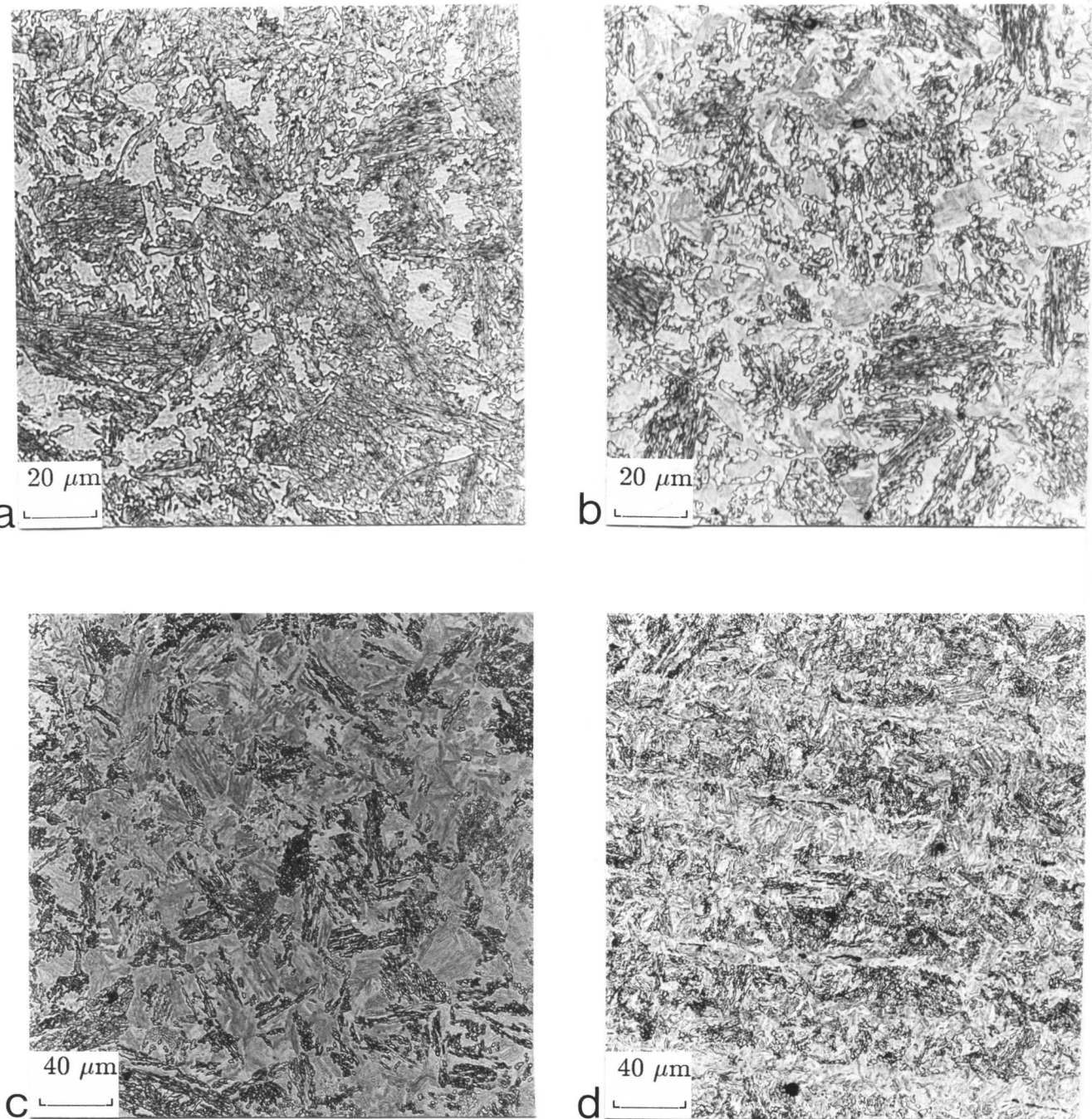


Fig. 8.4: Metallographic confirmation of the curves shown in figure 8.1:

- (a) Optical micrograph of the homogeneous specimen, from 'US83' steel, isothermally transformed at 400 °C.
- (b) Optical micrograph of the heterogeneous specimen, from 'US83' steel, isothermally transformed at 400 °C.
- (c) Optical micrograph of the homogeneous specimen, from 'US83' steel, isothermally transformed at 420 °C.
- (d) Optical micrograph of the heterogeneous specimen, from 'US83' steel, isothermally transformed at 420 °C.

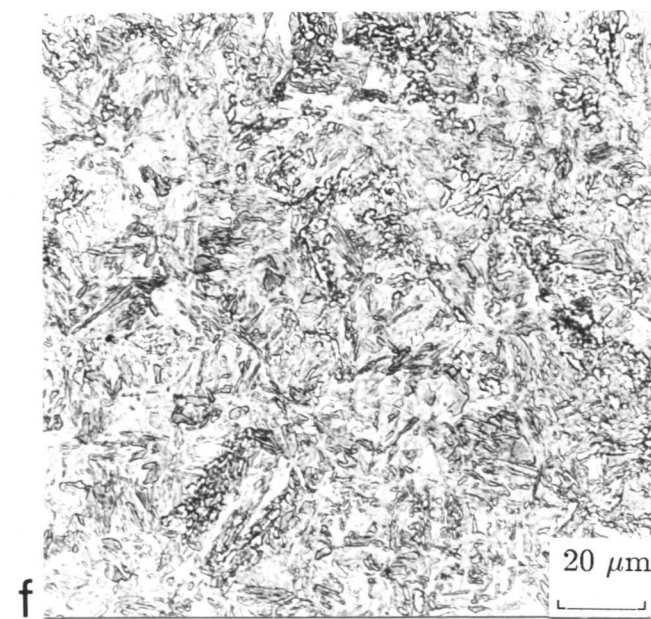
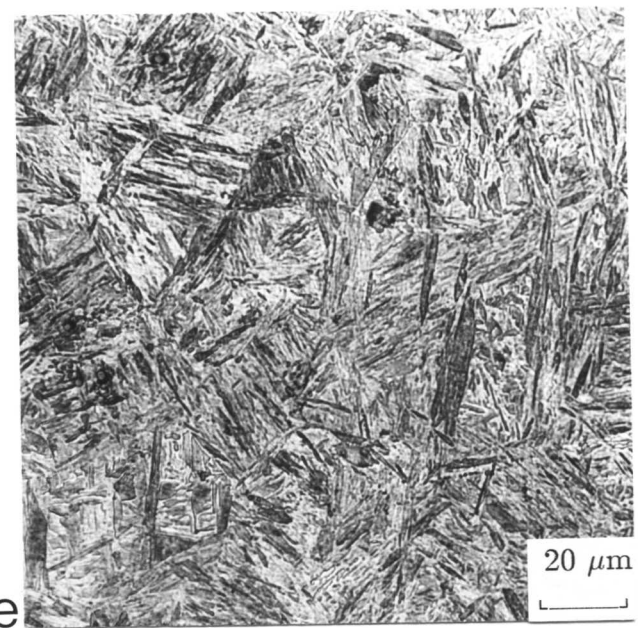


Fig. 8.4: (continued)

- (e) Optical micrograph of the homogeneous specimen, from 'US83' steel, isothermally transformed at 440°C .
- (f) Optical micrograph of the heterogeneous specimen, from 'US83' steel, isothermally transformed at 440°C .

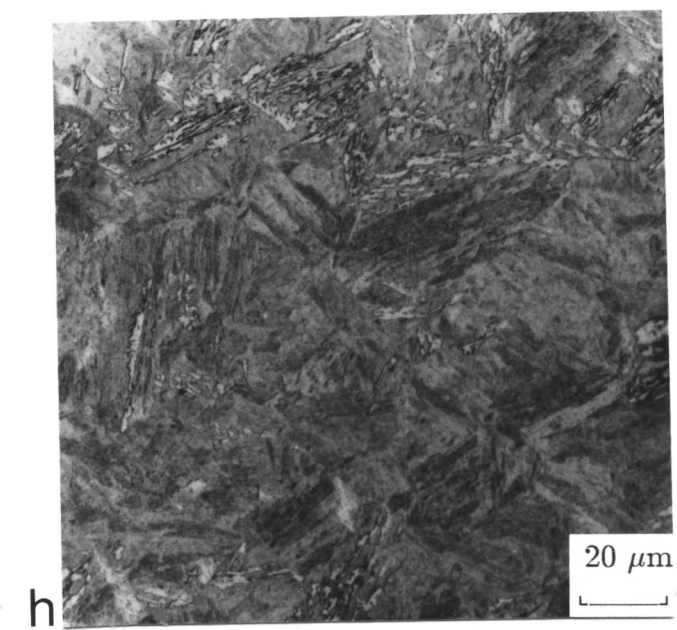
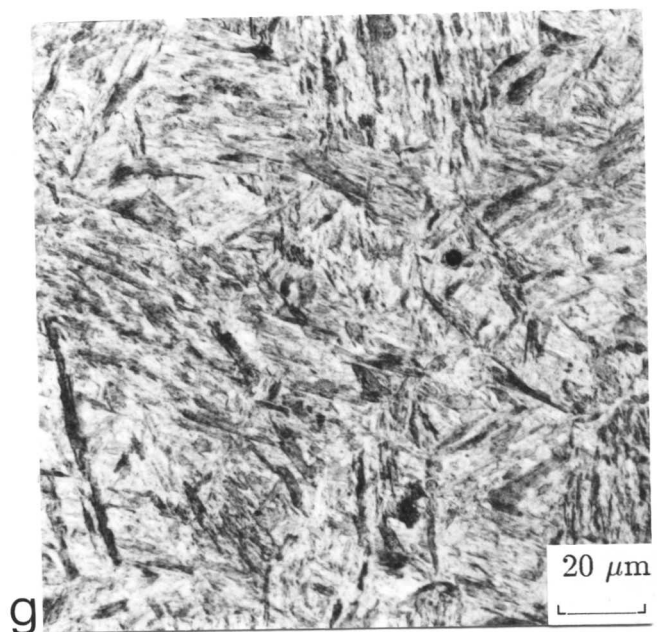


Fig. 8.4: (continued)

- (g) Optical micrograph of the homogeneous specimen, from 'US83' steel, isothermally transformed at 460 °C.
- (h) Optical micrograph of the heterogeneous specimen, from 'US83' steel, isothermally transformed at 460 °C.

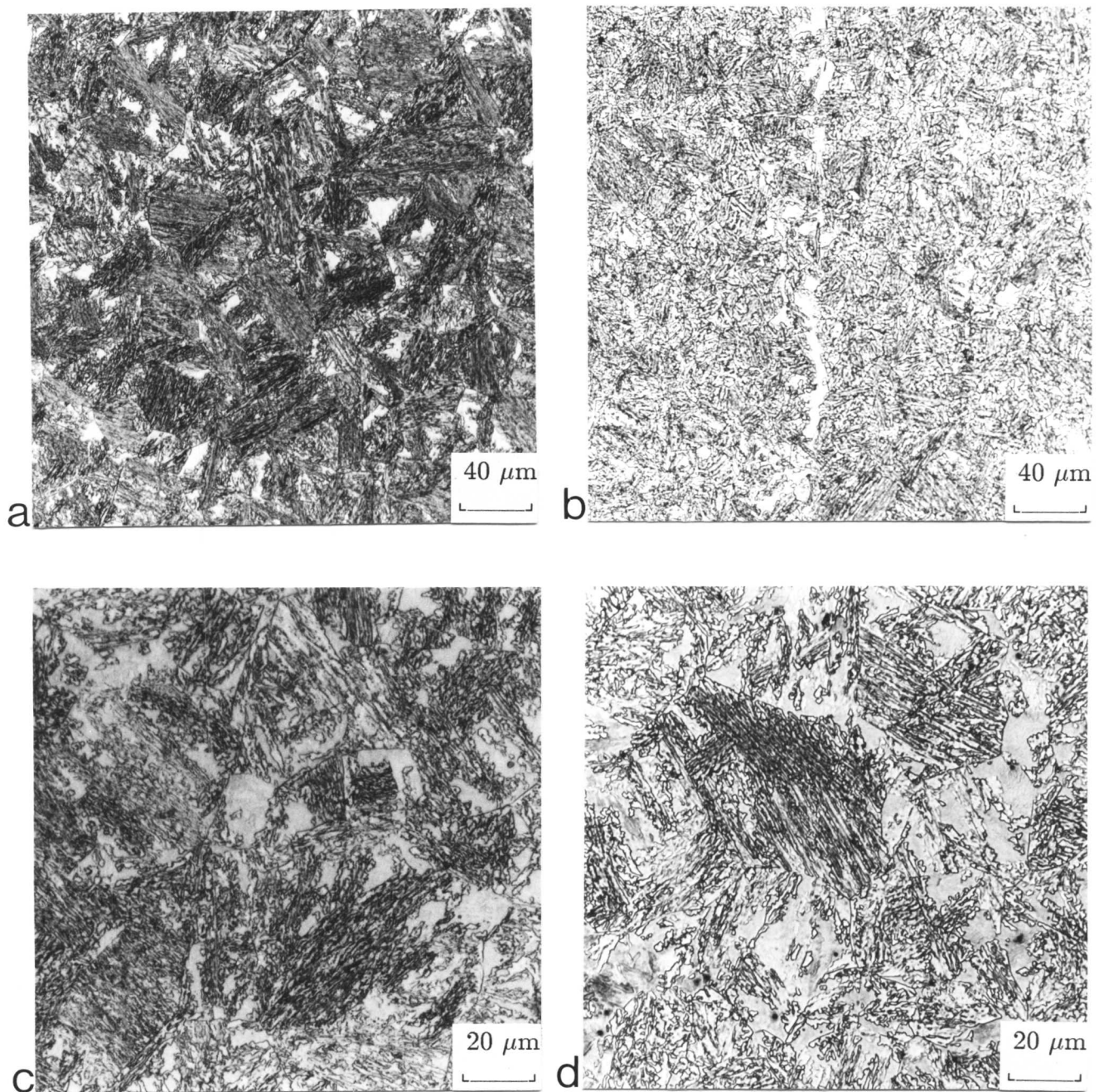


Fig. 8.5: Metallographic confirmation of the curves shown in figure 8.1:

(a) Optical micrograph of the homogeneous specimen, from ‘US24’ steel, isothermally transformed at 400°C .

(b) Optical micrograph of the heterogeneous specimen, from ‘US24’ steel, isothermally transformed at 400°C .

(c) Optical micrograph of the homogeneous specimen, from ‘US24’ steel, isothermally transformed at 420°C .

(d) Optical micrograph of the heterogeneous specimen, from ‘US24’ steel, isothermally transformed at 420°C .

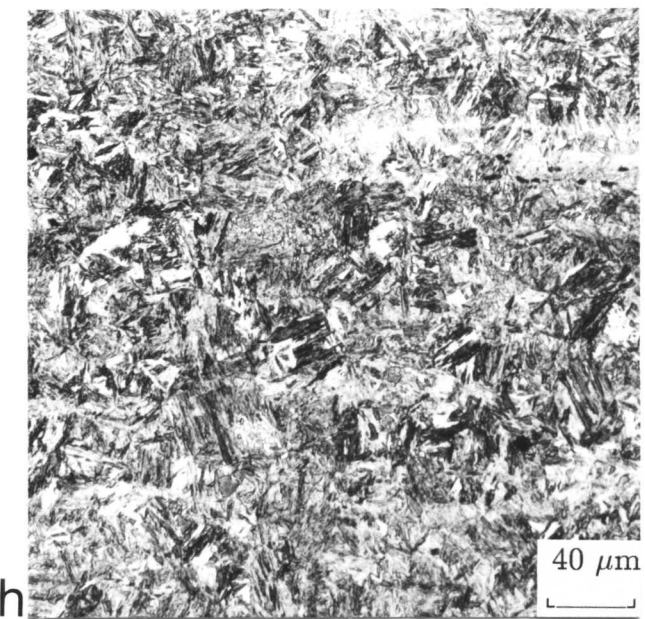
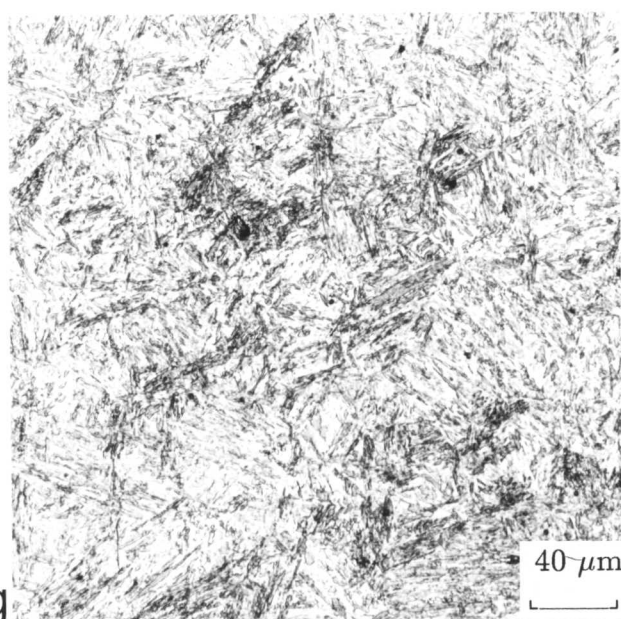
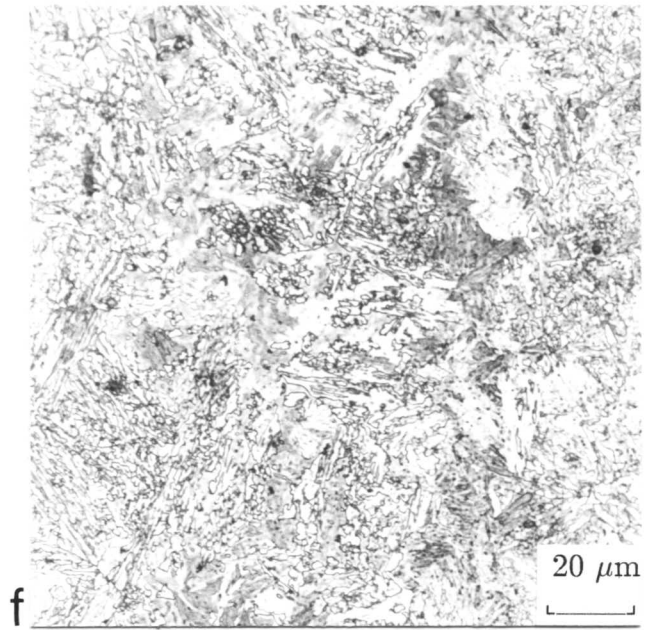
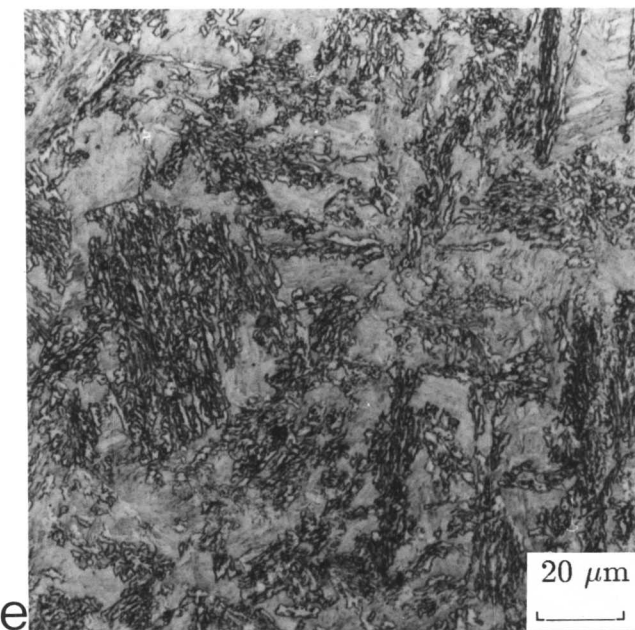


Fig. 8.5: (continued)

(e) Optical micrograph of the homogeneous specimen, from 'US24' steel, isothermally transformed at 440 °C.

(f) Optical micrograph of the heterogeneous specimen, from 'US24' steel, isothermally transformed at 440 °C.

(g) Optical micrograph of the homogeneous specimen, from 'US24' steel, isothermally transformed at 460 °C.

(h) Optical micrograph of the heterogeneous specimen, from 'US24' steel, isothermally transformed at 460 °C.

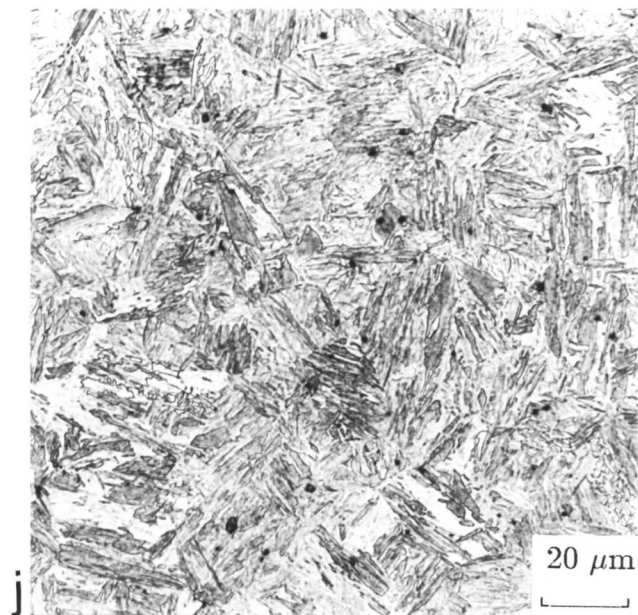
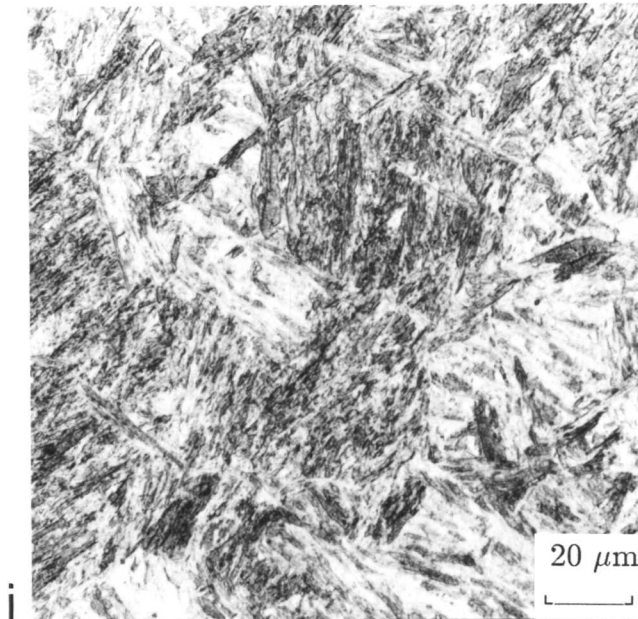
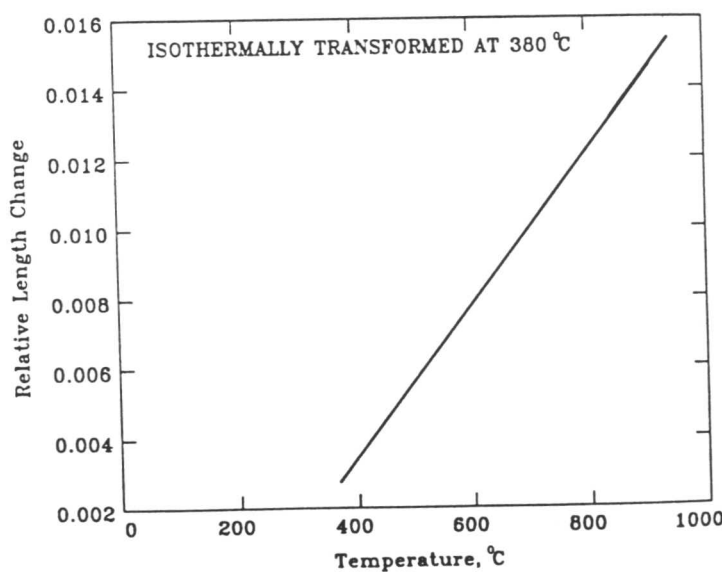
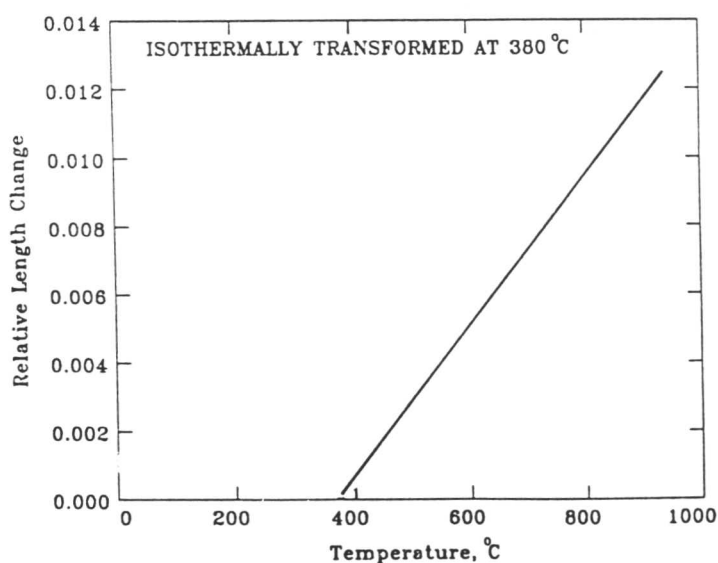


Fig. 8.5: (continued)

- (i) Optical micrograph of the homogeneous specimen, from 'US24' steel, isothermally transformed at 480 °C.
- (j) Optical micrograph of the heterogeneous specimen, from 'US24' steel, isothermally transformed at 480 °C.



a

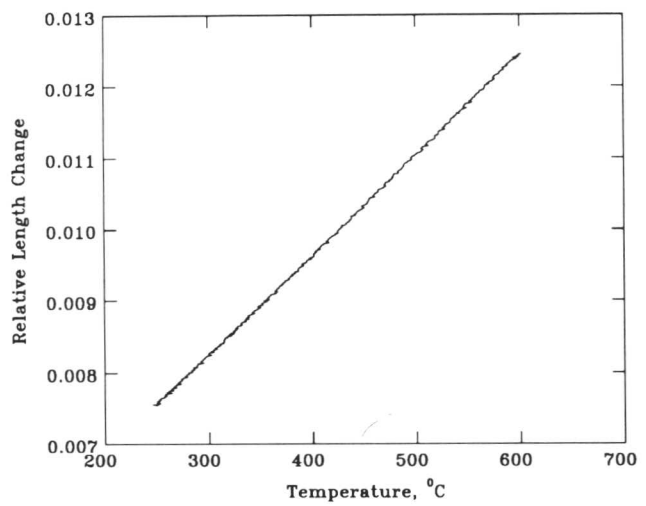


b

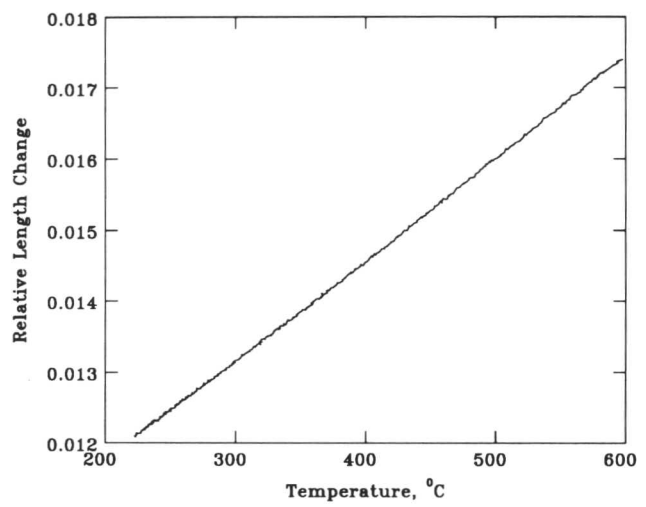
Fig. 8.6: Dilatometric curves showing the linear variation of relative specimen length as a function of temperature during cooling from the austenitising temperature to the isothermal transformation temperature.

(a) Heterogeneous 'US83' steel.

(b) Heterogeneous 'US24' steel.



a

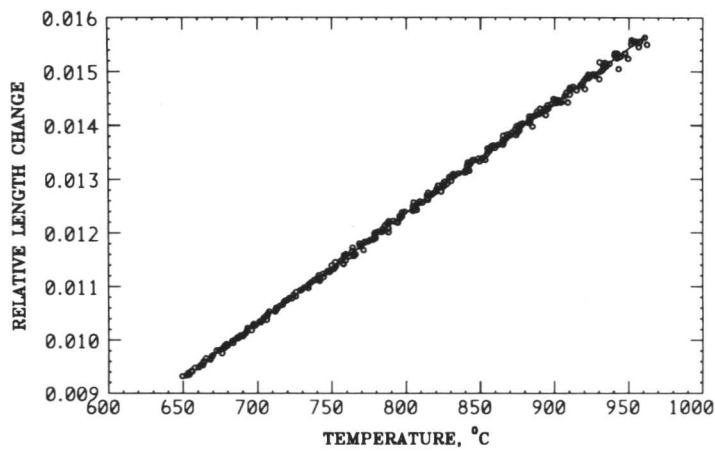


b

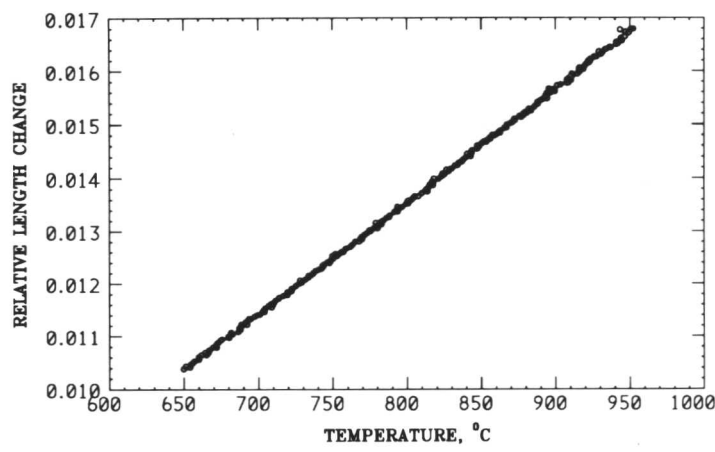
Fig. 8.7: Graph of relative length change versus temperature, from which the linear expansion coefficient of ferrite is obtained.

(a) 'US83' steel.

(b) 'US24' steel.



a

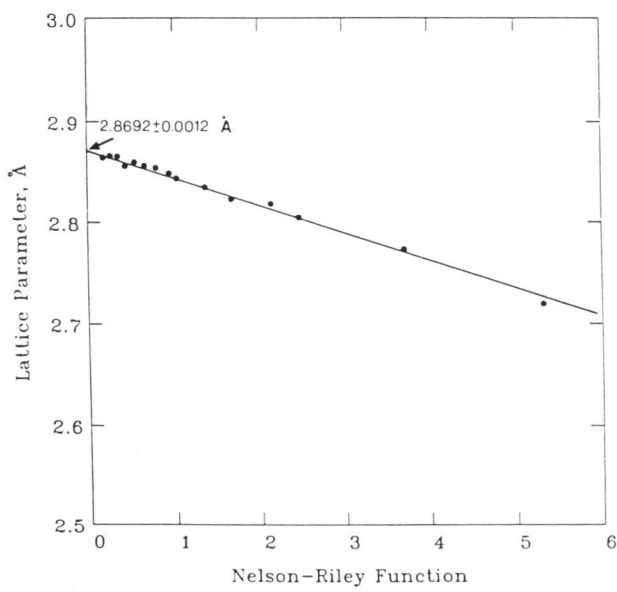


b

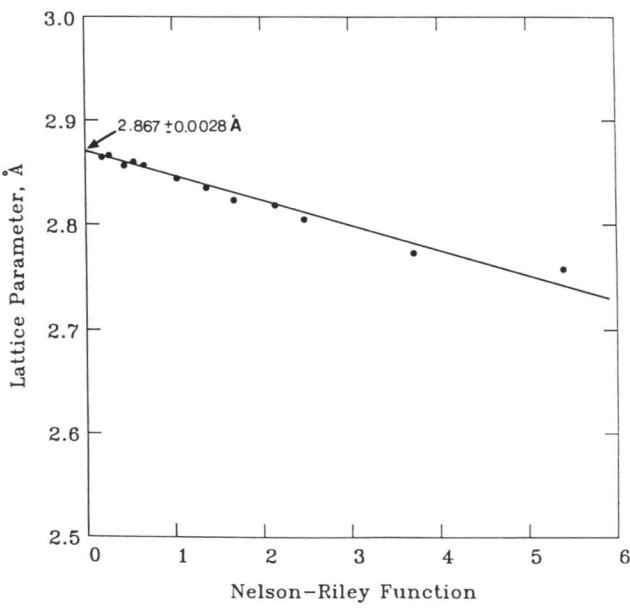
Fig. 8.8: Graph of relative length change versus temperature, from which the linear expansion coefficient of austenite is obtained.

(a) 'US83' steel.

(b) 'US24' steel.



a



b

Fig. 8.9: Extrapolation of measured lattice parameter against Nelson-Riley function (i.e., $\frac{\cos^2 \theta}{\sin \theta} + \frac{\cos^2 \theta}{\theta}$). θ is the diffraction angle.

(a) 'US83' steel.

(b) 'US24' steel.

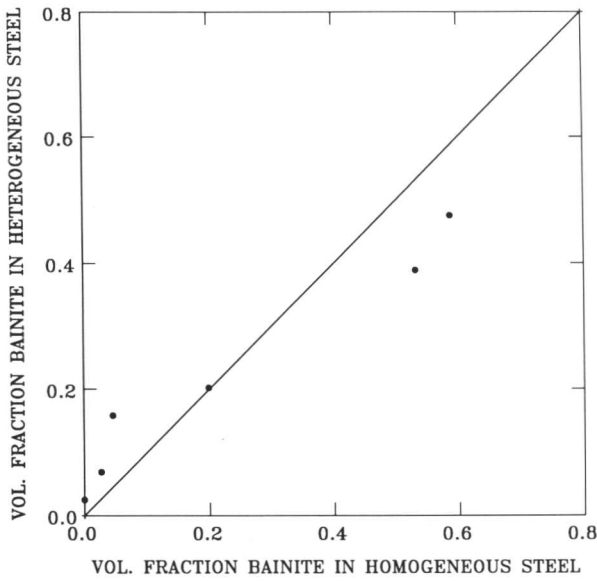


Fig. 8.10: A plot of the maximum volume fraction of bainitic ferrite obtained in homogenised 'US83' steel, versus the corresponding volume fraction for as-received 'US83' steel. The line has a slope of unity and serves to illustrate that except at the transformation temperatures near B_s , the extent of transformation is larger in the homogenised samples.

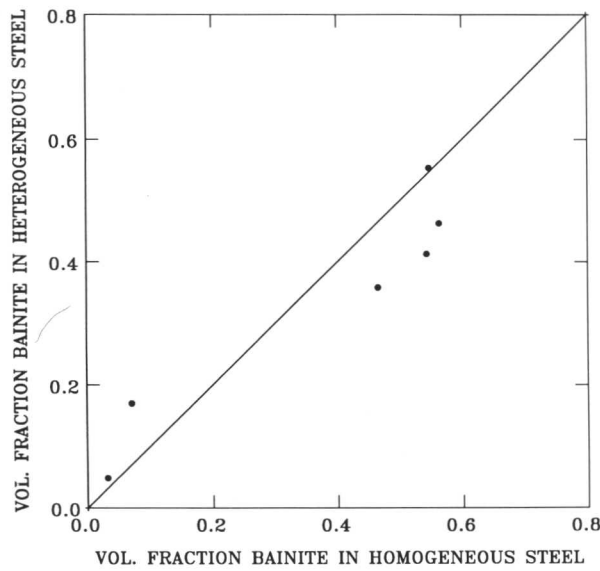


Fig. 8.11: A plot of the maximum volume fraction of bainitic ferrite obtained in homogenised 'US24' steel, versus the corresponding volume fraction for as-received 'US24' steel. The line has a slope of unity and serves to illustrate that except at the transformation temperatures near B_s , the extent of transformation is larger in the homogenised samples.

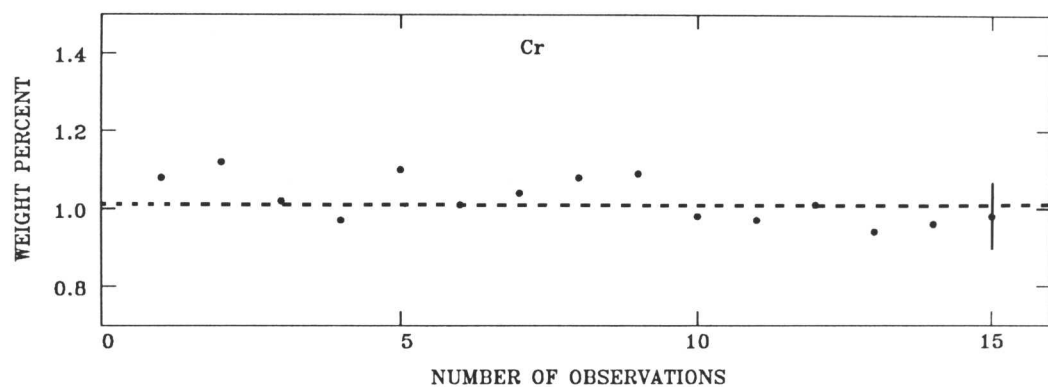
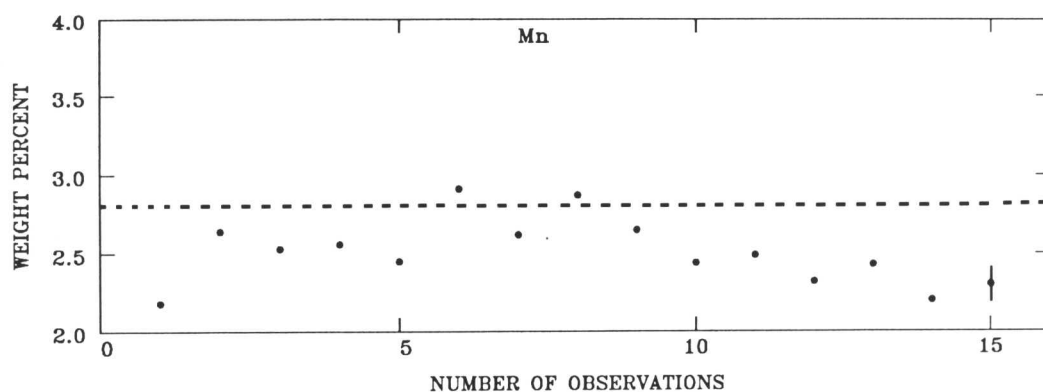
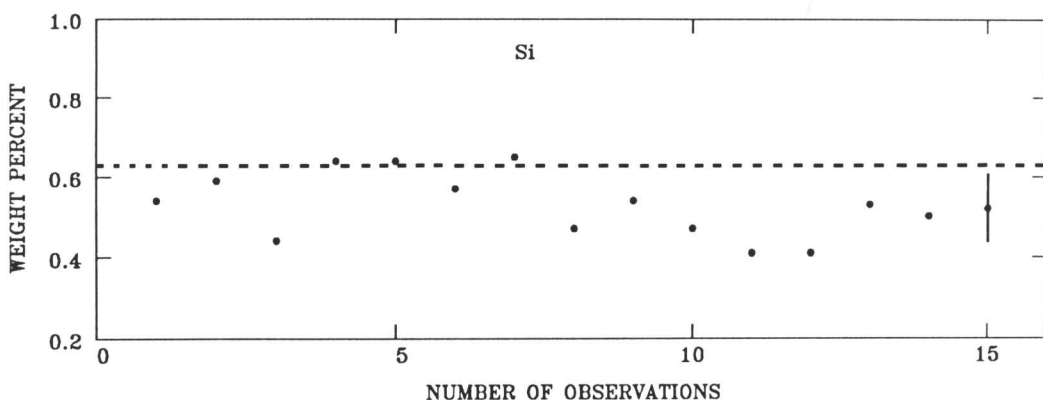


Fig. 8.12a: Microanalysis data from the bainitic regions in a heterogeneous sample of 'US83' steel. The error bars indicate the typical 95% confidence statistical error and the average composition is in each case indicated by the dashed horizontal line.

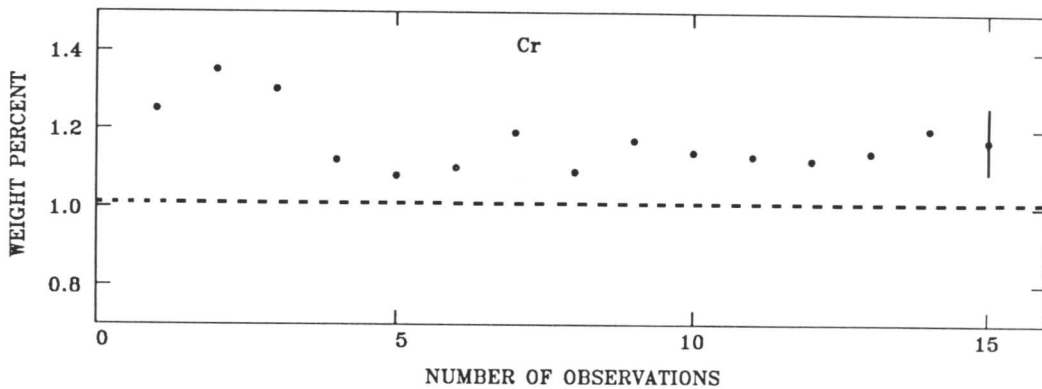
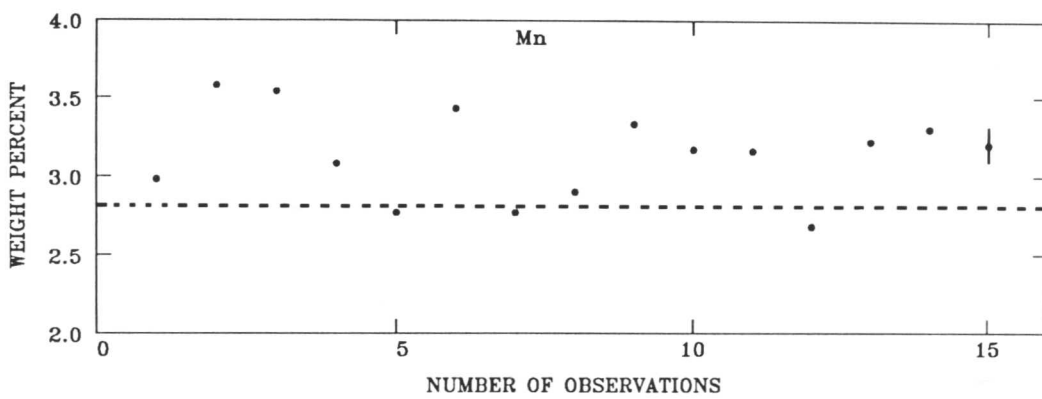
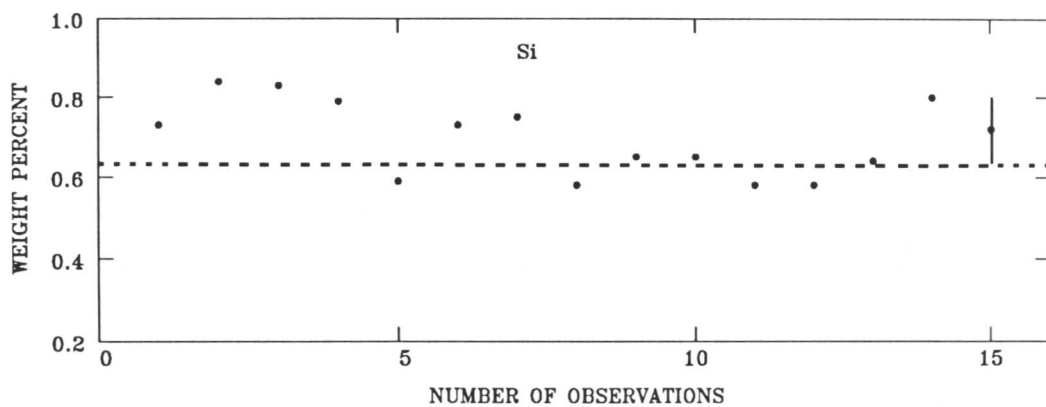


Fig. 8.12b: Microanalysis data from the martensitic regions in a heterogeneous sample of 'US83' steel. The error bars indicate the typical 95% confidence statistical error and the average composition is in each case indicated by the dashed horizontal line.

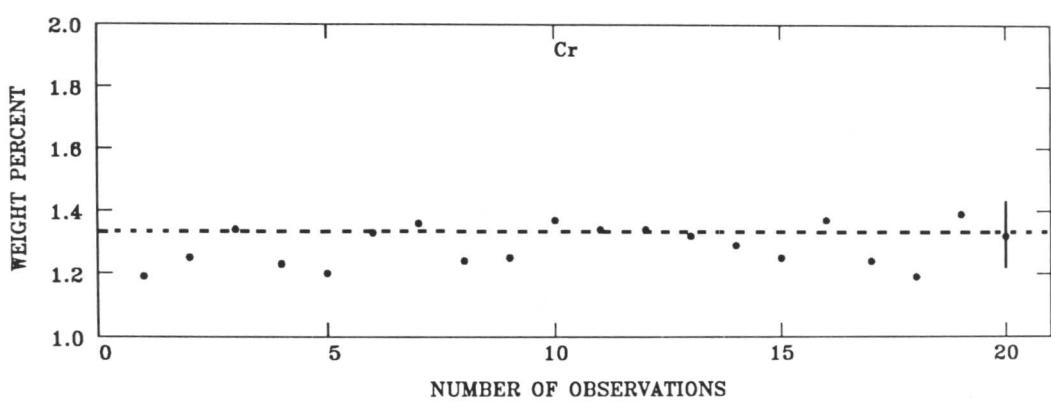
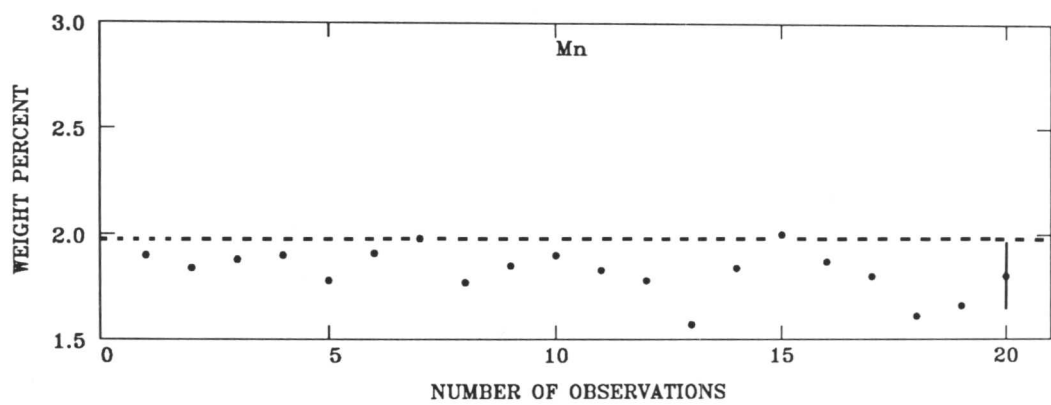
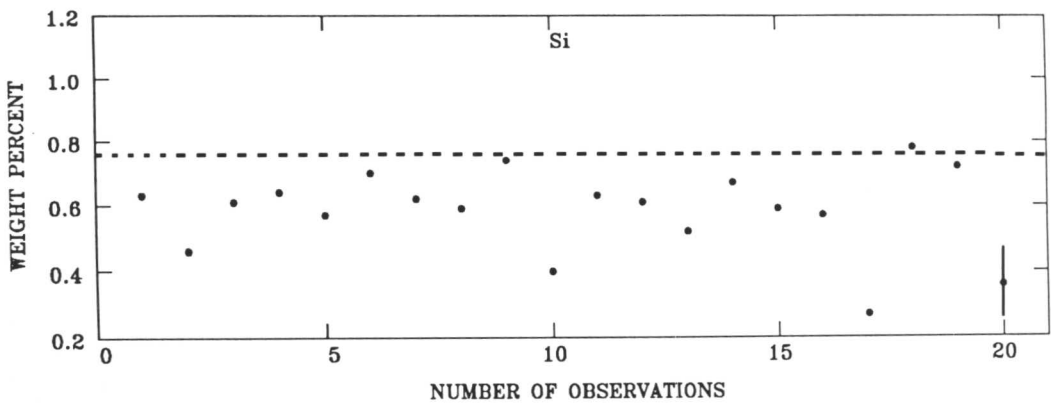


Fig. 8.13a: Microanalysis data from the bainitic regions in a heterogeneous sample of 'US24' steel. The error bars indicate the typical 95% confidence statistical error and the average composition is in each case indicated by the dashed horizontal line.

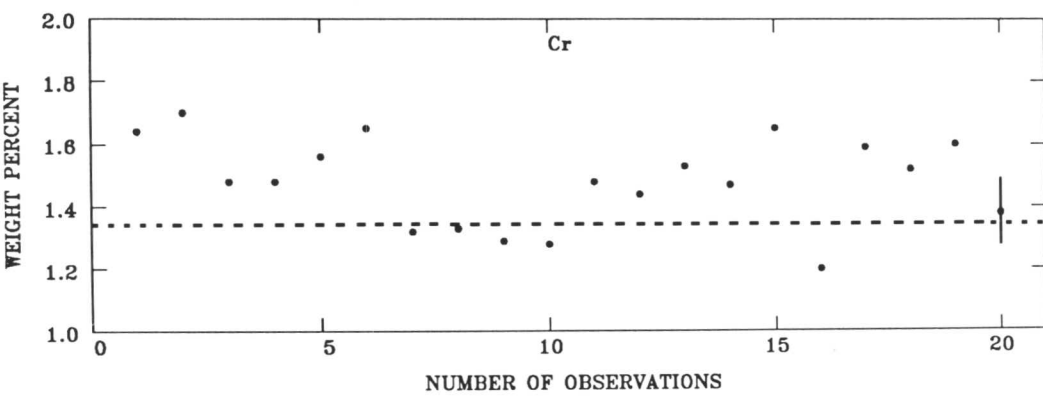
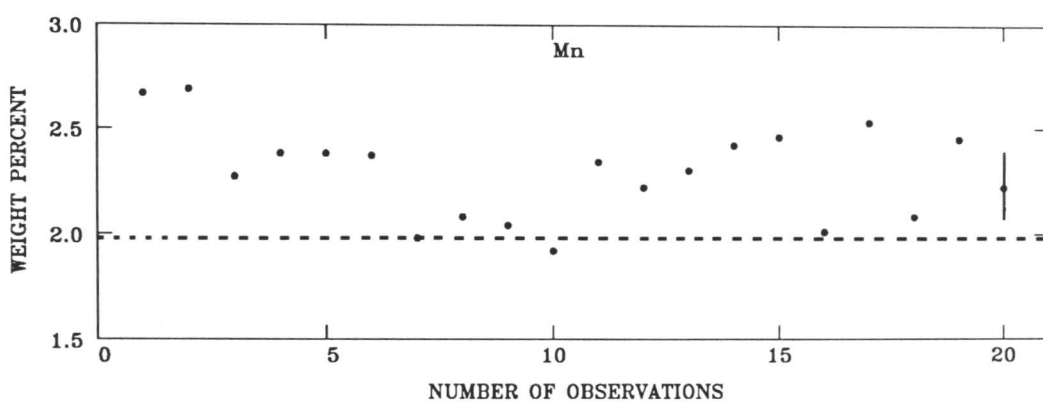
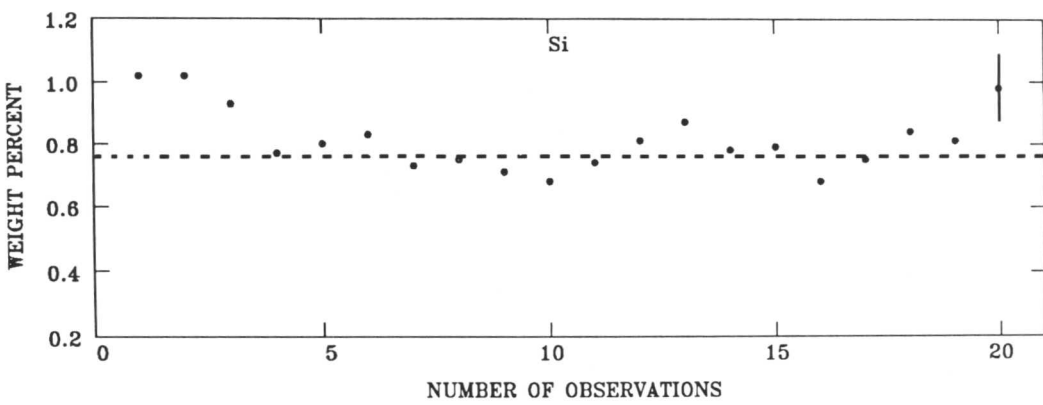
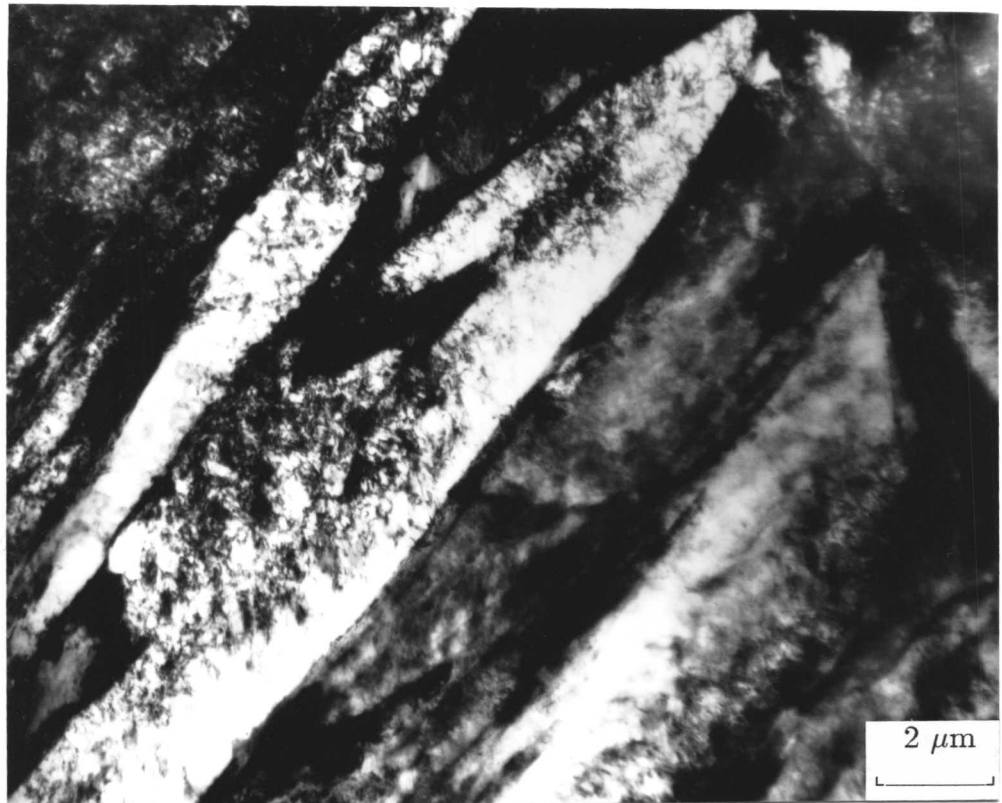
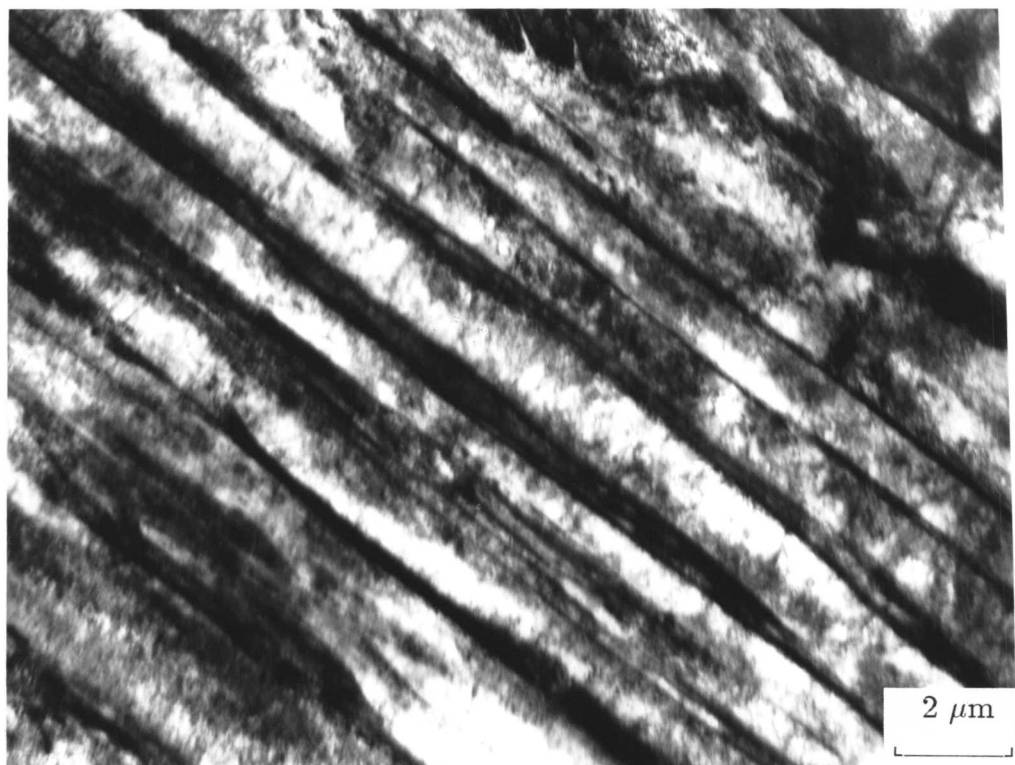


Fig. 8.13b: Microanalysis data from the martensitic regions in a heterogeneous sample of 'US24' steel. The error bars indicate the typical 95% confidence statistical error and the average composition is in each case indicated by the dashed horizontal line.



a



b

Fig. 8.14: Bright field transmission electron micrograph showing upper bainite in a heterogeneous sample of 'US83' steel.

(a) Isothermally transformed to bainitic ferrite at 400 °C for approximately 90 minutes before quenching to ambient temperature.

(b) Isothermally transformed to bainitic ferrite at 420 °C for approximately 90 minutes before quenching to ambient temperature.

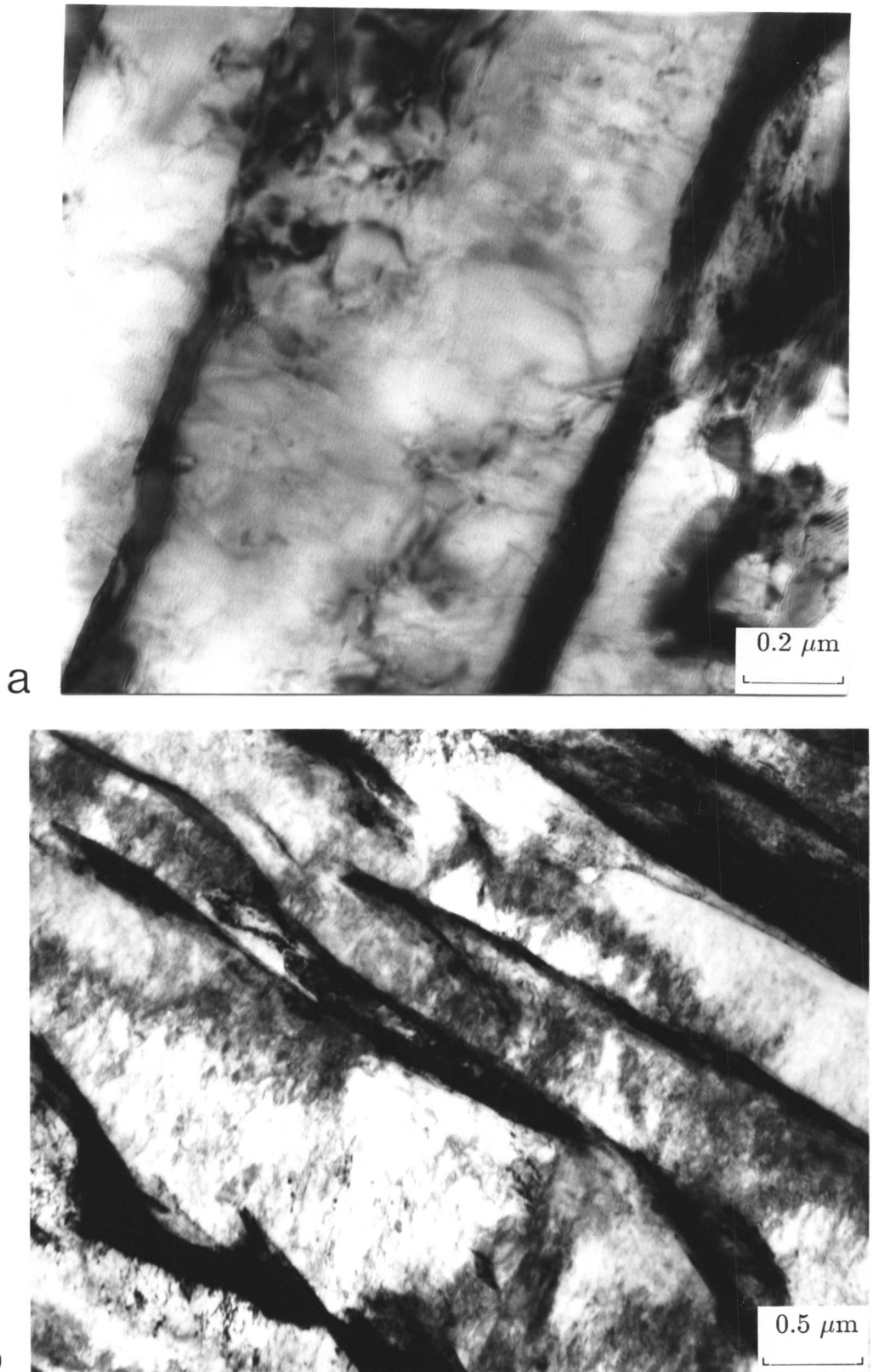


Fig. 8.15: Bright field transmission electron micrograph showing upper bainite in a heterogeneous sample of 'US24' steel.

- Isothermally transformed to bainitic ferrite at 400°C for approximately 90 minutes before quenching to ambient temperature.
- Isothermally transformed to bainitic ferrite at 420°C for approximately 90 minutes before quenching to ambient temperature.

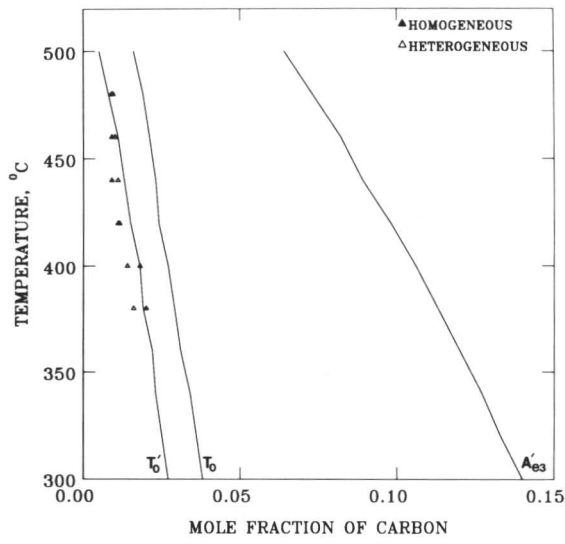


Fig. 8.16: Calculated^[3,4] T'_0 , A'_e3 and A_e3 phase boundaries for ‘US83’ steel. The experimental data are for samples transformed isothermally to bainitic ferrite and carbon enriched residual austenite at a variety of temperatures.

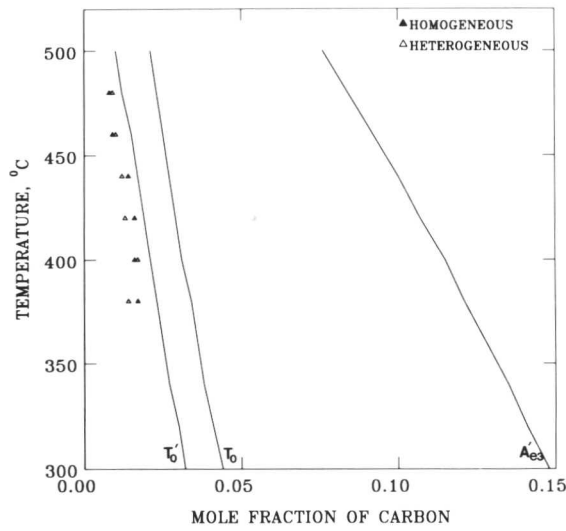
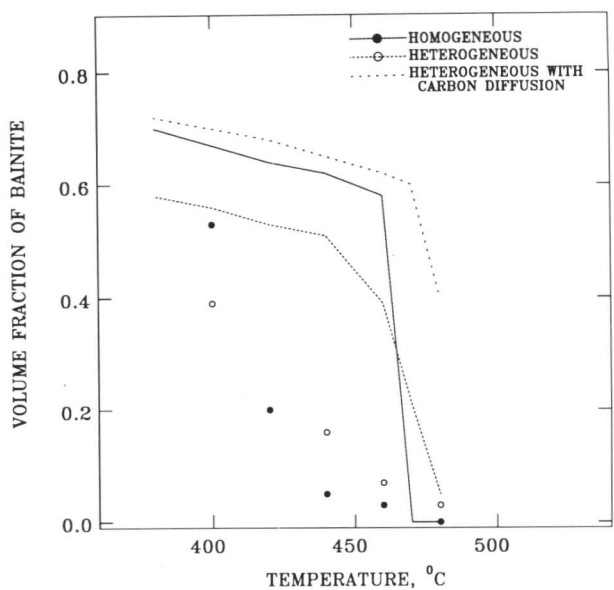
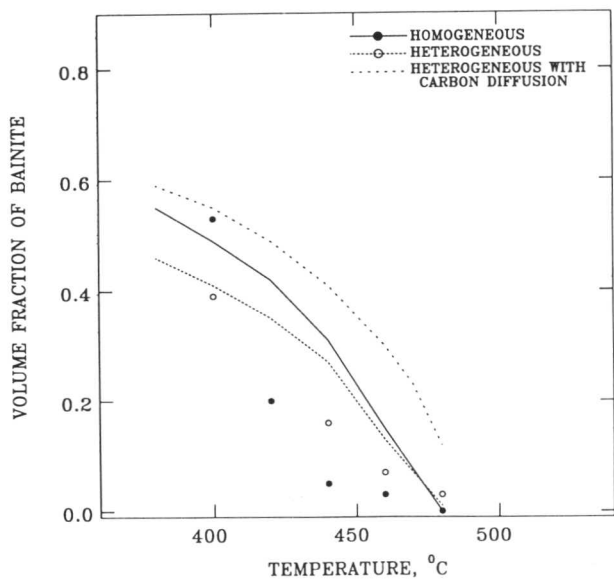


Fig. 8.17: Calculated^[3,4] T'_0 , A'_e3 and A_e3 phase boundaries for ‘US24’ steel. The experimental data are for samples transformed isothermally to bainitic ferrite and carbon enriched residual austenite at a variety of temperatures.



a

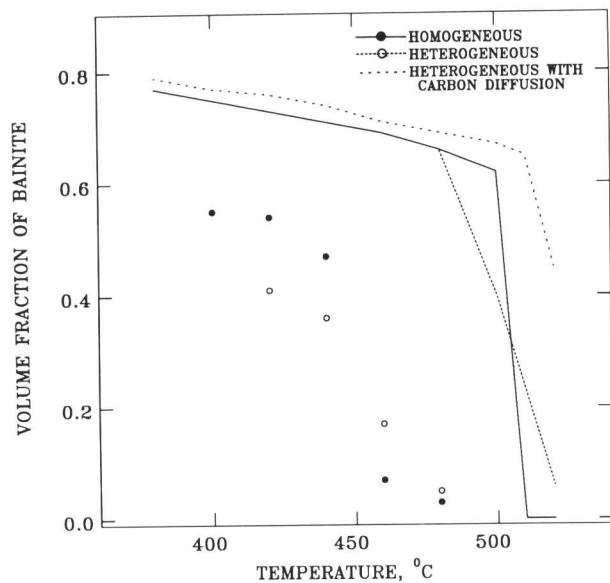


b

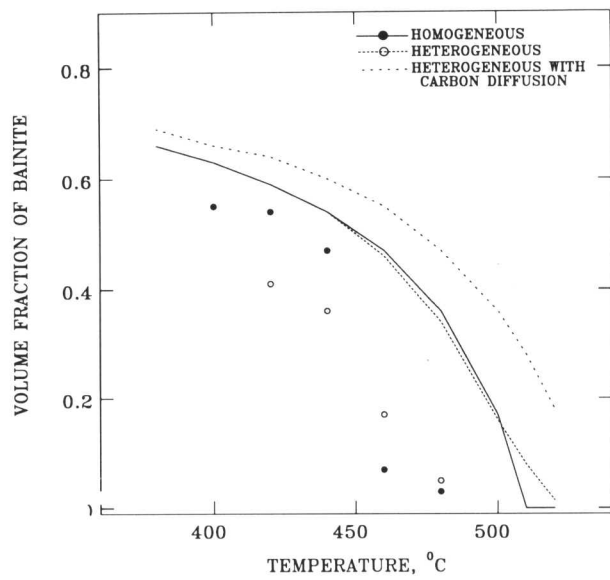
Fig. 8.18: Results from the slice model calculations for as-received and homogenised samples of 'US83' steel. Points in the graph represent the experimental data.

(a) Calculations based on T_0 curve.

(b) Calculations based on T'_0 curve.



a

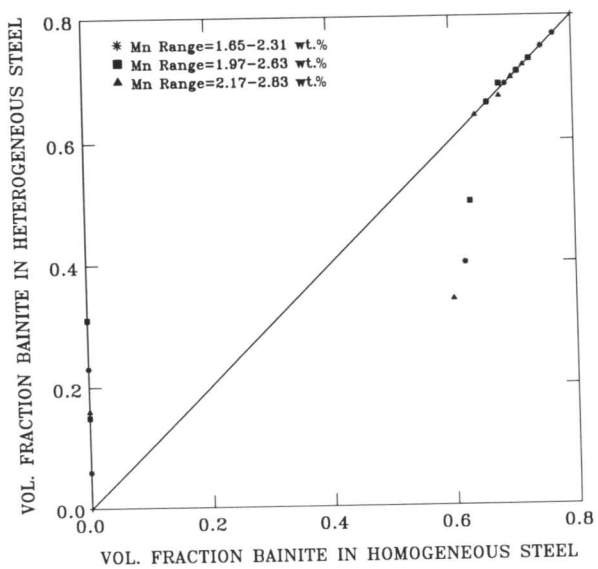


b

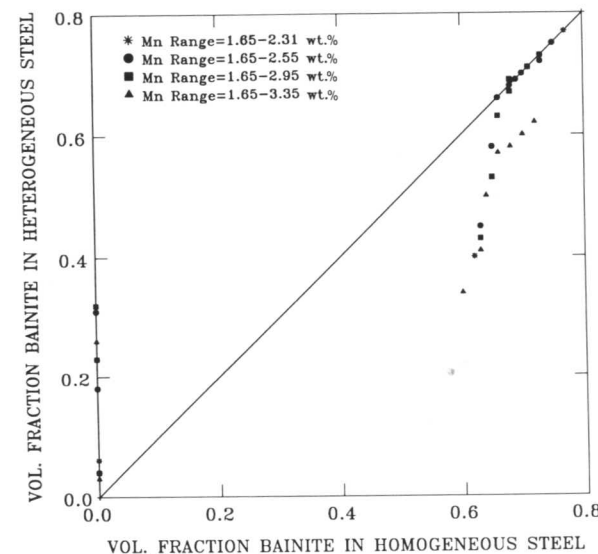
Fig. 8.19: Results from the slice model calculations for as-received and homogenised samples of 'US24' steel. Points in the graph represent the experimental data.

(a) Calculations based on T_0 curve.

(b) Calculations based on T'_0 curve.



a



b

Fig. 8.20: Graphs showing the differences in the volume fraction of bainite in the homogeneous and heterogeneous “US24” steel samples as a function of Mn concentration.

- The average Mn concentration was varied keeping the absolute range same.
- The Mn concentration range was varied keeping the minimum at a constant.

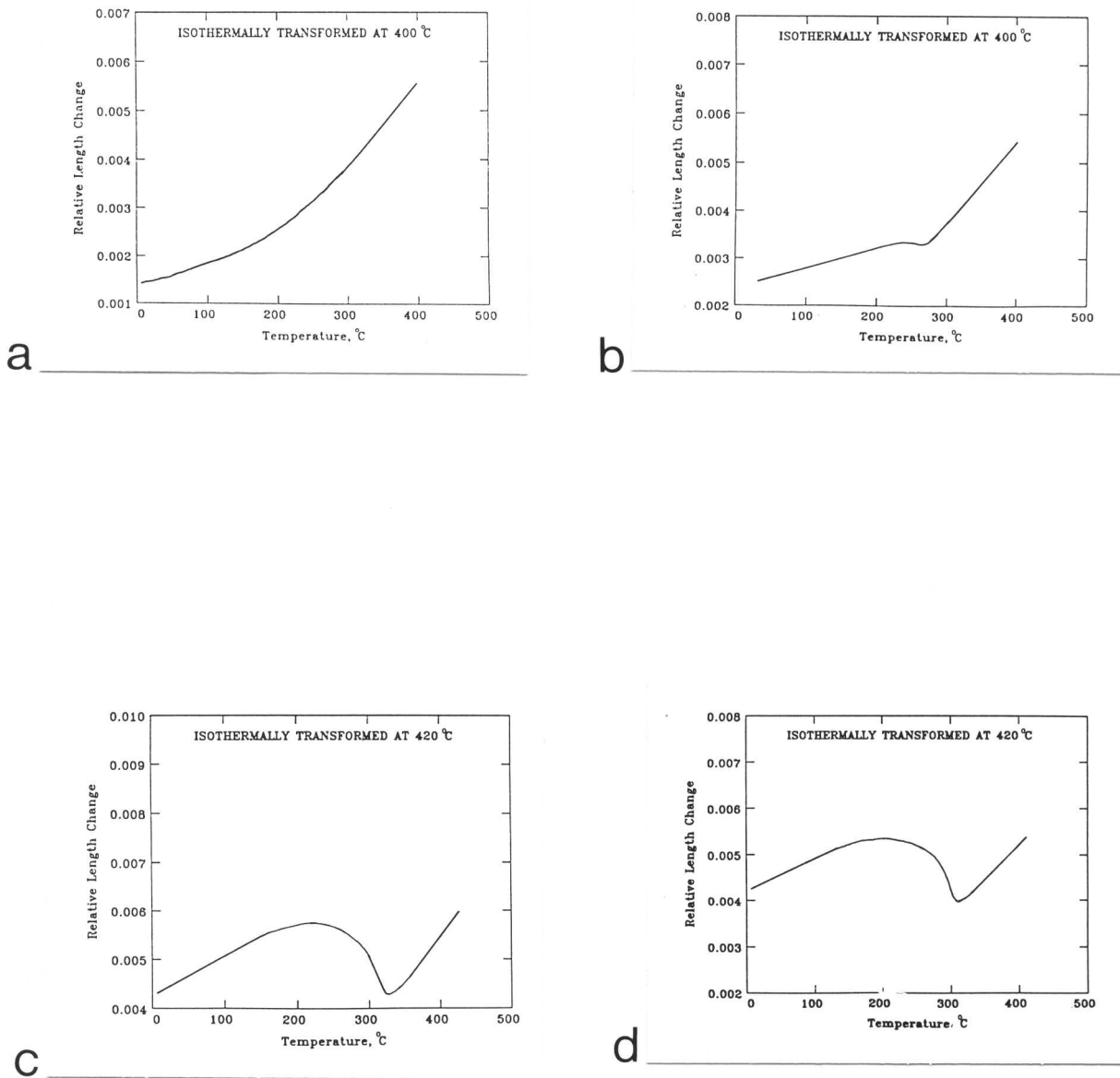
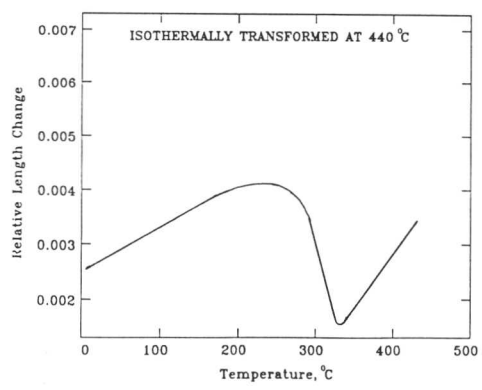
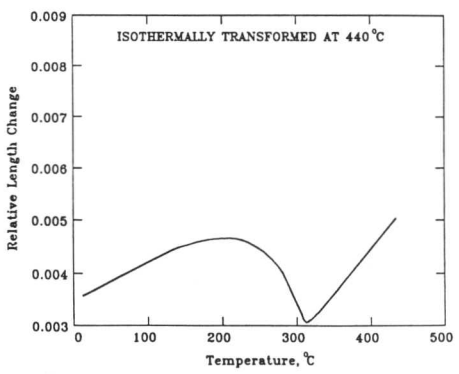


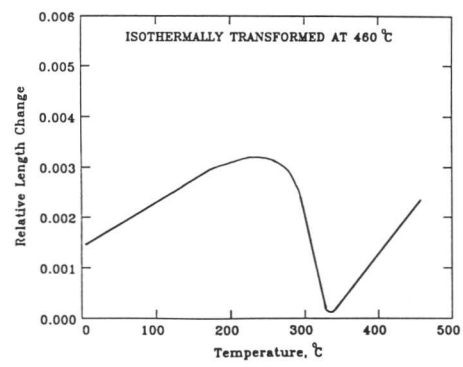
Fig. 8.21: Dilatometric curves showing the transformation to martensite in heterogeneous and homogeneous 'US83' steels, after the specimens were isothermally transformed to bainite at different temperatures, with enough time at each isothermal transformation temperature to ensure that bainitic ferrite formation stopped. Graphs (a), (c), (e), (g) and (i) are for homogeneous samples and (b), (d), (f), (h) and (j) are from heterogeneous samples.



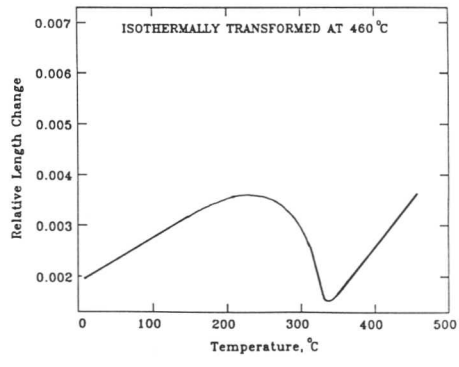
e



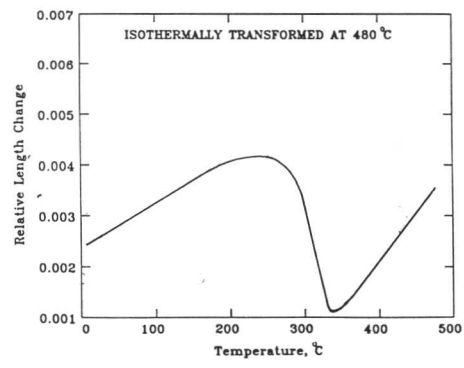
f



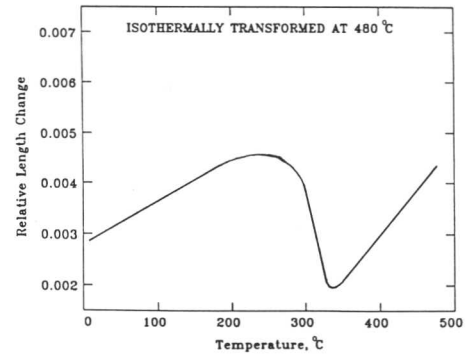
g



h



i



j

Fig. 8.21:(continued)

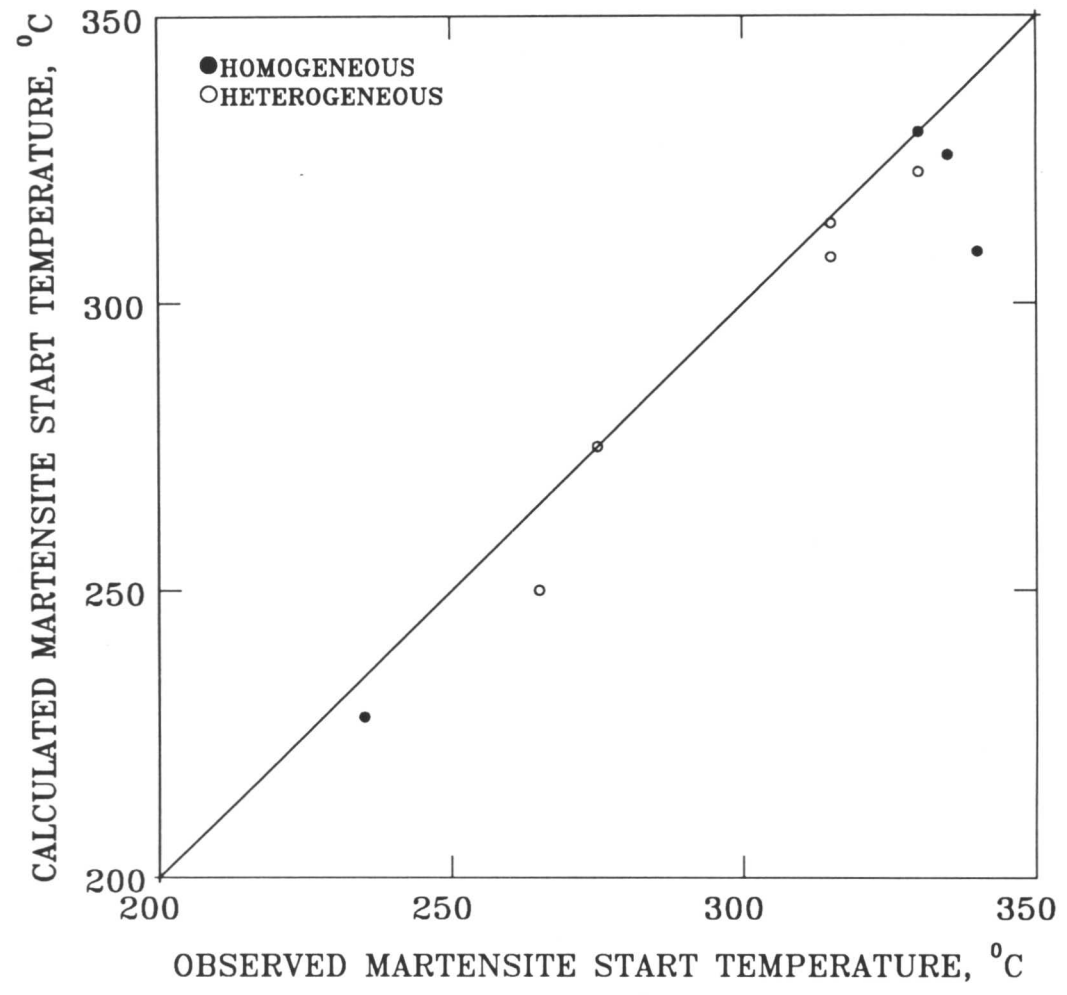


Fig. 8.22: Thermodynamically calculated^[7,8] and experimentally determined M_S temperatures for homogenised and heterogeneous samples, after partial isothermal transformation to bainite.

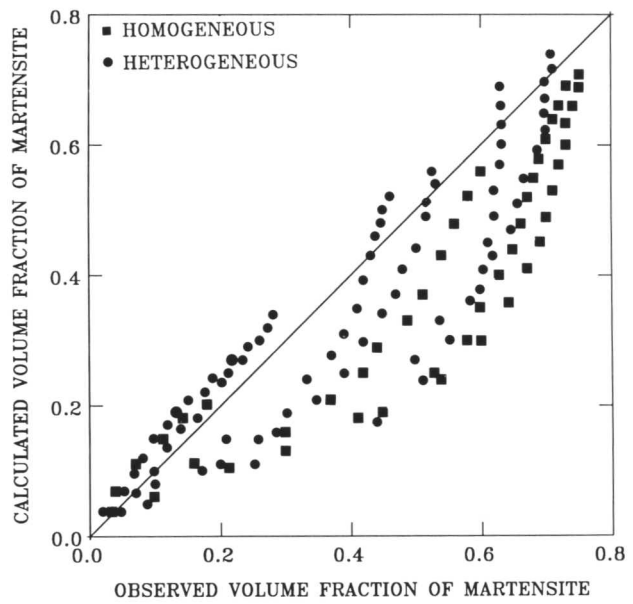


Fig. 8.23: Comparison of the observed and calculated volume fractions of martensite. The calculations utilise the Koistinen and Marburger's equation^[9]. A common value of 0.004 was assigned to C_1 for all these calculations.

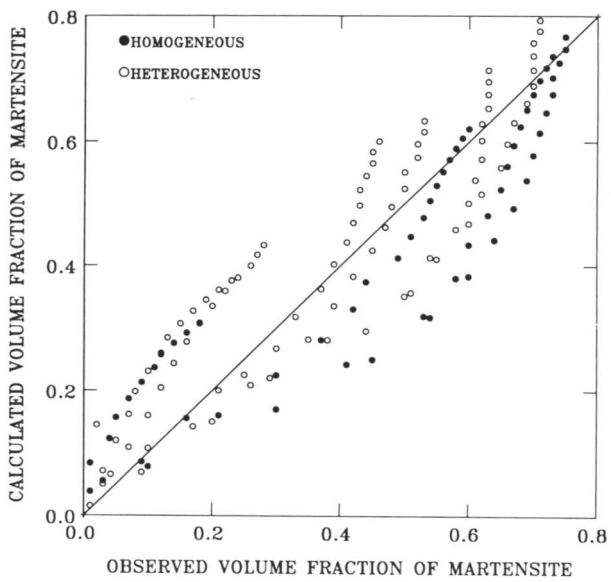
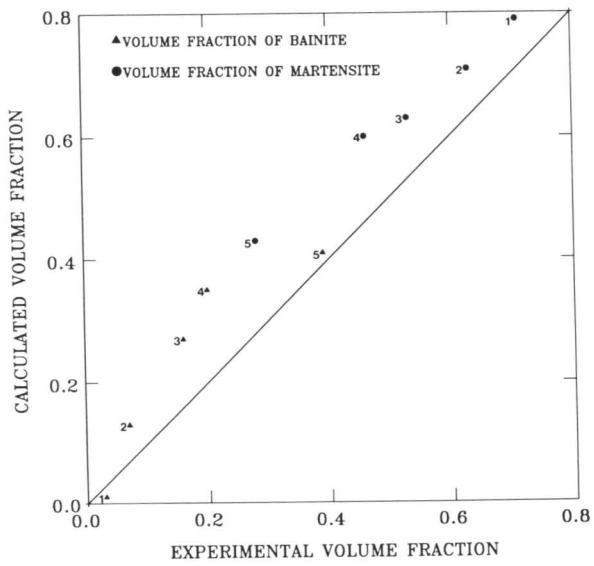
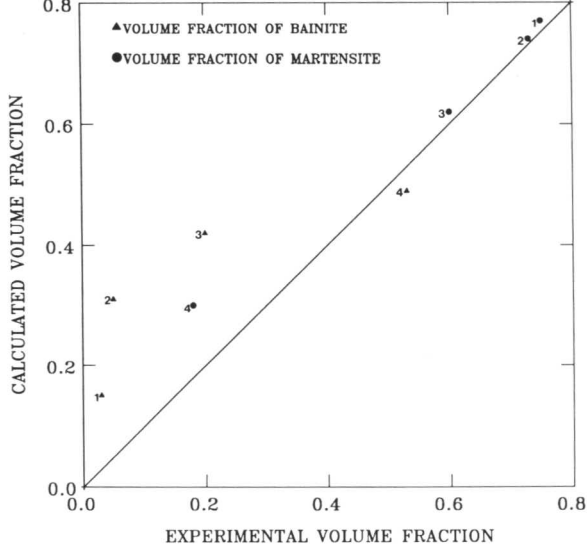


Fig. 8.24: Comparison of experimental results with those calculated by the new model based on equation 8.9.



a



b

Fig. 8.25: Comparison of the calculated and experimental maximum volume fractions of bainite and martensite in the “US83” steel. Data points marked with the same number are from the same heat treatment.

(a) Heterogeneous alloy.

(b) Homogeneous alloy.

REFERENCES

1. B. D. Cullity: *Elements of X-ray Diffraction*, Addison-Wesley, Reading, N.Y., 1956.
2. W. C. Leslie: *The Physical Metallurgy of Steels*, McGraw-Hill Int. Book Company, New York, 1982.
3. H. K. D. H. Bhadeshia and D. V. Edmonds: *Acta Metall.*, 1980, vol. 28, p. 1265.
4. H. K. D. H. Bhadeshia: *Acta Metall.*, 1981, vol. 29, p. 1117.
5. S. A. Khan and H. K. D. H. Bhadeshia: *Metall. Trans. A*, 1990, in press.
6. H. K. D. H. Bhadeshia: *J. De. Physique*, 1982, vol. 43, p. C4-443.
7. H. K. D. H. Bhadeshia: *Metal Science*, 1981, vol. 15, p. 175.
8. H. K. D. H. Bhadeshia: *Metal Science*, 1981, vol. 15, p. 178.
9. P. P. Koistinen and R. E. Marburger: *Acta Met.*, 1959, vol. 7, p. 59.
10. G. B. Olson and M. Cohen: *Ann. Rev. Mater. Sci.*, eds. R. A. Huggins, R. H. Bube and D. A. Vermilyea, Annual Reviews Inc., California, U. S. A., 1981, p. 1.
11. C. H. Shih, B. L. Averbach and M. Cohen: *Trans. AIME*, 1955, vol. 203, p. 183.
12. S. R. Pati and M. Cohen: *Acta Met.*, 1971, vol. 19, p. 1327.
13. H. K. D. H. Bhadeshia: *Metal Science* 1982, vol. 16, p. 159.

Chapter 9

SUMMARY AND FURTHER WORK

9.1 Summary

Phase transformations in different heterogeneous steels have been investigated using thermodynamic analysis and phase transformation theory, backed by experimental confirmation. It is found that the maximum volume fraction of bainite formed at any temperature (except above the B_s of homogeneous alloy) is lower in samples containing chemical segregation when compared with corresponding homogeneous alloy. A model has been developed which explains the results quantitatively, as long as the carbon distribution in the austenite does not homogenise during the course of bainite transformation. That it does not do so has been confirmed, since the M_s temperatures of partially bainitic specimen have been found to be much higher than expected. It has also been shown that if an opportunity is provided for carbon to distribute evenly throughout the residual austenite during the development of the bainitic microstructure, then the extent of transformation is always larger for the heterogeneous samples when compared with the homogenised samples. The later case was found to be more applicable in the formation of allotriomorphic ferrite in a heterogeneous alloy, where due to higher transformation temperatures involved carbon can distribute evenly throughout the residual austenite to facilitate still more transformation.

The major effect of chemical segregation on martensite transformation, in the steel studied, is to extend the range over which the reaction occurs relative to homogenised samples. It was also found that the presence of bainitic ferrite does not significantly alter the way in which the subsequent transformation to martensite occurs. All the data from homogeneous and heterogeneous samples have been rationalised using a new model of athermal martensite kinetics, which includes an effect of autocatalytic nucleation

Reaustenitisation from a mixture of bainite and austenite, in homogeneous and heterogeneous samples has also been studied under isothermal conditions and in circumstances where the nucleation of austenite is not necessary. Dilatometric results can

be explained well by a published theory for reaustenitisation. As initially higher volume fractions of bainite were obtained in the homogeneous alloy its reaustenitisation start temperature will be lower than the heterogeneous alloy. The temperature at which the completion of reaustenitisation occurs, being dependent on average carbon content of the alloy should be the same for homogeneous and heterogeneous alloys.

9.2 Further Work

The present work has been on relatively higher Si content alloys, it will be interesting to study the effect of heterogeneities on the bainite reaction in alloys where carbide precipitation also accompanies ferrite formation. It will be worth checking for any correlation between banding and austenite grain structure. The existing model could be extended to investigate the phase transformations in heterogeneous austempered ductile cast irons which are becoming commercially important in automobile industry. Although this work is a part of a project into prediction of complete microstructure of steel weld deposits, all the experiments were done on wrought alloys. Some weld deposits should be tried and tested for this purpose. A study into a heterogeneous steel with an artificially modulated composition profile can help refine this model.

The model presented for the kinetics of martensitic transformation assumes that all the plates of martensite have identical volume. Moreover, it considers that all nucleation sites have the same activation energy. These approximations require much further research and characterisation.

This work needs to be related quantitatively to the influence of segregation on mechanical properties particularly as some qualitative and quantitative relationships can be found in the literature for homogeneous alloys.

More generally, it would be fascinating to investigate all the problems of heterogeneity using artificially modulated steels, in which not only the modulation wavelength but also its morphology can be controlled. The kinetics need to be developed further to treat the complete evolution of microstructure as a function of time, rather than just the maximum degrees of reaction obtained during isothermal reaction. In this respect, the experimental data accumulated here could be of considerable value in testing any overall transformation kinetics models for heterogeneous steels.

APPENDIX-1

```

C Copyright S. A. Khan and H. K. D. H. Bhadeshia
C University of Cambridge, Department of Materials Science and Metallurgy,
C Pembroke Street, Cambridge CB2 3QZ, U. K.
C
C Program for the analysis of bainitic transformation in heterogeneous, Si
C containing steels. The steel is divided into slices of different compositions,
C the maximum volume fraction of bainite, for a given transformation temperature
C is then computed for each slice; taking care of nucleation (Bs temperature)
C & growth (T0 limit). Slices transform independent of each other and the
C carbon is not allowed to homogenise among the slices. The results averaged
C and compared with a steel of the corresponding average composition.
C This program calculates volume fraction of martensite also, Ms temperatureis
C calculated from the carbon content of residual austenite left after the
C isothermallyformed bainite at any specific temperature in every slice
C individually!!!
C Typical data set follows:
C 673 (temperature in Kelvin)
C 0.43 0.50 0.60 0.70 0.80 0.90 1.00 (Composition of slice 1 in wt.%)
C 0.43 0.60 0.60 0.70 0.80 0.90 1.90 (Composition of slice 2 in wt.%)
C C Si Mn Ni Mo Cr V
C

IMPLICIT REAL*8(A-H,K-Z), INTEGER(I,J)
DOUBLE PRECISION C(8),D(8),XTO(150),XTO400(150)
&,E(8),F(8),MS(150),BS(150),IA(150),XGAMMA(150),VOLF(150)
&,CN(150),SI(150),MN(150),NI(150),MO(150),V(150),FE(150)
&,CR(150),WD(8),VG(150),CD(8),XG(150),VMF(150)
VINCR=0.00005D+00
ISTOP=0
AVEVOL=0.0
XGMS=0.00
C1=0.0
C2=0.0
C3=0.0
C4=0.0
C5=0.0
C6=0.0
C7=0.0
READ(5,*)KELVIN
TISO=KELVIN-273.0
XALPHA=XALPH(KELVIN)
WRITE(6,9)KELVIN,XALPHA,VINCR
DO 1 I=1,200
READ(5,*),END=2)NIL,C(1),C(2),C(3),C(4),C(5),C(6),C(7)
CN(I)=C(1)
S(I)=C(2)
MN(I)=C(3)
NI(I)=C(4)
MO(I)=C(5)
CR(I)=C(6)
V(I)=C(7)
FE(I)=100.0D+0-(C(1)+C(2)+C(3)+C(4)+C(5)+C(6)+C(7))
C1=C1+C(1)
C2=C2+C(2)
C3=C3+C(3)
C4=C4+C(4)
C5=C5+C(5)
C6=C6+C(6)
C7=C7+C(7)
DO 43 IJI=1,7
E(IJI)=C(IJI)
43 CONTINUE
CALL TZERO(C,KELVIN,XTO(I),XTO400(I))
CALL MUC(E,MS,BS(I))
XBAR=C(1)
WRITE(6,10)I,XTO(I),BS(I)
1 CONTINUE

```

```

2 ISLICE=I-1
D(1)=C1/ISLICE
D(2)=C2/ISLICE
D(3)=C3/ISLICE
D(4)=C4/ISLICE
D(5)=C5/ISLICE
D(6)=C6/ISLICE
D(7)=C7/ISLICE
DO 70 JII=1,7
WD(JII)=D(JII)
70 CONTINUE
DO 56 JII=1,7
F(JII)=D(JII)
56 CONTINUE
CALL TZERO(D,KELVIN,XTOH,XTO4H)
CALL MUC(F,MS,BSH)
WRITE(6,75)BSH,XTOH
75 FORMAT(' BSH= ',D10.4,' XTOH= ',D10.4)
IF (BSH .LT. TISO) GOTO 789
GOTO 85
85 IF (XTOH .LE. D(1)) GOTO 789
GOTO 79
79 IF (XTOH .GT. XALPHA) GOTO 987
GOTO 789
789 VOLH=0.00
GOTO 678
987 VOLH=(XTOH-D(1))/(XTOH-XALPHA)
678 VGH=1.0D+0-VOLH
XGM=WD(1)*((VOLH*WD(1))/(1.0D+00-VOLH))
C Getting new composition (wt%) of residual austenite for Ms calculation
RTH=(100.0D+00-XGM)/(100.0D+00-WD(1))
WD(1)=XGM
DO 242 IIN=2,8
WD(IIN)=WD(IIN)*RTH
242 CONTINUE
CALL MUC(WD,MSH,BS)
IF (MSH .GE. 20.0) GOTO 564
GOTO 465
465 VMH=0.00
GOTO 45
564 VMH=(1.0D+00-DEXP(-0.0054D+00*(MSH-20.0D+00)))*VGH
45 WRITE(6,151)VMH
WRITE(6,252)MSH
252 FORMAT(' MSH= ',D10.4)
WRITE(6,15)VOLH
DO 6 I=1,100000
IF(ISTOP .EQ. ISLICE) GOTO 14
DO 4 J=1,ISLICE
IF(IA(J) .EQ. 1) GOTO 4
IF (BS(J) .LT. TISO) GOTO 5329
GOTO 9352
5329 VOLP(J)=0.00
GOTO 5
9352 VOLP(J)=VOLP(J) + VINCR
XGAMMA(J)=XBAR + ((VOLP(J)*(XBAR-XALPHA))/(
&(1.0D+00-VOLP(J))))
IF(XGAMMA(J) .GE. XTO(J)) GOTO 5
GOTO 4
5 IA(J)=1
ISTOP=ISTOP+IA(J)
VOLP(J)=VOLP(J)-VINCR
IF (VOLP(J) .LE. 0.00) GOTO 115
GOTO 4
115 VOLP(J)=0.00
XGAMMA(J)=XBAR
4 CONTINUE
6 CONTINUE
14 DO 12 J=1,ISLICE
VG(J)=1.0D+00-VOLP(J)

```

```

C Recalling the original composition(wt%) for each slice.....
CD(1)=CN(J)
CD(2)=SI(J)
CD(3)=MN(J)
CD(4)=NI(J)
CD(5)=MO(J)
CD(6)=CR(J)
CD(7)=V(J)
XG(J)=CD(1)+((VOLF(J)*CD(1))/(1.0D+00-VOLF(J)))

C Getting new composition (wt%) of residual austenite in each slice
C for Ms calculation...
RT=(100.0D+00-XG(J))/(100.0D+00-CD(1))
CD(1)=XG(J)
DO 262 NIN=2,7
CD(NIN)=CD(NIN)*RT
262  CONTINUE
CALL MUC(CD,MS(J),BS)
IF (MS(J) .GE. 20.0) GOTO 468
GOTO 864
864  VMF(J)=0.00
GOTO 464
468  VMP(J)=(1.0D+00-DEXP(-0.0054D+00*(MS(J)-20.0D+00)))*VG(J)
464  WRITE(6,909)J,MS(J),VMF(J),VOLF(J),XGAMMA(J)
909  FORMAT(' J= ',I3,' MS= ',D10.4,' VMF= ',D12.4,' VOLF= ',D12.4
     &,' XGM= ',D12.4)
XGMS=XGMS+XGAMMA(J)
AVEVOL=AVEVOL+VOLF(J)
VMT=VMT+VMR(J)
AVMS=AVMS+MS(J)
12  CONTINUE
XGMS=XGMS/ISLICE
AVEVOL=AVEVOL/ISLICE
VMT=VMT/ISLICE
AVMS=AVMS/ISLICE
WRITE(6,166)XGMS
166  FORMAT(' Average carbon in residual austenite= ',F8.3)
WRITE(6,13)AVEVOL
WRITE(6,2539)AVMS
WRITE(6,131)VMT
2539  FORMAT(' Average MS temperature= ',F8.3)
131  FORMAT(' Average volume fraction of MARTENSITE',
     &' in heterogeneous alloy =',F8.3)
151  FORMAT(' Maximum volume fraction of MARTENSITE in ',
     &' an alloy of average composition = ',F8.3)
13  FORMAT(' Average volume fraction of transformation',
     &' in heterogeneous alloy =',F8.3)
9   FORMAT(' KELVIN = ',F7.0,' XALPHA, mol. fraction =',D12.4
     &,' VOL INCREMENT=',D12.4)
10  FORMAT(' Slice Number ',I3,' XTO ',D12.4,
     &' BS ',D12.4)
15  FORMAT(' Maximum volume fraction of bainitic ferrite in ',
     &' an alloy of average composition = ',F8.3)
STOP
END
C Subroutine*****MUC*****
SUBROUTINE MUC(C,MS,BS)
DOUBLE PRECISION X,X1,T,R,A,A1,AFE,A1FE,DA1,DA2,DA1FE,H,H1,S,S1
INTEGER T1,I,NO,C100,U,B4,B5,J99,C99,C98,C97
DOUBLE PRECISION D11,FTO,FTO400,XTO400,G9400,SHEART,DIFTT,
D144,A44,AFE44,DA44,DAFE44,DD44,F44,X44,DF441,DT4(40),DDFTO(40),
V13,V14,G9,V10,V11,V12,XTO,DFTO,INCEPT,SLOPE,CORR,
1DEQ,ETEQ,T10,T20,XA,AFEQ,AEQ,ETEQ2,TEQ,
1,J1,D,D1,W,W1,F,TEST,GMAX,ERROR,T4,XEQ,FSON,FPRO
1,C(8),B1,B2,P(7),Y(7),B3,BS,WS,WS1,MS
C100=
DO 24 I=1,C100,1
B5=111
B3=0
C(8)=(100.0-C(1)-C(2)-C(3)-C(4)-C(5)-C(6)-(C7))/55.84

```

```

C(1)=C(1)/12.0115
C(2)=C(2)/28.09
C(3)=C(3)/54.94
C(4)=C(4)/58.71
C(5)=C(5)/95.94
C(6)=C(6)/52.0
C(7)=C(7)/50.94
B1=C(1)+C(2)+C(3)+C(4)+C(5)+C(6)+C(7)+C(8)
DO 107 U=2,7
Y(U)=C(U)/C(8)
107 CONTINUE
DO 106 U=1,7
C(U)=C(U)/B1
106 CONTINUE
B2=0.0
T10=Y(2)*(-.3)+Y(3)*2+Y(4)*12+Y(5)*(-.9)+Y(6)*(-.1)+Y(7)*(-.12)
T20=-3*Y(2)-37.5*Y(3)-6*Y(4)-26*Y(5)-19*Y(6)-44*Y(7)
P(2)=2013.0341+763.8167*C(2)+45802.87*C(2)**2-280061.63*C(2)**3
1+3.864D+06*C(2)**4-2.4233D+07*C(2)**5+6.9547D+07*C(2)**6
P(3)=2012.067-1764.095*C(3)+6287.52*C(3)**2-21647.96*C(3)**3
12.0119D+06*C(3)**4+3.1716D+07*C(3)**5-1.3885D+08*C(3)**6
P(4)=2006.8017+2330.2424*C(4)-54915.32*C(4)**2+1.6216D+06*C(4)**3
1-2.4968D+07*C(4)**4+1.8838D+08*C(4)**5-5.5531D+08*C(4)**6
P(5)=2006.834-2997.314*C(5)-37906.61*C(5)**2+1.0328D+06*C(5)**3
1-1.3306D+07*C(5)**4+8.411D+07*C(5)**5-2.0826D+08*C(5)**6
P(6)=2012.367-9224.2655*C(6)+33657.8*C(6)**2-566827.83*C(6)**3
1+8.5676D+06*C(6)**4-6.7482D+07*C(6)**5 +2.0837D+08*C(6)**6
P(7)=2011.9996-6247.9118*C(7)+5411.7566*C(7)**2
1+250118.1085*C(7)**3-4.1676D+06*C(7)**4
DO 108 U=2,7
B3=B3+P(U)*Y(U)
B2=B2+Y(U)
108 CONTINUE
IF(B2 .EQ. 0.0) GOTO 455
W=(B3/B2)*4.187
GOTO 456
455 W=8054.0
456 FTO=-1.0
X1=C(1)
XA=0.001
R=8.31432
W1=48570.0
H=38575.0
S=13.48
XEQ=0.2
XTO=0.07
XTO400=0.06
X44=0.1
INCEPT=1.0D+00
CORR=1.0D+00
SLOPE=1.0D+00
C98=0
C97=0
WS=0.0
DO 9 T1=473,1173,20
C98=C98+1
J98=0
J99=0
XTO=XTO+0.0001
XTO400=XTO400+0.0001
X44=0.3*XEQ
T=T1
IF (T .LE. 1000) GOTO 20
H1=105525
S1=45.34521
GOTO 19
20 H1=111918
S1=51.44
19 F=ENERGY(T,T10,T20)

```

```

J=1-DEXP(-W/(R*T))
51 DEQ=DSQRT(1-2*(1+2*J)*XEQ+(1+8*J)*XEQ*XEQ)
TEQ=5*DLOG((1-XEQ)/(1-2*XEQ))
TEQ=TEQ+DLOG(((1-2*J+(4*J-1)*XEQ-DEQ)/(2*J*(2*XEQ-1)))**6)
TEQ=TEQ*R*T-F
IF (DABS(TEQ) .LT. 1.0) GOTO 50
ETEQ=5*((1/(XEQ-1))-2/(1-2*XEQ))
ETEQ2=6*((4*J-1-(0.5/DEQ)*(-2-4*J+2*XEQ+16*XEQ*J))/(1-2*J+(4*J
1-1)*XEQ-DEQ))+6*(4*J/(2*J*(2*XEQ-1)))
ETEQ=(ETEQ+ETEQ2)*R*T
XEQ=XEQ-TEQ/ETEQ
GOTO 51
50 AEQ=5*DLOG((1-2*XEQ)/XEQ)+6*W/(R*T)+(H)-(S)*T)/(R*T)
AEQ=AEQ+DLOG(((DEQ-1+3*XEQ)/(DEQ+1-3*XEQ))**6)
AFEQ=5*DLOG((1-XEQ)/(1-2*XEQ))+DLOG(((1-2*J+(4*J-1)*XEQ-DEQ)/(2*J
1*(2*XEQ-1)))**6)
IF (XEQ .LT. X1) GOTO 2443
GOTO 2442
2443 IF(W<=0.0) GOTO 2441
GOTO 2444
2441 WS=T4
GOTO 2444
2442 D=DSQRT(1-2*(1+2*J)*X1+(1+8*J)*X1*X1)
A=6*W/(R*T)+DLOG(((D-1+3*X1)/(D+1-3*X1))**6)

A=A+5*DLOG((1-2*X1)/X1)
A=A+(H-S*T)/(R*T)
AFE=5*DLOG((1-X1)/(1-2*X1))
AFE=AFE+DLOG(((1-2*J+(4*J-1)*X1-D)/(2*J*(2*X1-1)))**6)
FSON=R*T*(XA*(AEQ-A)+(1-XA)*(AFEQ-AFE))
FPRO=R*T*(X1*(AEQ-A)+(1-X1)*(AFEQ-AFE))
V14=3.251745029*(T-273)-2183.014
IF (V14 .GE. 0.0) GOTO 452
IF (FPRO .GE. V14) GOTO 105
103 D44=DSQRT(1-2*(1+2*J)*X44+(1+8*J)*X44*X44)
DD44=(0.5/D44)*(-2-4*J+2*X44+16*J*X44)
A44=5*DLOG((1-2*X44)/X44)+6*W/(R*T)+(H)-(S)*T)/(R*T)
A44=A44+DLOG(((D44-1+3*X44)/(D44+1-3*X44))**6)
AFE44=5*DLOG((1-X44)/(1-2*X44))+DLOG(((1-2*J+(4*J-1)*X44-D44
1)/(2*J*(2*X44-1)))**6)
F44=R*T*(X44*(AEQ-A44)+(1-X44)*(AFEQ-AFE44))
F44=F44-V14
IF (DABS(F44) .GE. 10.0) GOTO 101
GOTO 102
101 DA44=-((10/(1-2*X44))+(5/X44))+6*((DD44+3)/(D44-1+3*X44
1)-(DD44-3)/(D44+1-3*X44))
DAFE44=10*(1-2*X44)-5*(1-X44)+6*((4*J-1-DD44)/(1-2*J+(4*
1J-1)*X44-D44)-2/(2*J*(2*X44-1)))
DF441=R*T*(AEQ-X44*DA44-AFEQ+X44*DAFE44-DAFE44-A44+AFE44)
X44=X44-F44/DF441
GOTO 103
105 X44=0.0
IF (C97 .GT. 0) GOTO 102
C97=1
WS=T4
GOTO 102
452 X44=9999999999.9999
IF(C97 .GT. 2) GOTO 9990
C97=3
WS1=T4
9990 WS=T4
102 FPROA=FPRO*((XEQ-XA)/(XEQ-X1))
X=0.000001
J1=1-DEXP(-W1/(R*T))
7 D1=DSQRT(9-6*X*(2*J1+3)+(9+16*J1)*X*X)
A1=3*DLOG((3-4*X)/X)+(4*W1)/(R*T)

```

```

A1=A1+DLOG(((D1-3+5*X)/(D1+3-5*X))**4)+(H1-S1*T)/(R*T)
A1FE=DLOG(1-X)
TEST=F+R*T*(A1FE-AFE) -R*T*(A1-A)
IF (DABS(TEST) .GT. 10.0) GOTO 5
GOTO 6
5 DA1=(3*X/(3-4*X))*(4*X-3)/(X**2)-4/X
DA2=(0.5*D1)*(-12*J1-18*X+32*J1*X)
DA2=4*((DA2+5)*(D1-3+5*X))-(DA2-5)*(D1+3-5*X))
DA1=DA1+DA2
DA1FE=1/(X-1)
ERROR=TEST/(R*T*(DA1FE-DA1))
IF (ERROR .GT. X) GOTO 30
GOTO 29
30 ERROR =0.3*X
29 X=X-ERROR
GOTO 7
6 GMAX=R*T*(A1-A)
D11=DSQRT(9-6*X1*(2*J1+3)+(9+16*J1)*X1*X1)
T4=T-273
IF (FTO .GE. 0.0) GOTO 22
FTO=FTO1(H,S,X1,T,W,W1,H1,S1,F,J,J1)
GOTO 21
22 FTO =0.0
21 DFTO=FTO1(H,S,XTO,T,W,W1,H1,S1,F,J,J1)
J98=J98+1
IF (DABS(DFTO) .LE. 10.0) GOTO 450
G9=G91(XTO,T,W,W1,H1,S1,F,J,J1)
IF (J98 .GE.9) GOTO 450
XTO=XTO-DFTO/G9
IF (XTO .LE. 0.0001) GOTO 94
GOTO 21
94 XTO=0.0000
450 FTO400=FTO1(H,S,XTO400,T,W,W1,H1,S1,F,J,J1)+400.0
J99=J99+1
IF(J99 .GE. 9) GOTO 92
IF (DABS(FTO400) .LE. 10.0) GOTO 92
G9400=G91(XTO400,T,W,W1,H1,S1,F,J,J1)
XTO400=XTO400-FTO400/G9400
IF (XTO400 .LE. 0.0001) GOTO 451
GOTO 450
451 XTO400=0.0000
92 V11=(XTO-X1)/(XTO-0.0013)
V12=(XEQ-X1)/(XEQ-0.0013)
V13=(X44-X1)/(X44-0.0013)
V11=FFF(V11)
V12=FFF(V12)
V13=FFF(V13)
SHEART=DEXP((0.2432D+06/(8.31432*T))-0.135D+03+20.0*DLOG(T)
1.5*DLOG(DABS(GMAX)))
DIFT=DEXP((0.6031D+06/(8.31432*T))-0.1905D+03+20.0*DLOG(T)
1.4*DLOG(DABS(GMAX)))
IF (X44 .EQ. 0.0) GOTO 453
GOTO 454
453 SHEART=1D+20
454 DDFTO(C98)=FTO
DT4(C98)=T4
9 CONTINUE
2444 C98=C98-1
CALL ANAL(C98,INCEPT,SLOPE,CORR,DT4,DDFTO)
BS=(-400.0-INCEPT)/SLOPE
MS=(-1120.0D+00-10568.0D+00*X1+94.1D+00-INCEPT)/SLOPE
IF (WS LT. BS) GOTO 9996
GOTO 24
9996 BS=WS
24 CONTINUE
RETURN
END
C Subroutine*****TZERO*****
SUBROUTINE TZERO(C,T,XTO,XTO400)

```

```

DOUBLE PRECISION X,X1,T,R,H,H1,S,S1
INTEGER I,U,B4,J99,C98,C97,B5
DOUBLE PRECISION D11,FTO,FTO400,XTO400,G9400,G9,XTO,DFTO,T10,T20,
1JJ1,D,W,W1,F,T4,C(8),B1,B2,P(7),Y(7),B3,WS
B3=0
C(8)=(100.0-C(1)-C(2)-C(3)-C(4)-C(5)-C(6)-(C7))/55.84
C DIVIDING BY ATOMIC WEIGHT.....  

C(1)=C(1)/12.0115
C(2)=C(2)/28.09
C(3)=C(3)/54.94
C(4)=C(4)/58.71
C(5)=C(5)/95.94
C(6)=C(6)/52.0
C(7)=C(7)/50.94
B1=C(1)+C(2)+C(3)+C(4)+C(5)+C(6)+C(7)+C(8)
DO 107 U=2,7
Y(U)=C(U)/C(8)
107 CONTINUE
C CALCULATING MOLE FRACTIONS.....  

DO 106 U=1,7
C(U)=C(U)/B1
106 CONTINUE
B2=0.0
T10=Y(2)*(-3)+Y(3)*2+Y(4)*12+Y(5)*(-9)+Y(6)*(-1)+Y(7)*(-12)
T20=-3*Y(2)-37.5*Y(3)-6*Y(4)-26*Y(5)-19*Y(6)-44*Y(7)
P(2)=2013.0341+763.8167*C(2)+45802.87*C(2)**2-280061.63*C(2)**3
1+3.864D+06*C(2)**4-2.4233D+07*C(2)**5+6.9547D+07*C(2)**6
P(3)=2012.067-1764.095*C(3)+6287.52*C(3)**2-21647.96*C(3)**3
12.0119D+06*C(3)**4+3.1716D+07*C(3)**5-1.3885D+08*C(3)**6
P(4)=2006.8017+2330.2424*C(4)-54915.32*C(4)**2+1.6216D+06*C(4)**3
1-2.4968D+07*C(4)**4+1.8838D+08*C(4)**5-5.5531D+08*C(4)**6
P(5)=2006.834-2997.314*C(5)-37906.61*C(5)**2+1.0328D+06*C(5)**3
1-1.3306D+07*C(5)**4+8.411D+07*C(5)**5-2.0826D+08*C(5)**6
P(6)=2012.367-9224.2655*C(6)+33657.8*C(6)**2-566827.83*C(6)**3
1+8.5676D+06*C(6)**4-6.7482D+07*C(6)**5+2.0837D+08*C(6)**6
P(7)=2011.9996-6247.9118*C(7)+5411.7566*C(7)**2
1+250118.1085*C(7)**3-4.1676D+06*C(7)**4
DO 108 U=2,7
B3=B3+P(U)*Y(U)
B2=B2+Y(U)
108 CONTINUE
IF(B2 .EQ. 0.0) GOTO 455
W=(B3/B2)*4.187
455 W=8054.0
FTO=-1.0
X1=C(1)
R=8.31432
W1=48570.0
C ENTHALPY OF CARBON IN AUSTENITE.....  

H=38575.0
C ENTROPY OF CARBON IN AUSTENITE.....  

S=13.48
XTO=0.04
XTO400=0.03
C98=0
C97=0
WS=0.0
J98=0
J99=0
IF (T .LE. 1000) GOTO 20
H1=105525
S1=45.34521
GOTO 19
20 H1=111918
S1=51.44
C Calling subroutine ENERGY———  

C DG FOR ALPHA—>GAMMA FOR PURE IRON.....  

C T10 & T20 ARE THE MAGNETIC & MAGN. EFFECTS OF ALLOY ADDITIONS ON
C DG FOR ALPHA—>GAMMA FOR PURE IRON (ZENER)

```

```

19 F=ENERGY(T,T10,T20)
C SITE EXCLUSION PARAMETER.....  

J=1-DEXP(-W/(R*T))
J1=1.0-DEXP(-W1/(R*T))
T4=T-273
C Calling subroutine FTO1-----  

FTO=FTO1(H,S,X1,T,W,W1,H1,S1,F,J,J1)
C Calling subroutine FTO1-----  

21 DFTO=FTO1(H,S,XTO,T,W,W1,H1,S1,F,J,J1)
J98=J98+1
IF (DABS(DFTO) .LE. 10.0) GOTO 450
C Calling subroutine G91-----  

G9=G91(XTO,T,W,W1,H1,S1,F,J,J1)
IF (J98 .GE.9) GOTO 450
XTO=XTO-DFTO/G9
IF (XTO .LE. 0.0001) GOTO 94
GOTO 21
94 XTO=0.0000
C Calling subroutine FTO1-----  

450 FTO400=FTO1(H,S,XTO400,T,W,W1,H1,S1,F,J,J1)+400.0
J99=J99+1
IF(J99 .GE. 10) GOTO 92
IF (DABS(FTO400) .LE. 10.0) GOTO 92
C Calling subroutine G91-----  

G9400=G91(XTO400,T,W,W1,H1,S1,F,J,J1)
XTO400=XTO400-FTO400/G9400
IF (XTO400 .LE. 0.0001) GOTO 451
GOTO 450
451 XTO400=0.0000
92 CONTINUE
RETURN
END
C Subroutine*****FTO1*****  

DOUBLE PRECISION FUNCTION FTO1(H,S,X,T,W,W1,H1,S1,F,J,J1)
DOUBLE PRECISION R,X,T,T60,ZEN1,ZEN2,ZENER,W,W1,H1,S1,F,
IJ1,D,D11,H,S
D=DSQRT(1-2*(1+2*J)*X+(1+8*J)*X*X)
D11=DSQRT(9-6*X*(2*J1+3)+(9+16*J1)*X*X)
T60=T*(1-X)/(28080*X)
IF (T60 .GT. 1.0) GOTO 18
IF (T60 .GT. 0.25) GOTO 17
C ZENER ORDERING.....  

ZEN1=0.2307+42.7974*T60-233.8631*T60*T60+645.4485*T60*T60*T60
1.954.3995*(T60**4)+711.8095*(T60**5)-211.5136*(T60**6)
ZEN2=-2.6702+45.6337*T60-225.3965*T60*T60+567.7112*(T60**3)
1.771.6466*(T60**4)+538.1778*(T60**5)-151.3818*(T60**6)
GOTO 16
17 ZEN2=1
ZEN1=3.295
16 ZENER=((ZEN2*X)**2)*(-50898.56)/(1-X)+ZEN1*T*X*0.6623741
ZENER=ZENER*4.187
GOTO 15
18 ZENER=0.0
15 R=-8.31432
FTO1=X*R*T*DLOG(X*X)+X*(H1-(H)-(S1-(S)
1)*T+4*W1-6*W)-R*T*(1-X)*DLOG((1-X)**4)+5*R*T*(1-2*X)*DLOG(1-2*X)
1-R*T*X*DLOG(((D-1+3*X)/(D+1-3*X))**6)-R*T*(1-X)*DLOG(((1-2*J+(4
1*J-1)*X-D)/(2*J*(2*X-1)))**6)+3*R*T*X*DLOG(3-4*X)+R*T*
1*X*DLOG(((D11-3+5*X)/(D11+3-5*X))**4)+(1-X)*F+ZENER
RETURN
END
C Subroutine*****G91*****  

DOUBLE PRECISION FUNCTION G91(XTO,T,W,W1,H1,S1,F,J,J1)
DOUBLE PRECISION R,XTO,T,W,W1,H1,S1,F,J,J1,FD,FD1,DT5,
1DT6,DZEN1,DZEN2,DZEN3,V1,V2,V3,V4,V5,V6,V7,V8,V9,G1,
1DZEN6,DZEN7,DZEN8
R=8.31432
FD=DSQRT(1-2*(1+2*J)*XTO+(1+8*J)*XTO*XTO)
FD1=DSQRT(9-6*XTO*(2*J1+3)+(9+16*J1)*XTO*XTO)

```

```

DT5=28080*XTO/(1-XTO)
DT6=T/DT5
IF (DT6 .GT. 1.0) GOTO 48
IF (DT6 .LT. 0.25) GOTO 47
DZEN1=0.2307+42.7974*DT6-233.8631*(DT6**2)+645.4485*(DT6**3)
1-954.3995*(DT6**4)+711.8095*(DT6**5)-211.5136*(DT6**6)
DZEN2=-2.6702+45.6337*DT6-225.3965*(DT6**2)+567.7112*(DT6**3)
1-771.6466*(DT6**4)+538.1778*(DT6**5)-151.3818*(DT6**6)
GOTO 46
47 DZEN2=1
DZEN1=3.295
46 DZEN3=((DZEN2*XTO)**2)*(-50898.56)/(1-XTO))+DZEN1*T*XTO*
1(0.6623741)
DZEN3=DZEN3*4.187
GOTO 45
48 DZEN3=0.0
45 V1=FD-1+3*XTO
V2=FD+1-3*XTO
V3=1-2*J+(4*J-1)*XTO-FD
V4=2*J*(2*XTO-1)
V5=FD1-3+5*XTO
V6=FD1+3-5*XTO
V7=(XTO-1-2*J+8*XTO*J)/FD
V8=(9*XTO-9-6*J1+16*J1*XTO)/FD1
V9=H1-(H)-(S1-(S))*T-6*W+4*W1
G1=2+DLOG(XTO**2)+4+DLOG((1-XTO)**4)-10-DLOG((1-2*XTO)**10)
1-DLOG((V1/V2)**6)-6*((XTO/V1)*(V7+3+V1*(3-V7)/V2))
1+DLOG((V3/V4)**6)-6*((1-XTO)/V3)*(4*J*(1-(V3/V4))-V7)
1+3*(DLOG(3-4*XTO)-4*XTO/(3-4*XTO))+DLOG((V5/V6)**4)+4*(XTO
1/V5)*(V8+5+(V5/V6)*(5-V8))
IF (DT6 .GT. 1.0) GOTO 90
DZEN6=(-3.3948+13.6112*DT6-13.4376*(DT6**2))*T/(28080*
1((1-XTO)**2))
DZEN7=(-3.3118+15.7462*DT6-23.2449*(DT6**2))*T/(28080*
1((1-XTO)**2))
DZEN8=50898*((DZEN2*XTO)**2)*((1-XTO)**2)+(-50898*(2*
1*DZEN2*DZEN6*(XTO**2)+2*XTO*(DZEN2**2))/(1-XTO))+DZEN1
1*T*0.6623741+DZEN7*T*XTO*0.6623741
GOTO 91
90 DZEN8=0.0
91 G91=V9+R*T*G1+DZEN8-F
RETURN
END
C Subroutine*****FFF*****
DOUBLE PRECISION FUNCTION FFF(V)
DOUBLE PRECISION V
IF (V .LE. 0.0) GOTO 1
IF (V .GT. 1.0) GOTO 1
2 GOTO 3
1 FFF=0.0
GOTO 4
3 FFF=V
4 RETURN
END
C Subroutine*****ENERGY*****
DOUBLE PRECISION FUNCTION ENERGY(T,T10,T20)
DOUBLE PRECISION T,T10,T20,F,T7
T7=T-100*T20
IF (T7 .LT. 300) GOTO 1
IF (T7 .LT. 700) GOTO 2
IF (T7 .LT. 940) GOTO 3
F=-8.88909+0.26557*(T7-1140)-1.04923D-3*((T7-1140)**2)
F=F+2.70013D-6*((T7-1140)**3)-3.58434D-9*((T7-1140)**4)
GOTO 4
1 F=1.38*T7-1499
GOTO 4
2 F=1.65786*T7-1581
GOTO 4
3 F=1.30089*T7-1331

```

```

4   ENERGY=(141*T10 + F)*4.187
RETURN
END
DOUBLE PRECISION FUNCTION XALPH(T)
DOUBLE PRECISION T,CTEMP
CTEMP=(T-273.0D+00)900.0D+00
XALPH=0.1528D-02-0.8816D-02*CTEMP+0.2450D-01*CTEMP*CTEMP
&-0.2417D-01 *CTEMP*CTEMP*CTEMP+
&0.6966D-02*CTEMP*CTEMP*CTEMP*CTEMP
RETURN
END
SUBROUTINE ANAL(C98,INCEPT,SLOPE,CORR,X,Y)
DOUBLE PRECISION AX,AX2,AY,AY2,AXY,INCEPT,CORR,SLOPE,
&X(40),Y(40)
INTEGER I,C98,I1
I1=C98
C98=C98-10
AX=0.0D+00
AY=0.0D+00
AX2=0.0D+00
AY2=0.0D+00
AXY=0.0D+00
DO 1 I=1,C98
AX=AX+X(I)
AY=AY+Y(I)
AXY=AXY+X(I)*Y(I)
AX2=AX2+X(I)*X(I)
AY2=AY2+Y(I)*Y(I)
1 CONTINUE
INCEPT=(AY*AX2-AX*AXY)/(C98*AX2-AX*AX)
SLOPE=((C98*AXY-AX*AY)/(C98*AX2-AX*AX))
CORR=(C98*AXY-AX*AY)/(DSQRT((C98*AX2-AX*AX)*
&(C98*AY2-AY*AY)))
C98=I1
RETURN
END

```

```

C Copyright S. A. Khan and H. K. D. H. Bhadeshia
C University of Cambridge, Department of Materials Science and Metallurgy,
C Pembroke Street, Cambridge CB2 3QZ, U. K.
C
C Program for the analysis of bainitic transformation in heterogeneous, Si
C containing steels. The steel is divided into slices of different compositions,
C the maximum volume fraction of bainite, for a given transformation temperature
C is then computed for each slice; taking care of nucleation (Bs temperature)
C & growth (T0 limit). The carbon is allowed to redistribute among the slices
C after each increment of transformation.
C The results averaged and compared with a steel of the corresponding average
C composition.
C
C Typical data set follows:
C 673 (temperature in Kelvin)
C 0.43 0.50 0.60 0.70 0.80 0.90 1.00 (Composition of slice 1 in wt.%)
C 0.43 0.60 0.60 0.70 0.80 0.90 1.90 (Composition of slice 2 in wt.%)
C C Si Mn Ni Mo Cr V
C
IMPLICIT REAL*8(A-H,K-Z), INTEGER(I,J)
DOUBLE PRECISION C(8),D(8),XTO(100),XTO400(100)
&,E(8),F(8),MS(100),BS(100),IA(100),XGAMMA(100),VOLF(100)
&,CN(100),SI(100),MN(100),NI(100),MO(100),V(100),FE(100)
&,CR(100),WD(8),VG(100),CD(8),XG(100),VMF(100)
VINCR=0.00005D+00
ISTOP=0
AVEVOL=0.0
C1=0.0
C2=0.0
C3=0.0
C4=0.0
C5=0.0
C6=0.0
C7=0.0
READ(5,*)KELVIN
TISO=KELVIN-273.0
XALPHA=XALPH(KELVIN)
WRITE(6,4444)
4444 FORMAT(' YOU ARE ALLOWING CARBON TO HOMOGENIZE!!! ')
WRITE(6,9)KELVIN,XALPHA,VINCR
DO 1 I=1,100
READ(5,*,END=2)C(1),C(2),C(3),C(4),C(5),C(6),C(7)
CN(I)=C(1)
SK(I)=C(2)
MN(I)=C(3)
NI(I)=C(4)
MO(I)=C(5)
CR(I)=C(6)
V(I)=C(7)
FE(I)=100.0D+0-(C(1)+C(2)+C(3)+C(4)+C(5)+C(6)+C(7))
C1=C1+C(1)
C2=C2+C(2)
C3=C3+C(3)
C4=C4+C(4)
C5=C5+C(5)
C6=C6+C(6)
C7=C7+C(7)
DO 43 JI=1,7
E(JI)=C(JI)
43 CONTINUE
CALL TZERO(C,KELVIN,XTO(I),XTO400(I))
CALL MUC(E,MS,BS(I))
XBAR=C(1)
WRITE(6,10)I,XTO(I),BS(I)
1 CONTINUE
2 ISLICE=I-1
D(1)=C1/ISLICE

```

```

D(2)=C2/ISLICE
D(3)=C3/ISLICE
D(4)=C4/ISLICE
D(5)=C5/ISLICE
D(6)=C6/ISLICE
D(7)=C7/ISLICE
DO 70 JII=1,7
WD(JII)=D(JII)
70  CONTINUE
DO 56 JII=1,7
F(JII)=D(JII)
56  CONTINUE
CALL TZERO(D,KELVIN,XTOH,XTO4H)
CALL MUC(F,MS,BSH)
WRITE(6,75)BSH,XTOH
75  FORMAT(' BSH= ',D10.4,' XTOH= ',D10.4)
IF (BSH .LT. TISO) GOTO 789
GOTO 85
85  IF (XTOH .LE. D(1)) GOTO 789
GOTO 79
79  IF (XTOH .GT. XALPHA) GOTO 987
GOTO 789
789 VOLH=0.00
GOTO 678
987 VOLH=(XTOH-D(1))/(XTOH-XALPHA)
678 VGH=1.0D+0-VOLH
DO 101 III=1,ISLICE
XGAMMA(III)=D(1)
VOLF(III)=0.0
IA(III)=0
101 CONTINUE
AVEX=D(1)
WRITE(6,15)VOLH
DO 6 I=1,100000
IF(ISTOP .EQ. ISLICE) GOTO 14
DO 4 J=1,ISLICE
IF(IA(J) .EQ. 1) GOTO 4
IF (BS(J) .LT. TISO) GOTO 5329
GOTO 9352
5329 VOLF(J)=0.00
GOTO 5
9352 VOLF(J)=VOLF(J) + VINCR
XGAMMA(J)=AVEX
IF(XGAMMA(J) .GE. XTO(J)) GOTO 5
GOTO 4
5  IA(J)=1
ISTOP=ISTOP+IA(J)
VOLF(J)=VOLF(J)-VINCR
IF (VOLF(J) .LE. 0.00) GOTO 115
GOTO 4
115 VOLF(J)=0.00
XGAMMA(J)=AVEX
4  CONTINUE
AVEVOL=0.0D+00
DO 90 J33=1,ISLICE
AVEVOL=AVEVOL+VOLF(J33)
90  CONTINUE
AVEVOL=AVEVOL/ISLICE
AVEX=D(1)+(AVEVOL*(D(1)-XALPHA))/(1.0D+00-AVEVOL)
6  CONTINUE
14 AVEVOL=0.0
DO 12 J=1,ISLICE
AVEVOL=AVEVOL+VOLF(J)
12  CONTINUE
XGMS=XGMS/ISLICE
AVEVOL=AVEVOL/ISLICE
WRITE(6,166)XGMS
166 FORMAT(' Average carbon in residual austenite= ',F8.3)
WRITE(6,13)AVEVOL

```

```

13  FORMAT(' Average volume fraction of transformation',
&' in heterogeneous alloy =',F8.3)
9   FORMAT(' KELVIN = ',F7.0,' XALPHA, mol. fraction =',D12.4
&,' VOL INCREMENT=',D12.4)
10  FORMAT(' Slice Number ',I3,' XTO ',D12.4,
&' BS ',D12.4)
15  FORMAT(' Maximum volume fraction of bainitic ferrite in ',
&' an alloy of average composition = ',F8.3)
      STOP
      END
C   Subroutine*****MUC*****
      SUBROUTINE MUC(C,MS,BS)
      DOUBLE PRECISION X,X1,T,R,A,A1,AFE,A1FE,DA1,DA2,DA1FE,H,H1,S,S1
      INTEGER T1,I,NO,C100,U,B4,B5,J99,C99,C98,C97
      DOUBLE PRECISION D11,FTO,FTO400,XTO400,G9400,SHEART,DIFTT,
      1D44,A44,AFE44,DA44,DAFE44,DD44,F44,X44,D441,DT4(40),DDFTO(40),
      1V13,V14,G9,V10,V11,V12,XTO,DFTO,INCEPT,SLOPE,CORR,
      1DEQ,ETEQ,T10,T20,XA,AFEQ,AEQ,ETEQ2,TEQ,
      1J,J1,D,D1,W,W1,F,TEST,GMAX,ERROR,T4,XEQ,FSON,FPRO
      1,C(8),B1,B2,P(7),Y(7),B3,BS,WS,WS1,MS
      C100=1
      DO 24 I=1,C100,1
      B5=111
      B3=0
      C(8)=(100.0-C(1)-C(2)-C(3)-C(4)-C(5)-C(6)-(C7))/55.84
      C(1)=C(1)/12.0115
      C(2)=C(2)/28.09
      C(3)=C(3)/54.94
      C(4)=C(4)/58.71
      C(5)=C(5)/95.94
      C(6)=C(6)/52.0
      C(7)=C(7)/50.94
      B1=C(1)+C(2)+C(3)+C(4)+C(5)+C(6)+C(7)+C(8)
      DO 107 U=2,7
      Y(U)=C(U)/C(8)
107  CONTINUE
      DO 106 U=1,7
      C(U)=C(U)/B1
106  CONTINUE
      B2=0.0
      T10=Y(2)*(-3)+Y(3)*2+Y(4)*12+Y(5)*(-9)+Y(6)*(-1)+Y(7)*(-12)
      T20=-3*Y(2)-37.5*Y(3)-6*Y(4)-26*Y(5)-19*Y(6)-44*Y(7)
      P(2)=2013.0341+763.8167*C(2)+45802.87*C(2)**2-280061.63*C(2)**3
      1+3.864D+06*C(2)**4-2.4233D+07*C(2)**5+6.9547D+07*C(2)**6
      P(3)=2012.067-1764.095*C(3)+6287.52*C(3)**2-21647.96*C(3)**3-
      12.0119D+06*C(3)**4+3.1716D+07*C(3)**5-1.3885D+08*C(3)**6
      P(4)=2006.8017+2330.2424*C(4)-54915.32*C(4)**2+1.6216D+06*C(4)**3
      1-2.4968D+07*C(4)**4+1.8838D+08*C(4)**5-5.5531D+08*C(4)**6
      P(5)=2006.834-2997.314*C(5)-37906.61*C(5)**2+1.0328D+06*C(5)**3
      1-1.3306D+07*C(5)**4+8.411D+07*C(5)**5-2.0826D+08*C(5)**6
      P(6)=2012.367-9224.2655*C(6)+33657.8*C(6)**2-566827.83*C(6)**3
      1+8.5676D+06*C(6)**4-6.7482D+07*C(6)**5+2.0837D+08*C(6)**6
      P(7)=2011.9996-6247.9118*C(7)+5411.7566*C(7)**2
      1+250118.1085*C(7)**3-4.1676D+06*C(7)**4
      DO 108 U=2,7
      B3=B3+P(U)*Y(U)
      B2=B2+Y(U)
108  CONTINUE
      IF(B2.EQ. 0.0) GOTO 455
      W=(B3/B2)*4.187
      GOTO 456
455  W=8054.0
456  FTO=1.0
      X1=C(1)
      XA=0.001
      R=8.31432
      W1=48570.0
      H=38575.0
      S=13.48

```

```

      XEQ=0.2
      XTO=0.07
      XTO400=0.06
      X44=0.1
      INCEPT=1.0D+00
      CORR=1.0D+00
      SLOPE=1.0D+00
      C98=0
      C97=0
      WS=0.0
      DO 9 T1=473,1173,20
      C98=C98+1
      J98=0
      J99=0
      XTO=XTO+0.0001
      XTO400=XTO400+0.0001
      X44=0.3*XEQ
      T=T1
      IF (T .LE. 1000) GOTO 20
      H1=105525
      S1=45.34521
      GOTO 19
20   H1=111918
      S1=51.44
19   F=ENERGY(T,T10,T20)
      J=1-DEXP(-W/(R*T))
51   DEQ=DSQRT(1-2*(1+2*J)*XEQ+(1+8*J)*XEQ*XEQ)
      TEQ=5*DLOG((1-XEQ)/(1-2*XEQ))
      TEQ=TEQ+DLOG(((1-2*J+(4*J-1)*XEQ-DEQ)/(2*J*(2*XEQ-1)))**6)
      TEQ=TEQ*R*T-F
      IF (DABS(TEQ) .LT. 1.0) GOTO 50
      ETEQ=5*((1/(XEQ-1))+2/(1-2*XEQ))
      ETEQ2=6*(4*J-1-(5/DEQ)*(-2-4*J+2*XEQ+16*XEQ*J))/(1-2*J+(4*J
      -1)*XEQ-DEQ))+6*(4*J/(2*J*(2*XEQ-1)))
      ETEQ=(ETEQ+ETEQ2)*R*T
      XEQ=XEQ-TEQ/ETEQ
      GOTO 51
50   AEQ=5*DLOG((1-2*XEQ)/XEQ)+6*W/(R*T)+(H)-(1
      S)*T)/(R*T)
      AEQ=AEQ+DLOG(((DEQ-1+3*XEQ)/(DEQ+1-3*XEQ))**6)
      AFEQ=5*DLOG((1-XEQ)/(1-2*XEQ))+DLOG(((1-2*J+(4*J-1)*XEQ-DEQ)/(2*J
      -1)*(2*XEQ-1)))**6)
      IF (XEQ .LT. X1) GOTO 2443
      GOTO 2442
2443  IF(WS .EQ. 0.0) GOTO 2441
      GOTO 2444
2441  WS=T
      GOTO 2444
2442  D=DSQRT(1-2*(1+2*J)*X1+(1+8*J)*X1*X1)
      A=6*W/(R*T)+DLOG((D-1+3*X1)/(D+1-3*X1))**6)
      A=A+5*DLOG((1-2*X1)/X1)
      A=A+(H-S*T)/(R*T)
      AFE=5*DLOG((1-X1)/(1-2*X1))
      AFE=AFE+DLOG(((1-2*J+(4*J-1)*X1-D)/(2*J*(2*X1-1)))**6)
      FSQN=R*T*(XA*(AEQ-A)+(1-XA)*(AFEQ-AFE))
      FPRO=R*T*(X1*(AEQ-A)+(1-X1)*(AFEQ-AFE))
      V14=3.251745029*(T-273)-2183.014
      IF (V14 .GE. 0.0) GOTO 452
      IF (FPRO .GE. V14) GOTO 105
103  D44=DSQRT(1-2*(1+2*J)*X44+(1+8*J)*X44*X44)
      DD44=(0.5/D44)*(-2-4*J+2*X44+16*J*X44)
      A44=5*DLOG((1-2*X44)/X44)+6*W/(R*T)+(H)-(1
      S)*T)/(R*T)
      A44=A44+DLOG(((D44-1+3*X44)/(D44+1-3*X44))**6)
      AFE44=5*DLOG((1-X44)/(1-2*X44))+DLOG(((1-2*J+(4*J-1)*X44-D44
      1)*(2*J*(2*X44-1)))**6)
      F44=R*T*(X44*(AEQ-A44)+(1-X44)*(AFEQ-AFE44))

```

```

F44=F44-V14
IF (DABS(F44) .GE. 10.0) GOTO 101
GOTO 102
101 DA44=-((10/(1-2*X44))+(5/X44))+6*((DD44+3)/(D44-1+3*X44
1)-(DD44-3)/(D44+1-3*X44))
DAFE44=10/(1-2*X44)-5/(1-X44)+6*((4*J-1-DD44)/(1-2*J+(4*
1-J)*X44-D44)-2*(2*J*(2*X44-1)))
DF441=R*T*(AEQ-X44*DA44-AFEQ+X44*DAFE44-DAFE44-A44+AFE44)
X44=X44-F44/DF441
GOTO 103
103 X44=0.0
IF (C97 .GT. 0) GOTO 102
C97=1
WS=T4
GOTO 102
452 X44=9999999999.9999
IF(C97 .GT. 2) GOTO 9990
C97=3
WS1=T4
9990 WS=T4
102 FPROA=FPRO*((XEQ-XA)/(XEQ-X1))
X=0.000001
J1=1-DEXP(-W1/(R*T))
7 D1=DSQRT(9-6*X*(2*J1+3)+(9+16*J1)*X*X)
A1=3*DLOG((3-4*X)/X)+(4*W1)/(R*T)
A1=A1+DLOG(((D1-3+5*X)/(D1+3-5*X))**4)+(H1-S1*T)/(R*T)
A1FE=DLOG(1-X)
TEST=F+R*T*(A1FE-AFE) -R*T*(A1-A)
IF (DABS(TEST) .GT. 10.0) GOTO 5
GOTO 6
5 DA1=(3*X/(3-4*X))*((4*X-3)/(X**2)-4/X)
DA2=(-5/D1)*(-12*J1-18+18*X+32*J1*X)
DA2=4*((DA2+5)/(D1-3+5*X))-((DA2-5)/(D1+3-5*X))
DA1=DA1+DA2
DA1FE=1/(X-1)
ERROR=TEST/(R*T*(DA1FE-DA1))
IF (ERROR .GT. X) GOTO 30
GOTO 29
30 ERROR =0.3*X
29 X=X-ERROR
GOTO 7
6 GMAX=R*T*(A1-A)
D11=DSQRT(9-6*X1*(2*J1+3)+(9+16*J1)*X1*X1)
T4=T-273
IF (FTO .GE. 0.0) GOTO 22
FTO=FTO1(H,S,X1,T,W,W1,H1,S1,F,J,J1)
GOTO 21
22 FTO =0.0
21 DFTO=FTO1(H,S,XTO,T,W,W1,H1,S1,F,J,J1)
J98=J98+1
IF (DABS(DFTO) .LE. 10.0) GOTO 450
G9=G91(XTO,T,W,W1,H1,S1,F,J,J1)
IF (J98 .GE.9) GOTO 450
XTO=XTO-DFTO/G9
IF (XTO .LE. 0.0001) GOTO 94
GOTO 21
94 XTO=0.0000
450 FTO400=FTO1(H,S,XTO400,T,W,W1,H1,S1,F,J,J1)+400.0
J99=J99+1
IF(J99 .GE. 9) GOTO 92
IF (DABS(FTO400) .LE. 10.0) GOTO 92
G9400=G91(XTO400,T,W,W1,H1,S1,F,J,J1)
XTO400=XTO400-FTO400/G9400
IF (XTO400 .LE. 0.0001) GOTO 451
GOTO 450
451 XTO400=0.0000
92 V11=(XTO-X1)/(XTO-0.0013)
V12=(XEQ-X1)/(XEQ-0.0013)
V13=(X44-X1)/(X44-0.0013)

```

```

V11=FFF(V11)
V12=FFF(V12)
V13=FFF(V13)
SHEART=DEXP((0.2432D+06/(8.31432*T))-0.135D+03+20.0*DLOG(T)
1.5*DLOG(DABS(GMAX)))
DIFFT=DEXP((0.6031D+06/(8.31432*T))-0.1905D+03+20.0*DLOG(T)
1.4*DLOG(DABS(GMAX)))
IF (X44 .EQ. 0.0) GOTO 453
GOTO 454
453  SHEART=1D+20
454  DDFTO(C98)=FTO
      DT4(C98)=T4
9    CONTINUE
2444 C98=C98-1
      CALL ANAL(C98,INCEPT,SLOPE,CORR,DT4,DDFTO)
      BS=(-400.0-INCEPT)/SLOPE
      MS=(-1120.0D+00-10568.0D+00*X1+94.1D+00-INCEPT)/SLOPE
      IF (WS .LT. BS) GOTO 9996
      GOTO 24
9996 BS=WS
24  CONTINUE
      RETURN
      END
C  Subroutine*****TZERO*****
SUBROUTINE TZERO(C,T,XTO,XTO400)
DOUBLE PRECISION X,X1,T,R,H,H1,S,S1
INTEGER I,U,B4,J99,C98,C97,B5
DOUBLE PRECISION D11,FTO,FTO400,XTO400,G9400,G9,XTO,DFTO,T10,T20,
1JJ1,D,W,W1,F,T4,C(8),B1,B2,P(7),Y(7),B3,WS
B3=0
C(8)=(100.0-C(1)-C(2)-C(3)-C(4)-C(5)-C(6)-(C7))/55.84
C  DIVIDING BY ATOMIC WEIGHT.....
C(1)=C(1)/12.0115
C(2)=C(2)/28.09
C(3)=C(3)/54.94
C(4)=C(4)/58.71
C(5)=C(5)/55.94
C(6)=C(6)/52.0
C(7)=C(7)/50.94
B1=C(1)+C(2)+C(3)+C(4)+C(5)+C(6)+C(7)+C(8)
DO 107 U=2,7
      Y(U)=C(U)/C(8)
107  CONTINUE
C  CALCULATING MOLE FRACTIONS.....
DO 106 U=1,7
      C(U)=C(U)/B1
106  CONTINUE
B2=0.0
T10=Y(2)*(-3)+Y(3)*2+Y(4)*12+Y(5)*(-9)+Y(6)*(-1)+Y(7)*(-12)
T20=-3*Y(2)-37.5*Y(3)-6*Y(4)-26*Y(5)-19*Y(6)-44*Y(7)
P(2)=2013.0341+763.8167*C(2)+45802.87*C(2)**2-280061.63*C(2)**3
1+3.864D+06*C(2)**4-2.4233D+07*C(2)**5+6.9547D+07*C(2)**6
P(3)=2012.067-1764.095*C(3)+6287.52*C(3)**2-21647.96*C(3)**3
12.0119D+06*C(3)**4+3.1716D+07*C(3)**5-1.3885D+08*C(3)**6
P(4)=2006.8017+2330.2424*C(4)-54915.32*C(4)**2+1.6216D+06*C(4)**3
1-2.4968D+07*C(4)**4+1.8838D+08*C(4)**5-5.5531D+08*C(4)**6
P(5)=2006.834-2997.314*C(5)-37906.61*C(5)**2+1.0328D+06*C(5)**3
1-1.3306D+07*C(5)**4+8.411D+07*C(5)**5-2.0826D+08*C(5)**6
P(6)=2012.367-9224.2655*C(6)+33657.8*C(6)**2-566827.83*C(6)**3
1+8.5676D+06*C(6)**4-6.7482D+07*C(6)**5 +2.0837D+08*C(6)**6
P(7)=2011.9996-6247.9118*C(7)-5411.7566*C(7)**2
1+250118.1085*C(7)**3-4.1676D+06*C(7)**4
DO 108 U=2,7
      B3=B3+P(U)*Y(U)
      B2=B2+Y(U)
108  CONTINUE
IF(B2 .EQ. 0.0) GOTO 455
W=(B3/B2)*4.187
455  W=8054.0

```

```

FTO=1.0
X1=C(1)
R=8.31432
W1=48570.0
C ENTHALPY OF CARBON IN AUSTENITE.....H=38575.0
C ENTROPY OF CARBON IN AUSTENITE.....S=13.48
XTO=0.04
XTO400=0.03
C98=0
C97=0
WS=0.0
J98=0
J99=0
IF (T .LE. 1000) GOTO 20
H1=105525
S1=45.34521
GOTO 19
20 H1=111918
S1=51.44
C Calling subroutine ENERGY———
C DG FOR ALPHA—>GAMMA FOR PURE IRON......
C T10 & T20 ARE THE MAGNETIC & MAGN. EFFECTS OF ALLOY ADDITIONS ON
C DG FOR ALPHA—>GAMMA FOR PURE IRON (ZENER)
19 F=ENERGY(T,T10,T20)
C SITE EXCLUSION PARAMETER......
J=1-DEXP(-W/(R*T))
J1=1.0-DEXP(-W1/(R*T))
T4=T-273
C Calling subroutine FTO1———
FTO=FTO1(H,S,X1,T,W,W1,H1,S1,F,J,J1)
C Calling subroutine FTO1———
21 DFTO=FTO1(H,S,XTO,T,W,W1,H1,S1,F,J,J1)
J98=J98+1
IF (DABS(DFTO) .LE. 10.0) GOTO 450
C Calling subroutine G91———
G9=G91(XTO,T,W,W1,H1,S1,F,J,J1)
IF (J98 .GE. 9) GOTO 450
XTO=XTO-DFTO/G9
IF (XTO .LE. 0.0001) GOTO 94
GOTO 21
94 XTO=0.0000
C Calling subroutine FTO1———
450 FTO400=FTO1(H,S,XTO400,T,W,W1,H1,S1,F,J,J1)+400.0
J99=J99+1
IF(J99 .GE. 10) GOTO 92
IF (DABS(FTO400) .LE. 10.0) GOTO 92
C Calling subroutine G91———
C9400=G91(XTO400,T,W,W1,H1,S1,F,J,J1)
XTO400=XTO400-FTO400/G9400
IF (XTO400 .LE. 0.0001) GOTO 451
GOTO 450
451 XTO400=0.0000
92 CONTINUE
RETURN
END
C Subroutine*****FTO1*****DOUBLE PRECISION FUNCTION FTO1(H,S,X,T,W,W1,H1,S1,F,J,J1)
DOUBLE PRECISION R,X,T,T60,ZEN1,ZEN2,ZENER,W,W1,H1,S1,F,
1J,J1,D,D11,H,S
D=DSQRT(1-2*(1+2*J)*X+(1+8*J)*X*X)
D11=DSQRT(9-6*X*(2*J1+3)-(9+16*J1)*X*X)
T60=T*(1-X)/(28080*X)
IF (T60 .GT. 1.0) GOTO 18
IF (T60 .GT. 0.25) GOTO 17
C ZENER ORDERING......
ZEN1=0.2307+42.7974*T60-233.8631*T60*T60+645.4485*T60*T60*T60
1-954.3995*(T60**4)+711.8095*(T60**5)-211.5136*(T60**6)

```

```

ZEN2=-2.6702+45.6337*T60-225.3965*T60*T60+567.7112*(T60**3)
1-771.6466*(T60**4)+538.1778*(T60**5)-151.3818*(T60**6)
GOTO 16
17 ZEN2=1
ZEN1=3.295
16 ZENER=((ZEN2*X)**2)*(-50898.56)/(1-X)+ZEN1*T*X*0.6623741
ZENER=ZENER*4.187
GOTO 15
18 ZENER=0.0
15 R=8.31432
FTO1=X*R*T*DLOG(X*X)+X*(H1-(H)-(S1-(S)
1)*T+4*W1-6*W)-R*T*(1-X)*DLOG((1-X)**4)+5*R*T*(1-2*X)*DLOG(1-2*X)
1-R*T*X*DLOG(((D-1+3*X)/(D+1-3*X))**6)-R*T*(1-X)*DLOG(((1-2*X)+(4
1*X-1)*X-D)/(2*X*(2*X-1)))**6)+3*R*T*X*DLOG(3-4*X)+R*T*
1X*DLOG(((D11-3+5*X)/(D11+3-5*X))**4)+(1-X)*F+ZENER
RETURN
END
C Subroutine*****G91*****
DOUBLE PRECISION FUNCTION G91(XTO,T,W,W1,H1,S1,F,J,J1)
DOUBLE PRECISION R,XTO,T,W,W1,H1,S1,F,J,J1,FD,FD1,DT5,
1DT6,DZEN1,DZEN2,DZEN3,V1,V2,V3,V4,V5,V6,V7,V8,V9,G1,
1DZEN6,DZEN7,DZEN8
R=8.31432
FD=DSQRT(1-2*(1+2*X)*XTO+(1+8*X)*XTO*XTO)
FD1=DSQRT(9-6*XTO*(2*X+3)+(9+16*X1)*XTO*XTO)
DT5=28080*XTO/(1-XTO)
DT6=T/DT5
IF (DT6 .GT. 1.0) GOTO 48
IF (DT6 .LT. 0.25) GOTO 47
DZEN1=0.2307+42.7974*DT6-233.8631*(DT6**2)+645.4485*(DT6**3)
1-954.3995*(DT6**4)+711.8095*(DT6**5)-211.5136*(DT6**6)
DZEN2=-2.6702+45.6337*DT6-225.3965*(DT6**2)+567.7112*(DT6**3)
1-771.6466*(DT6**4)+538.1778*(DT6**5)-151.3818*(DT6**6)
GOTO 46
47 DZEN2=1
DZEN1=3.295
46 DZEN3=((DZEN2*XTO)**2)*(-50898.56)/(1-XTO)+DZEN1*T*XTO*
1(0.6623741)
DZEN3=DZEN3*4.187
GOTO 45
48 DZEN3=0.0
45 V1=FD-1+3*XTO
V2=FD+1-3*XTO
V3=1-2*X+(4*X-1)*XTO-FD
V4=2*X*(2*XTO-1)
V5=FD1-3+5*XTO
V6=FD1+3-5*XTO
V7=(XTO-1-2*X+8*XTO*X)/FD
V8=(9*XTO-9-6*X1+16*X1*XTO)/FD1
V9=H1-(H)-(S1-(S))*T-6*W+4*W1
G1=2*DLOG(XTO**2)+4*DLOG((1-XTO)**4)-10*DLOG((1-2*XTO)**10)
1-DLOG((V1/V2)**6)-6*((XTO/V1)*(V7+3+V1*(3-V7)/V2))
1+DLOG((V3/V4)**6)-6*((1-XTO)/V3)*(4*X*(1-(V3/V4))-V7)
1+3*(DLOG(3-4*XTO)-4*XTO/(3-4*XTO))+DLOG((V5/V6)**4)+4*(XTO
1/V5)*(V8+5+(V5/V6)*(5-V8))
IF (DT6 .GT. 1.0) GOTO 90
DZEN6=(-3.3948+13.6112*DT6-13.4376*(DT6**2))/T/(28080*
1((1-XTO)**2))
DZEN7=(-3.3118+15.7462*DT6-23.2449*(DT6**2))/T/(28080*
1((1-XTO)**2))
DZEN8=50898*((DZEN2*XTO)**2)/((1-XTO)**2)+(-50898*(2*
1DZEN2*DZEN6*(XTO**2)+2*XTO*(DZEN2**2))/(1-XTO))+DZEN1
1*T*0.6623741+DZEN7*T*XTO*0.6623741
GOTO 91
90 DZEN8=0.0
91 G91=V9+R*T*G1+DZEN8-F
RETURN
END
C Subroutine*****FFF*****

```

```

DOUBLE PRECISION FUNCTION FFF(V)
DOUBLE PRECISION V
IF (V .LE. 0.0) GOTO 1
IF (V .GT. 1.0) GOTO 1
2   GOTO 3
1   FFF=0.0
GOTO 4
3   FFF=V
4   RETURN
END
C   Subroutine*****ENERGY*****
DOUBLE PRECISION FUNCTION ENERGY(T,T10,T20)
DOUBLE PRECISION T,T10,T20,F,T7
T7=T-100*T20
IF (T7 .LT. 300) GOTO 1
IF (T7 .LT. 700) GOTO 2
IF (T7 .LT. 940) GOTO 3
F=-8.88909+0.26557*(T7-1140)-1.04923D-3*((T7-1140)**2)
F=F+2.70013D-6*((T7-1140)**3)-3.58434D-9*((T7-1140)**4)
GOTO 4
1   F=1.38*T7-1499
GOTO 4
2   F=1.65786*T7-1581
GOTO 4
3   F=1.30089*T7-1331
4   ENERGY=(141*T10 + F)*4.187
RETURN
END
DOUBLE PRECISION FUNCTION XALPH(T)
DOUBLE PRECISION T,CTEMP
CTEMP=(T-273.0D+00)/900.0D+00
XALPH=0.1528D-02-0.8816D-02*CTEMP+0.2450D-01*CTEMP*CTEMP
&-0.2417D-01*CTEMP*CTEMP*CTEMP+
&0.6966D-02*CTEMP*CTEMP*CTEMP*CTEMP
RETURN
END
SUBROUTINE ANAL(C98,INCEPT,SLOPE,CORR,X,Y)
DOUBLE PRECISION AX,AX2,AY,AY2,AXY,INCEPT,CORR,SLOPE,
&X(40),Y(40)
INTEGER I,C98,I1
I1=C98
C98=C98-10
AX=0.0D+00
AY=0.0D+00
AX2=0.0D+00
AY2=0.0D+00
AXY=0.0D+00
DO 1 I=1,C98
AX=AX+X(I)
AY=AY+Y(I)
AXY=AXY+X(I)*Y(I)
AX2=AX2+X(I)*X(I)
AY2=AY2+Y(I)*Y(I)
1 CONTINUE
INCEPT=(AY*AX2-AX*AXY)/(C98*AX2-AX*AX)
SLOPE=((C98*AXY-AX*AY)/(C98*AX2-AX*AX))
CORR=(C98*AXY-AX*AY)/(DSQRT((C98*AX2-AX*AX)*
&(C98*AY2-AY*AY)))
C98=I1
RETURN
END

```

APPENDIX-3

```

C Copyright S. A. Khan and H. K. D. H. Bhadeshia
C University of Cambridge, Department of Materials Science and Metallurgy,
C Pembroke Street, Cambridge CB2 3QZ, U. K.
C
C PROG. FOR THE ANALYSIS OF ALLOTRIOMORPHIC FERRITE TRANSFORMATION IN
C HETEROGENEOUS STEELS.
C
C The motion of austenite/ferrite interface is considered to be parallel to the
C isoconcentration planes.
C
C The steel is divided into slices of different compositions, Ac3 temperature
C of each slice is calculated and transformation is allowed only in slices
C whose Ac3 temperature is higher than the concerned transformation
C temperature. The extent of transformation is limited by paraequilibrium
C mechanism. The carbon is permitted to redistribute among the slices after
C each increment of transformation. The results averaged and compared with a
C steel of the corresponding average composition.
C Typical data set follows:
C 673 (temperature in Kelvin)
C 0.43 0.50 0.60 0.70 0.80 0.90 1.00 (Composition of slice 1 in wt.%)
C 0.43 0.60 0.60 0.70 0.80 0.90 1.90 (Composition of slice 2 in wt.%)
C C Si Mn Ni Mo Cr V
C
IMPLICIT REAL*8(A-H,K-Z), INTEGER(I,J)
DOUBLE PRECISION C(8),D(8),XEQ(200)
&,E(8),F(8),MS(100),IA(100),XGAMMA(200),VOLP(200)
&,CN(200),SI(200),MN(200),NI(200),MO(200),V(200),FE(200)
&,CR(200),WD(8),VG(200),CD(8),XG(200),TAE3(200)
&,TAE3H,XEQH,TVOLF,AVEVOL,MOMENT,TISO
VINCR=0.00005D+00
ISTOP=0
AVEVOL=0.0D+0
TVOLF=0.0D+0
C1=0.0
C2=0.0
C3=0.0
C4=0.0
C5=0.0
C6=0.0
C7=0.0
READ(5,*)KELVIN
TISO=KELVIN-273.0D+0
XALPHA=XALPH(KELVIN)
WRITE(6,4444)
4444 FORMAT(' ****CARBON IS ALLOWED TO DIFFUSE!!!!*****')
WRITE(6,9)KELVIN,XALPHA,VINCR
WRITE(6,9090)
9090 FORMAT('
&_____
DO 1 I=1,101
READ(5,*),END=2)C(1),C(2),C(3),C(4),C(5),C(6),C(7)
CN(I)=C(1)
SI(I)=C(2)
MN(I)=C(3)
NI(I)=C(4)
MO(I)=C(5)
CR(I)=C(6)
V(I)=C(7)
FE(I)=100.0D+0-(C(1)+C(2)+C(3)+C(4)+C(5)+C(6)+C(7))
C1=C1+C(1)
C2=C2+C(2)
C3=C3+C(3)
C4=C4+C(4)
C5=C5+C(5)
C6=C6+C(6)
C7=C7+C(7)
DO 43 II=1,7

```

```

E(JI)=C(JI)
43  CONTINUE
CALL XEQ3(KELVIN,C,XEQ(I))
CALL TEMP3(E,TAE3(I))
XBAR=C(1)
WRITE(6,10)I,XEQ(I),TAE3(I)
WRITE(6,6161)

6161 FORMAT('*****')
&*****
1  CONTINUE
2  ISLICE=I-1
WRITE(*,*) ISLICE
D(1)=C1/ISLICE
D(2)=C2/ISLICE
D(3)=C3/ISLICE
D(4)=C4/ISLICE
D(5)=C5/ISLICE
D(6)=C6/ISLICE
D(7)=C7/ISLICE
DO 70 JII=1,7
WD(JII)=D(JII)
70  CONTINUE
DO 56 JU=1,7
F(JU)=D(JU)
56  CONTINUE
CALL XEQ3(KELVIN,D,XEQH)
CALL TEMP3(F,TAE3H)
WRITE(6,75)TAE3H
75  FORMAT( ' A3H-' D10.4)
WRITE(*,*)D(1)
IF (TAE3H .LT. TISO) GOTO 789
GOTO 85
85  IF (XEQH .LE. D(1)) GOTO 789
GOTO 79
79  IF (XEQH .GT. XALPHA) GOTO 987
GOTO 789
789  VOLH=0.00
GOTO 678
987  VOLH=(XEQH-D(1))/(XEQH-XALPHA)
678  VGH=1.0D+0-VOLH
WRITE(6,15)VOLH
DO 1020 III=1,ISLICE
XGAMMA(III)=D(1)
VOLF(III)=0.0D+0
1020 CONTINUE
AVEX=D(1)
DO 6 I=1,100000
IF (ISTOP .EQ. ISLICE) GO TO 14
DO 4 J=1,ISLICE
IF (IA(J) .EQ. 1) GOTO 4
IF (TAE3(J) .LT. TISO) GOTO 5329
GOTO 9352
5329  VOLF(J)=0.00
GOTO 5
9352  VOLF(J)=VOLF(J)+VINCR
XGAMMA(J)=AVEX
IF (XGAMMA(J) .GT. XEQ(J)) GOTO 5
GOTO 4
5  IA(J)=1
ISTOP=ISTOP+IA(J)
VOLF(J)=VOLF(J)-VINCR
IF (VOLF(J) .LE. 0.0D+0) GOTO 115
GOTO 4
115  VOLF(J)=0.0D+0
XGAMMA(J)=AVEX
4  CONTINUE
AVEVOL=0.0D+0
DO 90 J33=1,ISLICE
AVEVOL=AVEVOL+VOLF(J33)

```

```

90  CONTINUE
    AVEVOL=AVEVOL/ISLICE
    AVEX=D(1)+(AVEVOL*(D(1)-XALPHA))/(1.0D+0-AVEVOL)
6   CONTINUE
14  AVEVOL=0.0D+0
    DO 12 J=1,ISLICE
        AVEVOL=AVEVOL+VOLF(J)
        WRITE(6,786)J,VOLF(J),XGAMMA(J),XEQ(J),TAE3(J),D(1),AVEVOL
786  FORMAT(' SLICE=',I3,' VOLF=',D10.3,' XGAMMA=',D10.3,' XEQ=',
     &D10.3,' TAE3=',D10.3,' D(1)=',D10.3,' AVEVOL=',D10.3)
12  CONTINUE
    AVEVOL=AVEVOL/ISLICE
    WRITE(6,13)AVEVOL
13  FORMAT(' Average volume fraction of transformation',
     &' in heterogeneous alloy =',D8.3)
9   FORMAT(' KELVIN = ',F7.0,' XALPHA, mol. fraction =',D12.4
     &,' VOL INCREMENT=',D12.4)
10  FORMAT(' Slice Number= ',I3,'      XEQ = ',D10.4,
     &          AE3-T= ',D10.4/)
15  FORMAT(' Maximum volume fraction of bainitic ferrite in ',
     &' an alloy of average composition = ',D8.3)
    STOP
    END

```

```

C*****
SUBROUTINE TEMP3(C,AE3T)
DOUBLE PRECISION X,X1,R,A,A1,AFE,A1FE,DA1,DA2,DA1FE,H,H1,S,S1
INTEGER T1,I,NO,U,B4,J99,C99,C98,C97
DOUBLE PRECISION D11,DTQ(40),DXEQ(40),
1INCEPT,SLOPE,CORR,
1DEQ,ETEQ,T10,T20,XA,AFEQ,AEQ,ETEQ2,TEQ,
1JJ1,D,D1,W,W1,F,TEST,ERROR,T4,XEQ,FPRO
1,(8),B1,B2,P(7),Y(7),B3,AE3T,EE(8)
WRITE(6,1100)C(1),C(2),C(3),C(4),C(5),C(6),C(7)
1100 FORMAT(7D11.3)
B3=0
C(8)=(100.0-C(1)-C(2)-C(3)-C(4)-C(5)-C(6)-(C7))/55.84
C(1)=C(1)/12.0115
C(2)=C(2)/28.09
C(3)=C(3)/54.94
C(4)=C(4)/58.71
C(5)=C(5)/95.94
C(6)=C(6)/52.0
C(7)=C(7)/50.94
B1=C(1)+C(2)+C(3)+C(4)+C(5)+C(6)+C(7)+C(8)
DO 107 U=2,7
Y(U)=C(U)/C(8)
107  CONTINUE
DO 106 U=1,7
C(U)=C(U)/B1
106  CONTINUE
B2=0.0
T10=Y(2)*(-3)+Y(3)*2+Y(4)*12+Y(5)*(-9)+Y(6)*(-1)+Y(7)*(-12)
T20=-3*Y(2)-37.5*Y(3)-6*Y(4)-26*Y(5)-19*Y(6)-44*Y(7)
P(2)=2013.0341+763.8167*C(2)+45802.87*C(2)**2-280061.63*C(2)**3
1+3.864D+06*C(2)**4-2.4233D+07*C(2)**5+6.9547D+07*C(2)**6
P(3)=2012.067-1764.095*C(3)+6287.52*C(3)**2-21647.96*C(3)**3
12.0119D+06*C(3)**4+3.1716D+07*C(3)**5-1.3885D+08*C(3)**6
P(4)=2006.8017+2330.2424*C(4)-54915.32*C(4)**2+1.6216D+06*C(4)**3
1-2.4968D+07*C(4)**4+1.8838D+08*C(4)**5-5.5531D+08*C(4)**6
P(5)=2006.834-2997.314*C(5)-37906.61*C(5)**2+1.0328D+06*C(5)**3
1-1.3306D+07*C(5)**4+8.411D+07*C(5)**5-2.0826D+08*C(5)**6
P(6)=2012.367-9224.2655*C(6)+33657.8*C(6)**2-566827.83*C(6)**3
1+8.5676D+06*C(6)**4-6.7482D+07*C(6)**5+2.0837D+08*C(6)**6
P(7)=2011.9996-6247.9118*C(7)+5411.7566*C(7)**2
1+250118.1085*C(7)**3-4.1676D+06*C(7)**4
DO 108 U=2,7
B3=B3+P(U)*Y(U)
B2=B2+Y(U)
108  CONTINUE

```

```

108  CONTINUE
    IF(B2 .EQ. 0.0) GOTO 455
    W=(B3/B2)*4.187
    GOTO 456
455  W=8054.0
456  CONTINUE
    X1=C(1)
    R=-8.31432
    W1=48570.0
    H=38575.0
    S=13.48
    II1=873
    II2=1173
    II3=15
    II=0
201  XEQ=0.1
    INCEPT=1.0D+00
    CORR=1.0D+00
    SLOPE=1.0D+00
    C98=0
    C97=0
    DO 9 T1=II1,II2,II3
    C98=C98+1
    T=T1
    IF (T .LE. 1000) GOTO 20
    H1=105525
    S1=45.34521
    GOTO 19
20   H1=111918
    S1=51.44
19   F=ENERGY(T,T10,T20)
    J=1-DEXP(-W/(R*T))
    DEQ=DSQRT((1-2*(1+2*J)*XEQ+(1+8*J)*XEQ*XEQ)
    TEQ=5*DLOG((1-XEQ)/(1-2*XEQ))
    TEQ=TEQ+DLOG(((1-2*J+(4*J-1)*XEQ-DEQ)/(2*J*(2*XEQ-1)))**6)
    TEQ=TEQ*R*T-F
    IF (DABS(TEQ) .LT. 1.0) GOTO 50
    ETEQ=5*((1/(XEQ-1))+2/(1-2*XEQ))
    ETEQ2=6*((4*J-1-(0.5/DEQ))*(-2-4*J+2*XEQ+16*XEQ*XEQ))/(1-2*J+(4*J
    1-1)*XEQ-DEQ))+6*(4*J/(2*J*(2*XEQ-1)))
    ETEQ=(ETEQ+ETEQ2)*R*T
    XEQ=XEQ-TEQ/ETEQ
    GOTO 51
50   IF (XEQ .LT. 0.001) GOTO 2444
    T4=T1-273.0
    DTQ(C98)=T4
    DXEQ(C98)=XEQ
9    CONTINUE
2444 C98=C98-1
    CALL ANAL(C98,INCEPT,SLOPE,CORR,DTQ,DXEQ)
    AE3T=(X1-INCEPT)/SLOPE
    IF(II .GT. 0) GOTO 802
    II=AE3T
    II1=II-9+273
    II2=II+9+273
    II3=1
    GOTO 201
802  RETURN
END
SUBROUTINE ANAL(C98,INCEPT,SLOPE,CORR,X,Y)
DOUBLE PRECISION AX,AX2,AY,AY2,AXY,INCEPT,CORR,SLOPE,
&X(40),Y(40)
INTEGER I,C98,I1
I1=C98
C98=C98-10
AX=0.0D+00
AY=0.0D+00
AX2=0.0D+00
AY2=0.0D+00

```

```

AXY=0.0D+00
DO 1 I=1,C98
AX=AX+X(I)
AY=AY+Y(I)
AXY=AXY+X(I)*Y(I)
AX2=AX2+X(I)*X(I)
AY2=AY2+Y(I)*Y(I)
1 CONTINUE
INCEPT=(AY*AX2-AX*AXY)/(C98*AX2-AX*AX)
SLOPE=((C98*AXY-AX*AY)/(C98*AX2-AX*AX))
CORR=(C98*AXY-AX*AY)/(DSQRT((C98*AX2-AX*AX)*
&(C98*AY2-AY*AY)))
C98=I1
RETURN
END
DOUBLE PRECISION FUNCTION ENERGY(T,T10,T20)
DOUBLE PRECISION T,T10,T20,F,T7
T7=T-100*T20
IF (T7 .LT. 300) GOTO 1
IF (T7 .LT. 700) GOTO 2
IF (T7 .LT. 940) GOTO 3
F=-8.88909+0.26557*(T7-1140)-1.04923D-3*((T7-1140)**2)
F=F+2.70013D-6*((T7-1140)**3)-3.58434D-9*((T7-1140)**4)
GOTO 4
1 F=1.38*T7-1499
GOTO 4
2 F=1.63786*T7-1581
GOTO 4
3 F=1.30089*T7-1331
4 ENERGY=(141*T10 + F)*4.187
RETURN
END

C*****
SUBROUTINE XEQ3(TT,C,XEQ)
DOUBLE PRECISION X,X1,T,R,A,A1,AFE,A1FE,DA1,DA2,DA1FE,H,H1,S,S1
&,TT
INTEGER I,NO,U,B4,J99,C99,C98,C97
DOUBLE PRECISION D11,
1DEQ,ETEQ,T10,T20,XA,AFEQ,AEQ,ETEQ2,TEQ,
1JJ1,D,D1,W,W1,F,TEST,ERROR,T4,XEQ,FPRO
1,C(8),B1,B2,P(7),Y(7),B3,AE3T,CC(8)

B3=0
C(8)=(100.0-C(1)-C(2)-C(3)-C(4)-C(5)-C(6)-(C7))/55.84
C(1)=C(1)/12.0115
C(2)=C(2)/28.09
C(3)=C(3)/54.94
C(4)=C(4)/58.71
C(5)=C(5)/55.94
C(6)=C(6)/52.0
C(7)=C(7)/50.94
B1=C(1)+C(2)+C(3)+C(4)+C(5)+C(6)+C(7)+C(8)
DO 107 U=2,7
Y(U)=C(U)/C(8)
107 CONTINUE
DO 106 U=1,7
C(U)=C(U)/B1
106 CONTINUE
B2=0.0
T10=Y(2)*(-3)+Y(3)*2+Y(4)*12+Y(5)*(-9)+Y(6)*(-1)+Y(7)*(-12)
T20=-3*Y(2)-37.5*Y(3)-6*Y(4)-26*Y(5)-19*Y(6)-44*Y(7)
P(2)=2013.0341+763.8167*C(2)+45802.87*C(2)**2-280061.63*C(2)**3
1+3.864D+06*C(2)**4-2.423D+07*C(2)**5+6.9547D+07*C(2)**6
P(3)=2012.067-1764.095*C(3)+6287.52*C(3)**2-21647.96*C(3)**3-
12.0119D+06*C(3)**4+3.1716D+07*C(3)**5-1.3885D+08*C(3)**6
P(4)=2006.8017+2330.2424*C(4)-54915.32*C(4)**2+1.6216D+06*C(4)**3
1-2.4968D+07*C(4)**4+1.8838D+08*C(4)**5-5.5531D+08*C(4)**6
P(5)=2006.834-2997.314*C(5)-37906.61*C(5)**2+1.0328D+06*C(5)**3

```

```

1-1.3306D+07*C(5)**4+8.411D+07*C(5)**5-2.0826D+08*C(5)**6
P(6)=2012.367-9224.2655*C(6)+33657.8*C(6)**2-566827.83*C(6)**3
1+8.5676D+06*C(6)**4-6.7482D+07*C(6)**5+2.0837D+08*C(6)**6
P(7)=2011.9996-6247.9118*C(7)+5411.7566*C(7)**2
1+250118.1085*C(7)**3-4.1676D+06*C(7)**4
DO 108 U=2,7
B3=B3+P(U)*Y(U)
B2=B2+Y(U)
108 CONTINUE
IF(B2 .EQ. 0.0) GOTO 455
W=(B3/B2)*4.187
GOTO 456
455 W=8054.0
456 CONTINUE
X1=C(1)
R=8.31432
W1=48570.0
H=38575.0
S=13.48
201 XEQ=0.1
T=TT
IF (T .LE. 1000) GOTO 20
H1=105525
S1=45.34521
GOTO 19
20 H1=111918
S1=51.44
19 F=ENERGY(T,T10,T20)
J=1-DEXP(-W/(R*T))
51 DEQ=DSQRT(1-2*(1+2*J)*XEQ+(1+8*J)*XEQ*XEQ)
TEQ=S*DLOG((1-XEQ)/(1-2*XEQ))
TEQ=TEQ+DLOG(((1-2*J+(4*J-1)*XEQ-DEQ)/(2*J*(2*XEQ-1)))**6)
TEQ=TEQ*R*T-F
IF (DABS(TEQ) .LT. 1.0) GOTO 50
ETEQ=5*((1/(XEQ-1))+2/(1-2*XEQ))
ETEQ2=6*((4*J-1-(0.5/DEQ)*(-2-4*J+2*XEQ+16*XEQ*XEQ))/(1-2*J+(4*J
1-1)*XEQ-DEQ))+6*(4*J/(2*J*(2*XEQ-1)))
ETEQ=(ETEQ+ETEQ2)*R*T
XEQ=XEQ-TEQ/ETEQ
GOTO 51
50 RETURN
END
DOUBLE PRECISION FUNCTION ENERGY(T,T10,T20)
DOUBLE PRECISION T,T10,T20,F,T7
T7=T-100*T20
IF (T7 .LT. 300) GOTO 1
IF (T7 .LT. 700) GOTO 2
IF (T7 .LT. 940) GOTO 3
F=-8.88909+0.26557*(T7-1140)-1.04923D-3*((T7-1140)**2)
F=F+2.70013D-6*((T7-1140)**3)-3.58434D-9*((T7-1140)**4)
GOTO 4
1 F=1.38*T7-1499
GOTO 4
2 F=1.65786*T7-1581
GOTO 4
3 F=1.30089*T7-1331
4 ENERGY=(141*T10 + F)*4.187
RETURN
END

DOUBLE PRECISION FUNCTION XALPH(T)
DOUBLE PRECISION T,CTEMP
CTEMP=(T-273.0D+00)/900.0D+00
XALPH=0.1528D-02-0.8816D-02*CTEMP+0.2450D-01*CTEMP*CTEMP
&-0.2417D-01*CTEMP*CTEMP*CTEMP+
&0.6966D-02*CTEMP*CTEMP*CTEMP*CTEMP
RETURN
END

```

APPENDIX-4

```

C Copyright S. A. Khan and H. K. D. H. Bhadeshia
C University of Cambridge, Department of Materials Science and Metallurgy,
C Pembroke Street, Cambridge CB2 3QZ, U. K.
C
C PROG. FOR THE ANALYSIS OF ALLOTRIOMORPHIC FERRITE TRANSFORMATION IN
C HETEROGENEOUS STEELS.
C
C The motion of austenite/ferrite interface is considered to be parallel to the
C isoconcentration planes.
C
C The steel is divided into slices of different compositions,  $Ae_3$  temperature
C of each slice is calculated and transformation is allowed only in slices
C whose  $Ae_3$  temperature is higher than the concerned transformation
C temperature. The extent of transformation is limited by paraequilibrium
C mechanism.
C
C The carbon is not allowed to redistribute among the slices after each
C increment of transformation. The results averaged and compared with a steel
C of the corresponding average composition.
C Typical data set follows:
C 673 (temperature in Kelvin)
C 0.43 0.50 0.60 0.70 0.80 0.90 1.00 (Composition of slice 1 in wt.%)
C 0.43 0.60 0.60 0.70 0.80 0.90 1.90 (Composition of slice 2 in wt.%)
C C Si Mn Ni Mo Cr V
C
IMPLICIT REAL*8(A-H,K-Z), INTEGER(I,J)
DOUBLE PRECISION C(8),D(8),XEQ(300)
&,E(8),F(8),MS(300),IA(300),XGAMMA(300),VOLF(300)
&,CN(300),S(300),MN(300),NI(300),MO(300),V(300),FE(300)
&,CR(300),WD(8),VG(300),CD(8),XG(300),TAE3(300)
&,TAE3H,XEQH,TVOLF,AVEVOL,MOMENT,TISO
VINCR=0.00005D+00
ISTOP=0
AVEVOL=0.0D+0
TVOLF=0.0D+0
C1=0.0
C2=0.0
C3=0.0
C4=0.0
C5=0.0
C6=0.0
C7=0.0
READ(5,*)KELVIN
TISO=KELVIN-273.0D+0
XALPHA=XALPH(KELVIN)
WRITE(6,9)KELVIN,XALPHA,VINCR
WRITE(6,9090)
9090 FORMAT('
&-----')
DO 1 I=1,300
READ(5,*,END=2)C(1),C(2),C(3),C(4),C(5),C(6),C(7)
CN(I)=C(1)
SI(I)=C(2)
MN(I)=C(3)
NI(I)=C(4)
MO(I)=C(5)
CR(I)=C(6)
V(I)=C(7)
FE(I)=100.0D+0-(C(1)+C(2)+C(3)+C(4)+C(5)+C(6)+C(7))
C1=C1+C(1)
C2=C2+C(2)
C3=C3+C(3)
C4=C4+C(4)
C5=C5+C(5)
C6=C6+C(6)
C7=C7+C(7)
DO 43 J=1,7

```

```

E(UI)=C(UI)
43  CONTINUE
CALL XEQ3(KELVIN,C,XEQ(I))
CALL TEMP3(E,TAE3(I))
XBAR=C(1)
WRITE(6,10)I,XEQ(I),TAE3(I)
WRITE(6,6161)

6161 FORMAT('*****')
&*****
1  CONTINUE
2  ISLICE=I-1
WRITE(*,*) ISLICE
D(1)=C1/ISLICE
D(2)=C2/ISLICE
D(3)=C3/ISLICE
D(4)=C4/ISLICE
D(5)=C5/ISLICE
D(6)=C6/ISLICE
D(7)=C7/ISLICE
DO 70 JII=1,7
WD(JII)=D(JII)
70  CONTINUE
DO 56 JIJ=1,7
F(JIJ)=D(JIJ)
56  CONTINUE
CALL XEQ3(KELVIN,D,XEQH)
CALL TEMP3(F,TAE3H)
WRITE(6,75)TAE3H

75  FORMAT( ' Ae3H= ',D10.4)
WRITE(*,*)D(1)
IF (TAE3H .LT. TISO) GOTO 789
GOTO 85

85  IF (XEQH .LE. D(1)) GOTO 789
GOTO 79

79  IF (XEQH .GT. XALPHA) GOTO 987
GOTO 789

789 VOLH=0.00
GOTO 678

987 VOLH=(XEQH-D(1))/(XEQH-XALPHA)
678 VGH=1.0D+0-VOLH
WRITE(6,15)VOLH
DO 6 I=1,100000
IF (ISTOP .EQ. ISLICE) GOTO 14
DO 4 J=1,ISLICE
IF (IA(J) .EQ. 1) GOTO 4
IF (TAE3(J) .LT. TISO) GOTO 5329
GOTO 9352

5329 VOLF(J)=0.00
GOTO 5

9352 VOLF(J)=VOLF(J)+VINCR
XGAMMA(J)=XBAR+((VOLF(J)*(XBAR-XALPHA))/(
&(1.0D+0-VOLF(J)))
IF (XGAMMA(J) .GE. XEQ(J)) GOTO 5
GOTO 4

5  IA(J)=1
ISTOP =ISTOP+IA(J)
VOLF(J)=VOLF(J)-VINCR
IF (VOLF(J) .LE. 0.0D+0) GOTO 115
GOTO 4

115 VOLF(J)=0.0D+0
XGAMMA(J)=XBAR

4  CONTINUE
6  CONTINUE
14 DO 12 JJ=1,ISLICE
AVEVOL=AVEVOL+VOLF(JJ)
WRITE(6,786)JJ,VOLF(JJ),XGAMMA(JJ),XEQ(JJ),TAE3(JJ),XBAR,AVEVOL

786 FORMAT(' SLICE=',I3,' VOLF=',D10.3,' XGAMMA=',D10.3,' XEQ=',
&D10.3,' TAE3=',D10.3,' XBAR=',D10.3,' AVEVOL(RUNNING SUM)=',D10.3)

12  CONTINUE

```

```

      WRITE(6,13)AVEVOL
13   FORMAT(' Average volume fraction of transformation',
     & ' in heterogeneous alloy =',D8.3)
9    FORMAT(' KELVIN = ',F7.0,' XALPHA, mol. fraction =',D12.4
     & , ' VOL INCREMENT=',D12.4)
10   FORMAT(' Slice Number= ',I3,'      XEQ = ',D10.4,
     & ' AE3-T= ',D10.4/)
15   FORMAT(' Maximum volume fraction of bainitic ferrite in ',
     & ' an alloy of average composition = ',D8.3)
      STOP
      END

C*****SUBROUTINE TEMP3(C,AE3T)
DOUBLE PRECISION X,X1,R,A,A1,AFE,A1FE,DA1,DA2,DA1FE,H,H1,S,S1
INTEGER T1,I,NO,U,B4,J99,C99,C98,C97
DOUBLE PRECISION D11,DTQ(40),DXEQ(40),
1INCEPT,SLOPE,CORR,
1DEQ,ETEQ,T10,T20,XA,AFEQ,AEQ,ETEQ2,TEQ,
1J1,D,D1,W,W1,F,TEST,ERROR,T4,SEQ,FPRO
1,C(8),B1,B2,P(7),Y(7),B3,AE3T,EE(8)
      WRITE(6,1100)C(1),C(2),C(3),C(4),C(5),C(6),C(7)
1100 FORMAT(7D11.3)
      B3=0
      C(8)=(100.0-C(1)-C(2)-C(3)-C(4)-C(5)-C(6)-(C7))/55.84
      C(1)=C(1)/12.0115
      C(2)=C(2)/28.09
      C(3)=C(3)/54.94
      C(4)=C(4)/58.71
      C(5)=C(5)/95.94
      C(6)=C(6)/52.0
      C(7)=C(7)/50.94
      B1=C(1)+C(2)+C(3)+C(4)+C(5)+C(6)+C(7)+C(8)
      DO 107 U=2,7
      Y(U)=C(U)/C(8)
107   CONTINUE
      DO 106 U=1,7
      C(U)=C(U)/B1
106   CONTINUE
      B2=0.0
      T10=Y(2)*(-3)+Y(3)*2+Y(4)*12+Y(5)*(-9)+Y(6)*(-1)+Y(7)*(-12)
      T20=-3*Y(2)-37.5*Y(3)-6*Y(4)-26*Y(5)-19*Y(6)-44*Y(7)
      P(2)=2013.0341+763.8167*C(2)+45802.87*C(2)**2-280061.63*C(2)**3
      +3.864D+06*C(2)**4-2.4233D+07*C(2)**5+6.9547D+07*C(2)**6
      P(3)=2012.067-1764.095*C(3)+6287.52*C(3)**2-21647.96*C(3)**3-
      12.0119D+06*C(3)**4+3.1716D+07*C(3)**5-1.3885D+08*C(3)**6
      P(4)=2006.8017+2330.2424*C(4)-54915.32*C(4)**2+1.6216D+06*C(4)**3
      -1.24968D+07*C(4)**4+1.8838D+08*C(4)**5-5.5531D+08*C(4)**6
      P(5)=2006.834-2997.314*C(5)-37906.61*C(5)**2+1.0328D+06*C(5)**3
      1.3306D+07*C(5)**4+8.411D+07*C(5)**5-2.0826D+08*C(5)**6
      P(6)=2012.367-9224.2655*C(6)+33657.8*C(6)**2-566827.83*C(6)**3
      +8.5676D+06*C(6)**4-6.7482D+07*C(6)**5 +2.0837D+08*C(6)**6
      P(7)=2011.9996-6247.9118*C(7)+5411.7566*C(7)**2
      1+250118.1085*C(7)**3-4.1676D+06*C(7)**4
      DO 108 U=2,7
      B3=B3+P(U)*Y(U)
      B2=B2+Y(U)
108   CONTINUE
      IF(B2 .EQ. 0.0) GOTO 455
      W=(B3/B2)*4.187
      GOTO 456
455  W=8054.0
456  CONTINUE
      X1=C(1)
      R=8.31432
      W1=48570.0
      H=38575.0
      S=13.48
      II1=873

```

```

II2=1173
II3=15
II=0
201 XEQ=0.1
INCEPT=1.0D+00
CORR=1.0D+00
SLOPE=1.0D+00
C98=0
C97=0
DO 9 T1=II1,II2,II3
C98=C98+1
T=T1
IF (T .LE. 1000) GOTO 20
H1=105525
S1=45.34521
GOTO 19
20 H1=111918
S1=51.44
19 F=ENERGY(T,T10,T20)
J=1-DEXPC(-W/(R*T))
51 DEQ=DSQRT(1-2*(1+2*J)*XEQ+(1+8*J)*XEQ*XEQ)
TEQ=5*DLOG((1-XEQ)/(1-2*XEQ))
TEQ=TEQ+DLOG(((1-2*J+(4*J-1)*XEQ-DEQ)/(2*J*(2*XEQ-1)))**6)
TEQ=TEQ*R*T-F
IF (DABS(TEQ) .LT. 1.0) GOTO 50
ETEQ=5*(1/(XEQ-1))+2/(1-2*XEQ))
ETEQ2=6*((4*J-1-(0.5/DEQ)*(-2-4*J+2*XEQ+16*XEQ*J))/(1-2*J+(4*J-1)*XEQ-DEQ))+6*(4*J/(2*J*(2*XEQ-1)))
ETEQ=(ETEQ+ETEQ2)*R*T
XEQ=XEQ-TEQ/ETEQ
GOTO 51
50 IF (XEQ .LT. 0.001) GOTO 2444
T4=T1-273.0
DTQ(C98)=T4
DXEQ(C98)=XEQ
9 CONTINUE
2444 C98=C98-1
CALL ANAL(C98,INCEPT,SLOPE,CORR,DTQ,DXEQ)
AE3T=(X1-INCEPT)/SLOPE
IF(II .GT. 0) GOTO 802
II=AE3T
II=II-9+273
II2=II+9+273
II3=1
GOTO 201
802 RETURN
END
SUBROUTINE ANAL(C98,INCEPT,SLOPE,CORR,X,Y)
DOUBLE PRECISION AX,AX2,AY,AY2,AXY,INCEPT,CORR,SLOPE,
&X(40),Y(40)
INTEGER I,C98,I1
I1=C98
C98=C98-10
AX=0.0D+00
AY=0.0D+00
AX2=0.0D+00
AY2=0.0D+00
AXY=0.0D+00
DO 1 I=1,C98
AX=AX+X(I)
AY=AY+Y(I)
AXY=AXY+X(I)*Y(I)
AX2=AX2+X(I)*X(I)
AY2=AY2+Y(I)*Y(I)
1 CONTINUE
INCEPT=(AY*AX2-AX*AXY)/(C98*AX2-AX*AX)
SLOPE=((C98*AXY-AX*AY)/(C98*AX2-AX*AX))
CORR=(C98*AXY-AX*AY)/(DSQRT((C98*AX2-AX*AX)*
&(C98*AY2-AY*AY)))

```

```

C98=l1
RETURN
END
DOUBLE PRECISION FUNCTION ENERGY(T,T10,T20)
DOUBLE PRECISION T,T10,T20,F,T7
T7=T-100*T20
IF (T7 .LT. 300) GOTO 1
IF (T7 .LT. 700) GOTO 2
IF (T7 .LT. 940) GOTO 3
F=-8.88909+0.26557*(T7-1140)-1.04923D-3*((T7-1140)**2)
F=F+2.70013D-6*((T7-1140)**3)-3.58434D-9*((T7-1140)**4)
GOTO 4
1 F=1.38*T7-1499
GOTO 4
2 F=1.65786*T7-1581
GOTO 4
3 F=1.30089*T7-1331
4 ENERGY=(141*T10 + F)*4.187
RETURN
END

C*****SUBROUTINE XEQ3(TT,C,XEQ)
SUBROUTINE XEQ3(TT,C,XEQ)
DOUBLE PRECISION X,X1,T,R,A,A1,AFE,A1FE,DA1,DA2,DA1FE,H,H1,S,S1
&,TT
INTEGER I,NO,U,B4,J99,C99,C98,C97
DOUBLE PRECISION D11,
1DEQ,ETEQ,T10,T20,XA,AFEQ,AEQ,ETEQ2,TEQ,
1J,J1,D,D1,W,W1,F,TEST,ERROR,T4,XEQ,FPRO
1,C(8),B1,B2,P(7),Y(7),B3,AE3T,CC(8)

B3=0
C(8)=(100.0-C(1)-C(2)-C(3)-C(4)-C(5)-C(6)-(C7))/55.84
C(1)=C(1)/12.0115
C(2)=C(2)/28.09
C(3)=C(3)/54.94
C(4)=C(4)/58.71
C(5)=C(5)/95.94
C(6)=C(6)/52.0
C(7)=C(7)/50.94
B1=C(1)+C(2)+C(3)+C(4)+C(5)+C(6)+C(7)+C(8)
DO 107 U=2,7
Y(U)=C(U)/C(8)
107 CONTINUE
DO 106 U=1,7
C(U)=C(U)/B1
106 CONTINUE
B2=0.0
T10=Y(2)*(-3)+Y(3)*2+Y(4)*12+Y(5)*(-9)+Y(6)*(-1)+Y(7)*(-12)
T20=-3*Y(2)-37.5*Y(3)-6*Y(4)-26*Y(5)-19*Y(6)-44*Y(7)
P(2)=2013.0341+763.8167*C(2)+45802.87*C(2)**2-280061.63*C(2)**3
1+3.864D+06*C(2)**4-2.4233D+07*C(2)**5+6.9547D+07*C(2)**6
P(3)=2012.067-1764.095*C(3)+6287.52*C(3)**2-21647.96*C(3)**3
12.0119D+06*C(3)**4+3.1716D+07*C(3)**5-1.3885D+08*C(3)**6
P(4)=2006.8017+2330.2424*C(4)-54915.32*C(4)**2+1.6216D+06*C(4)**3
1-2.4968D+07*C(4)**4+1.8838D+08*C(4)**5-5.5531D+08*C(4)**6
P(5)=2006.834-2997.314*C(5)-37906.61*C(5)**2+1.0328D+06*C(5)**3
1-1.3306D+07*C(5)**4+8.411D+07*C(5)**5-2.0826D+08*C(5)**6
P(6)=2012.367-9224.2655*C(6)+33657.8*C(6)**2-566827.83*C(6)**3
1+8.5676D+06*C(6)**4-6.7482D+07*C(6)**5+2.0837D+08*C(6)**6
P(7)=2011.9996-6247.9118*C(7)+5411.7566*C(7)**2
1+250118.1085*C(7)**3-4.1676D+06*C(7)**4
DO 108 U=2,7
B3=B3+P(U)*Y(U)
B2=B2+Y(U)
108 CONTINUE
IF(B2 .EQ. 0.0) GOTO 455
W=(B3/B2)*4.187
GOTO 456

```

```

455  W=8054.0
456  CONTINUE
      X1=C(1)
      R=8.31432
      W1=48570.0
      H=38575.0
      S=13.48
201  XEQ=0.1
      T=TT
      IF (T .LE. 1000) GOTO 20
      H1=105525
      S1=45.34521
      GOTO 19
20   H1=111918
      S1=51.44
19   F=ENERGY(T,T10,T20)
      J=1-DEXP(-W/(R*T))
51   DEQ=DSQRT(1-2*(1+2*J)*XEQ+(1+8*J)*XEQ*XEQ)
      TEQ=5*DLOG((1-XEQ)/(1-2*XEQ))
      TEQ=TEQ+DLOG(((1-2*J+(4*J-1)*XEQ-DEQ)/(2*J*(2*XEQ-1)))**6)
      TEQ=TEQ*R*T-F
      IF (DABS(TEQ) .LT. 1.0) GOTO 50
      ETEQ=5*((1/(XEQ-1))+2/(1-2*XEQ))
      ETEQ2=6*((4*J-1-(0.5/DEQ)*(-2-4*J+2*XEQ+16*XEQ*J))/(1-2*J+(4*J
      1-1)*XEQ-DEQ))+6*(4*J/(2*J*(2*XEQ-1)))
      ETEQ=(ETEQ+ETEQ2)*R*T
      XEQ=XEQ-TEQ/ETEQ
      GOTO 51
50   RETURN
      END
      DOUBLE PRECISION FUNCTION ENERGY(T,T10,T20)
      DOUBLE PRECISION T,T10,T20,F,T7
      T7=T-100*T20
      IF (T7 .LT. 300) GOTO 1
      IF (T7 .LT. 700) GOTO 2
      IF (T7 .LT. 940) GOTO 3
      F=-8.88909+0.26557*(T7-1140)-1.04923D-3*((T7-1140)**2)
      F=F+2.70013D-6*((T7-1140)**3)-3.58434D-9*((T7-1140)**4)
      GOTO 4
1    F=1.38*T7-1499
      GOTO 4
2    F=1.65786*T7-1581
      GOTO 4
3    F=1.30089*T7-1331
4    ENERGY=(141*T10 + F)*4.187
      RETURN
      END

      DOUBLE PRECISION FUNCTION XALPH(T)
      DOUBLE PRECISION T,CTEMP
      CTEMP=(T-273.0D+00)/900.0D+00
      XALPH=0.1528D-02-0.8816D-02*CTEMP+0.2450D-01*CTEMP*CTEMP
      &-0.2417D-01*CTEMP*CTEMP*CTEMP+
      &0.6966D-02*CTEMP*CTEMP*CTEMP*CTEMP
      RETURN
      END

```

```

C Copyright S. A. Khan, H. K. D. H. Bhadeshia.
C
C Program calculates volume fraction of martensite from dilatometric data.
C Typical dataset follows
C VBAIN-wt% C in residual aust-Ms
C 0.142 0.508 262.0
C relative length change-respective temp
C 0.0057 100.00
C 0.0053 120.00
C VBAIN calculated from dilatometry using prog length
C wt% C in residual aust.from dilatometry using prog .length
C Ms from cooling curve from dilatometry
C Relative length change-&-respective temp obtained from cooling curve
C A1, C1, G1 are the martensite a, martensite c and austenite lattice parameters
C See Andrews and Speich for details of parameters as a function of alloy
C For lattice parameter equations, substitutional alloy content in atomic %
C but carbon in wt%
C VBAIN = bainite volume fraction
C MS = martensite start temperature XWT = carbon content of residual austenite
C T = Centigrade (all temps in these units) L = relative length change
IMPLICIT REAL*8 (A-H,L-Z), INTEGER (I-K)
DOUBLE PRECISION X(500),Y(500),RESULT(200)
READ(5,*)
VBAIN,XWT,MS
VG=1.0D+00-VBAIN
WRITE(6,9)VG
9 FORMAT('VOLUME FRACTION OF AUSTENITE=',F8.4)
EXA=1.1103E-05
EXY=.7951E-05
WRITE(6,4)VBAIN,XWT,MS
WRITE(6,6)EXA,EXY
MN=0.66
SI=3.35
VAN=0.1
CR=0.86
NI=1.70
MO=0.22
WRITE(6,7)XWT,SI,MN,NI,MO,CR,VAN
ALLOY1=0.0010*MN-0.0002*Ni+0.0006*CR+0.0053*MO+0.0017*VAN
ALLOY2=0.0006*MN+0.0007*Ni+0.0005*CR-0.0003*SI
G1=3.573+ALLOY1+0.033*XWT
A1=2.8661+ALLOY2- 0.013*XWT
C1=2.8661+ALLOY2+0.116*XWT
WRITE(6,5)
DO 1 K=1,500
READ(5,*)
L,T
C Calculation of lattice parameters at temperature T
G2=G1*(1.0D+00+(T-20)*EXY)
A2=A1*(1.0D+00+(T-20)*EXA)
C2=C1*(1.0D+00+(T-20)*EXA)
C Calculation of the volume fraction of martensite
V2=(3*L*G2**3)/(VG*(2*A2*A2*C2-G2**3))
C V2 is the fraction of residual austenite that transforms into martensite
C V2 = f = VM/Vg
C Calculation of ln(1-f)
IF (V2 .GT. 1) GOTO 22
GOTO 23
22 V2=0.999
23 Y(K)=DLOG(1.0D+00-(V2))
X(K)=MS-T
VGR=VG-(V2*VG)
C TO read every 3rd data from the computed (dilatometric) length change data.
NO=NO+1
IF (NO .EQ. 3) GOTO 67
GOTO 68
C Not to consider data below 15.0 degree centigrade.
67 IF (T .LT. 15.0) GOTO 68
GOTO 71

```

```

71  WRITE(6,3) L,T,V2,G2,A2,C2,X(K),Y(K),VGR
C Calculation of the absolute volume fraction
  IF (T .LE. 20.0) GOTO 123
  GOTO 321
123  VAB=V2*VG
  WRITE(6,66)T,VAB
66  FORMAT(' ABSOLUTE VALUE OF MARTENSITE AT',F4.0,' IS= ',F8.3)
321  NO=0
68  III=III+1
3  FORMAT(F8.5,F5.0,F7.3,F10.5,F10.5,F7.0,F10.3,F10.4)
1  CONTINUE
2  III=K-1
STOP
4  FORMAT(' Volume Fraction of Bainite = ',F8.4/
  & ' C in residual austenite, at ',
  & ' termination of bainite reaction, wt.%, =',F8.3/
  & ' Martensite start temperature, centigrade, = ',F8.2)
7  FORMAT(' C, wt.% =',F8.3,2X,'Si, At.% =',
  & F8.2,2X,'Mn, At.% =',F8.2,
  & 2X,'Ni, At.% =',F10.4,'Mo, At.% =',F10.4,2X,
  & ' Cr, At.% =',F8.2,2X,'V, At.% =',F10.4//)
6  FORMAT(' Linear Expansivity, alpha = ',D12.4/
  & ' Linear Expansivity, gamma = ',D12.4)
5  FORMAT(' Length Ctemp Vmart   G2    A2    C2 ',
  & ' Ms-Tq   LN(1-F)   VGR')
END

```

APPENDIX-6

```

C Copyright S. A. Khan and H. K. D. H. Bhadeshia
C University of Cambridge, Department of Materials Science and Metallurgy,
C Pembroke Street, Cambridge CB2 3QZ, U. K.
C
C PROG. FOR THE ANALYSIS OF ALLOTRIMORPHIC FERRITE TRANSFORMATION IN
C HETEROGENEOUS ALLOY, AS INTERFACE MOTION IS NORMAL TO THE ISOCONCENTRATION
C PLANES.
C
C The steel is divided into slices of different compositions,
C Ae3 temperature and XEQ of the first slice (solute depleted) is calculated.
C Transformation is allowed to go to 100% in slice J=1 if its Ae3 temperature
C is higher than the isothermal temperature, the carbon thus
C rejected is allowed to homogenise in the residual austenite.
C Transformation now shifts to slice J=2 if its Ae3 temperature, calculated
C from the its new composition (i.e., due to increase in carbon content), is
C higher than the concerned transformation temprature. The extent of
C transformation is limited by paraequilibrium mechanism.
C The results averaged and compared with a steel of the corresponding average
C composition.
C Typical data set follows:
C 673 (temperature in Kelvin)
C 0.43 0.50 0.60 0.70 0.80 0.90 1.00 (Composition of slice 1 in wt.%)
C 0.43 0.60 0.60 0.70 0.80 0.90 1.90 (Composition of slice 2 in wt.%)
C C Si Mn Ni Mo Cr V
C
IMPLICIT REAL*8(A-H,K-Z), INTEGER(I,J)
DOUBLE PRECISION C(8),D(8),XEQ(200)
&,E(8),F(8),MS(100),IA(100),XGAMMA(200),VOLF(200)
&,CN(200),SI(200),MN(200),NI(200),MO(200),V(200),FE(200)
&,CR(200),WD(8),VG(200),CD(8),XG(200),TAE3(200)
&,TAE3H,XEQH,TOLF,AVEVOL,MOMENT,TISO,CE(8),SLICEN,TSlice
DIMENSION VOLFD(200)
VINCR=0.00005D+00
ISTOP=0
AVEVOL=0.0D+0
TVOLF=0.0D+0
C1=0.0
C2=0.0
C3=0.0
C4=0.0
C5=0.0
C6=0.0
C7=0.0
READ(5,*),KELVIN
TISO=KELVIN-273.0D+0
XALPHA=XALPH(KELVIN)
WRITE(6,4444)
4444 FORMAT(' *****CARBON IS ALLOWED TO DIFFUSE!!!!*****')
WRITE(6,9)KELVIN,XALPHA,VINCR
WRITE(6,9090)
9090 FORMAT('
&-----')
DO 1 I=1,200
READ(5,*),END=2,C(1),C(2),C(3),C(4),C(5),C(6),C(7)
CN(I)=C(1)
SI(I)=C(2)
MN(I)=C(3)
NI(I)=C(4)
MO(I)=C(5)
CR(I)=C(6)
V(I)=C(7)
FE(I)=100.0D+0-(C(1)+C(2)+C(3)+C(4)+C(5)+C(6)+C(7))
C1=C1+C(1)
C2=C2+C(2)
C3=C3+C(3)
C4=C4+C(4)
C5=C5+C(5)

```

```

C6=C6+C(6)
C7=C7+C(7)
DO 43 JI=1,7
E(JI)=C(JI)
43  CONTINUE
CALL XEQ3(KELVIN,C,XEQ(I))
CALL TEMP3(E,TAE3(I))
XBAR=C(1)
WRITE(6,10)I,XEQ(I),TAE3(I)
WRITE(6,6161)

6161 FORMAT('*****')
&*****
1  CONTINUE
2  ISLICE=I-1
WRITE(*,*) ISLICE
D(1)=C1/ISLICE
D(2)=C2/ISLICE
D(3)=C3/ISLICE
D(4)=C4/ISLICE
D(5)=C5/ISLICE
D(6)=C6/ISLICE
D(7)=C7/ISLICE
DO 70 JII=1,7
WD(JII)=D(JII)
70  CONTINUE
DO 56 JIJ=1,7
F(JIJ)=D(JIJ)
56  CONTINUE
CALL XEQ3(KELVIN,D,XEQH)
CALL TEMP3(F,TAE3H)
WRITE(6,75)TAE3H
75  FORMAT(' A3H= ',D10.4)
C   IF (TAE3H .LT. TISO) GOTO 789
C   GOTO 85
IF (XEQH .LE. D(1)) GOTO 789
GOTO 79
79  IF (XEQH .GT. XALPHA) GOTO 987
GOTO 789
789  VOLH=0.00
GOTO 678
987  VOLH=(XEQH-D(1))/(XEQH-XALPHA)
678  VGH=1.0D+0-VOLH
WRITE(6,15)VOLH
AVEX=D(1)
DO 4 J=1,ISLICE
SLICEN=J
TSLICE=ISLICE
IF (XEQ(J) .LE. AVEX) GOTO 5
GOTO 7007
7007  IF (TAE3(J) .LT. TISO) GOTO 5
GOTO 9352
9352  AVEVOL=SLICEN/TSLICE
VOLF(J)=AVEVOL
AVEX=D(1)+(AVEVOL*(D(1)-XALPHA))/(1.0D+0-AVEVOL)
WRITE(6,886)J,XEQ(J),TAE3(J),D(1),AVEVOL,AVEX,VOLF(J)
886  FORMAT(' SLICE=',I3,' XEQ=',
&D10.3,' TAE3=',D10.3,' D(1)=',D10.3,' AVEVOL=',D10.3,' AVEX=',
&D10.3,' VOLF(J)=',D10.3)
C Recalling the original composition(wt%) for each slice.....
CD(1)=CN(J+1)
CD(2)=SI(J+1)
CD(3)=MN(J+1)
CD(4)=NI(J+1)
CD(5)=MO(J+1)
CD(6)=CR(J+1)
CD(7)=V(J+1)
XG(J+1)=CD(1)+((VOLF(J)*CD(1))/(1.0D+00-VOLP(J)))
C Getting new composition (wt%) of residual austenite in each slice
RT=(100.0D+00-XG(J+1))/(100.0D+00-CD(1))

```

```

CD(1)=XG(J+1)
DO 262 NIN=2,7
CD(NIN)=CD(NIN)*RT
262 CONTINUE
DO 161 NO=1,7
CE(NO)=CD(NO)
161 CONTINUE
CALL XEQ3(KELVIN,CD,XEQ(J+1))
CALL TEMP3(CE,TAE3(J+1))
GOTO 4
5 GOTO 786
4 CONTINUE
786 WRITE(6,13)AVEVOL
13 FORMAT(' Average volume fraction of transformation',
&' in heterogeneous alloy =',D8.3)
9 FORMAT(' KELVIN = ',F7.0,' XALPHA, mol. fraction =',D12.4
&,' VOL INCREMENT=',D12.4)
10 FORMAT(' Slice Number= ',I3,'      XEQ = ',D10.4,
&          AE3-T= ',D10.4/)
15 FORMAT(' Maximum volume fraction of bainitic ferrite in ',
&' an alloy of average composition = ',D8.3)
STOP
END

C*****
SUBROUTINE TEMP3(C,AE3T)
DOUBLE PRECISION X,X1,R,A,A1,AFE,A1FE,DA1,DA2,DA1FE,H,H1,S,S1
INTEGER T1,I,NO,U,B4,J99,C99,C98,C97
DOUBLE PRECISION D11,DTQ(40),DXEQ(40),
1INCEPT,SLOPE,CORR,
1DEQ,ETEQ,T10,T20,XA,AFEQ,AEQ,ETEQ2,TEQ,
1JJ1,D,D1,W,W1,F,TEST,ERROR,T4,XEQ,FPRO
1,C(8),B1,B2,P(7),Y(7),B3,AE3T,EE(8)
WRITE(6,1100)C(1),C(2),C(3),C(4),C(5),C(6),C(7)
1100 FORMAT(7D11.3)
B3=0
C(8)=(100.0-C(1)-C(2)-C(3)-C(4)-C(5)-C(6)-(C7))/55.84
C(1)=C(1)/12.0115
C(2)=C(2)/28.09
C(3)=C(3)/54.94
C(4)=C(4)/58.71
C(5)=C(5)/95.94
C(6)=C(6)/52.0
C(7)=C(7)/50.94
B1=C(1)+C(2)+C(3)+C(4)+C(5)+C(6)+C(7)+C(8)
DO 107 U=2,7
Y(U)=C(U)/C(8)
107 CONTINUE
DO 106 U=1,7
C(U)=C(U)/B1
106 CONTINUE
B2=0.0
T10=Y(2)*(-3)+Y(3)*2+Y(4)*12+Y(5)*(-9)+Y(6)*(-1)+Y(7)*(-12)
T20=-3*Y(2)-37.5*Y(3)-6*Y(4)-26*Y(5)-19*Y(6)-44*Y(7)
P(2)=2013.0341+763.8167*C(2)+45802.87*C(2)**2-280061.63*C(2)**3
1+3.864D+06*C(2)**4-2.4233D+07*C(2)**5+6.9547D+07*C(2)**6
P(3)=2012.067-1764.095*C(3)+6287.52*C(3)**2-21647.96*C(3)**3-
12.0119D+06*C(3)**4+3.1716D+07*C(3)**5-1.3885D+08*C(3)**6
P(4)=2006.8017+2330.2424*C(4)-54915.32*C(4)**2+1.6216D+06*C(4)**3
1-2.4968D+07*C(4)**4+1.8838D+08*C(4)**5-5.5531D+08*(C(4)**6
P(5)=2006.834-2997.314*C(5)-37906.61*C(5)**2+1.0328D+06*C(5)**3
1-1.3306D+07*C(5)**4+8.411D+07*C(5)**5-2.0826D+08*C(5)**6
P(6)=2012.367-9224.2655*C(6)+33657.8*C(6)**2-566827.83*C(6)**3
1+8.5676D+06*C(6)**4-6.7482D+07*C(6)**5 +2.0837D+08*C(6)**6
P(7)=2011.9996-6247.9118*C(7)+5411.7566*C(7)**2
1+250118.1085*C(7)**3-4.1676D+06*C(7)**4
DO 108 U=2,7
B3=B3+P(U)*Y(U)
B2=B2+Y(U)

```

```

108  CONTINUE
    IF(B2 .EQ. 0.0) GOTO 455
    W=(B3/B2)*4.187
    GOTO 456
455  W=8054.0
456  CONTINUE
    X1=C(1)
    R=8.31432
    W1=48570.0
    H=38575.0
    S=13.48
    II1=873
    II2=1173
    II3=15
    II=0
201  XEQ=0.1
    INCEPT=1.0D+00
    CORR=1.0D+00
    SLOPE=1.0D+00
    C98=0
    C97=0
    DO 9 T1=II1,II2,II3
    C98=C98+1
    T=T1
    IF (T .LE. 1000) GOTO 20
    H1=105525
    S1=45.34521
    GOTO 19
20   H1=111918
    S1=51.44
19   F=ENERGY(T,T10,T20)
    J=1-DEXP(-W/(R*T))
51   DEQ=DSQRT(1-2*(1+2*J)*XEQ+(1+8*J)*XEQ*XEQ)
    TEQ=5*DLOG((1-XEQ)/(1-2*XEQ))
    TEQ=TEQ+DLOG(((1-2*J+(4*J-1)*XEQ-DEQ)/(2*J*(2*XEQ-1)))**6)
    TEQ=TEQ*R*T-F
    IF (DABS(TEQ) .LT. 1.0) GOTO 50
    ETEQ=5*((1/(XEQ-1))+2/(1-2*XEQ))
    ETEQ2=6*((4*J-1-(0.5/DEQ)*(-2-4*J+2*XEQ+16*XEQ*J))/(1-2*J+(4*J
    1-1)*XEQ-DEQ))+6*(4*J/(2*J*(2*XEQ-1)))
    ETEQ=(ETEQ+ETEQ2)*R*T
    XEQ=XEQ-TEQ/ETEQ
    GOTO 51
50   IF (XEQ .LT. 0.001) GOTO 2444
    T4=T1-273.0
    DTQ(C98)=T4
    DXEQ(C98)=XEQ
9    CONTINUE
2444 C98=C98-1
    CALL ANAL(C98,INCEPT,SLOPE,CORR,DTQ,DXEQ)
    AE3T=(X1-INCEPT)/SLOPE
    IF(II .GT. 0) GOTO 802
    II=AE3T
    II1=II-9+273
    II2=II+9+273
    II3=1
    GOTO 201
802  RETURN
END
SUBROUTINE ANAL(C98,INCEPT,SLOPE,CORR,X,Y)
DOUBLE PRECISION AX,AX2,AY,AY2,AXY,INCEPT,CORR,SLOPE,
&X(40),Y(40)
INTEGER I,C98,II
II=C98
C98=C98-10
AX=0.0D+00
AY=0.0D+00
AX2=0.0D+00
AY2=0.0D+00

```

```

AXY=0.0D+00
DO 1 I=1,C98
AX=AX+X(I)
AY=AY+Y(I)
AXY=AXY+X(I)*Y(I)
AX2=AX2+X(I)*X(I)
AY2=AY2+Y(I)*Y(I)
1 CONTINUE
INCEPT=(AY*AX2-AX*AXY)/(C98*AX2-AX*AX)
SLOPE=((C98*AXY-AX*AY)/(C98*AX2-AX*AX))
CORR=(C98*AXY-AX*AY)/(DSQRT((C98*AX2-AX*AX)*
&(C98*AY2-AY*AY)))
C98=11
RETURN
END
DOUBLE PRECISION FUNCTION ENERGY(T,T10,T20)
DOUBLE PRECISION T,T10,T20,F,T7
T7=T-100*T20
IF (T7 .LT. 300) GOTO 1
IF (T7 .LT. 700) GOTO 2
IF (T7 .LT. 940) GOTO 3
F=-8.88909+0.26557*(T7-1140)-1.04923D-3*((T7-1140)**2)
F=F+2.70013D-6*((T7-1140)**3)-3.58434D-9*((T7-1140)**4)
GOTO 4
1 F=1.38*T7-1499
GOTO 4
2 F=1.65786*T7-1581
GOTO 4
3 F=1.30089*T7-1331
4 ENERGY=(141*T10 + F)*4.187
RETURN
END

C*****
SUBROUTINE XEQ3(TT,C,XEQ)
DOUBLE PRECISION X,X1,T,R,A,A1,AFE,A1FE,DA1,DA2,DA1FE,H,H1,S,S1
&TT
INTEGER I,NO,U,B4,J99,C99,C98,C97
DOUBLE PRECISION D11,
1DEQ,ETEQ,T10,T20,XA,AFEQ,AEQ,ETEQ2,TEQ,
1JJ1,D,D1,W,W1,F,TEST,ERROR,T4,XEQ,FPRO
1,C(8),B1,B2,P(7),Y(7),B3,AE3T,CC(8)

B3=0
C(8)=(100.0-C(1)-C(2)-C(3)-C(4)-C(5)-C(6)-(C7))/55.84
C(1)=C(1)/12.0115
C(2)=C(2)/28.09
C(3)=C(3)/54.94
C(4)=C(4)/58.71
C(5)=C(5)/95.94
C(6)=C(6)/52.0
C(7)=C(7)/50.94
B1=C(1)+C(2)+C(3)+C(4)+C(5)+C(6)+C(7)+C(8)
DO 107 U=2,7
Y(U)=C(U)/C(8)
107 CONTINUE
DO 106 U=1,7
C(U)=C(U)/B1
106 CONTINUE
B2=0.0
T10=Y(2)*(-3)+Y(3)*2+Y(4)*12+Y(5)*(-9)+Y(6)*(-1)+Y(7)*(-12)
T20=-3*Y(2)-37.5*Y(3)-6*Y(4)-26*Y(5)-19*Y(6)-44*Y(7)
P(2)=2013.0341+763.8167*C(2)+45802.87*C(2)**2-280061.63*C(2)**3
1+3.864D+06*C(2)**4-2.4233D+07*C(2)**5+6.9547D+07*C(2)**6
P(3)=2012.067-1764.095*C(3)+6287.52*C(3)**2-21647.96*C(3)**3
12.0119D+06*C(3)**4+3.1716D+07*C(3)**5-1.3885D+08*C(3)**6
P(4)=2006.8017+2330.2424*C(4)-54915.32*C(4)**2+1.6216D+06*C(4)**3
1-2.4968D+07*C(4)**4+1.8838D+08*C(4)**5-5.5531D+08*C(4)**6
P(5)=2006.834-2997.314*C(5)-37906.61*C(5)**2+1.0328D+06*C(5)**3

```

```

1-1.3306D+07*C(5)**4+8.411D+07*C(5)**5-2.0826D+08*C(5)**6
P(6)=2012.367-9224.2655*C(6)+33657.8*C(6)**2-566827.83*C(6)**3
1+8.5676D+06*C(6)**4-6.7482D+07*C(6)**5 +2.0837D+08*C(6)**6
P(7)=2011.9996-6247.9118*C(7)+5411.7566*C(7)**2
1+250118.1085*C(7)**3-4.1676D+06*C(7)**4
DO 108 U=2,7
B3=B3+P(U)*Y(U)
B2=B2+Y(U)
108 CONTINUE
IF(B2 .EQ. 0.0) GOTO 455
W=(B3/B2)*4.187
GOTO 456
455 W=8054.0
456 CONTINUE
X1=C(1)
R=8.31432
W1=48570.0
H=38575.0
S=13.48
201 XEQ=0.1
T=TT
IF (T .LE. 1000) GOTO 20
H1=105525
S1=45.34521
GOTO 19
20 H1=111918
S1=51.44
19 F=ENERGY(T,T10,T20)
J=1-DEXPC(-W/(R*T))
51 DEQ=DSQRT(1-2*(1+2*J)*XEQ+(1+8*J)*XEQ*XEQ)
TEQ=5*DLOG((1-XEQ)/(1-2*XEQ))
TEQ=TEQ+DLOG(((1-2*J+(4*J-1)*XEQ-DEQ)/(2*J*(2*XEQ-1)))**6)
TEQ=TEQ*R*T-F
IF (DABS(TEQ) .LT. 1.0) GOTO 50
ETEQ=5*((1/(XEQ-1))+2/(1-2*XEQ))
ETEQ2=6*((4*J-1-(0.5/DEQ)*(-2-4*J+2*XEQ+16*XEQ*XEQ))/(1-2*J+(4*J
-1)*XEQ-DEQ))+6*(4*J/(2*J*(2*XEQ-1)))
ETEQ=(ETEQ+ETEQ2)*R*T
XEQ=XEQ-TEQ/ETEQ
GOTO 51
50 RETURN
END
DOUBLE PRECISION FUNCTION ENERGY(T,T10,T20)
DOUBLE PRECISION T,T10,T20,F,T7
T7=T-100*T20
IF (T7 .LT. 300) GOTO 1
IF (T7 .LT. 700) GOTO 2
IF (T7 .LT. 940) GOTO 3
F=-8.88909+0.26557*(T7-1140)-1.04923D-3*((T7-1140)**2)
F=F+2.70013D-6*((T7-1140)**3)-3.58434D-9*((T7-1140)**4)
GOTO 4
1 F=1.38*T7-1499
GOTO 4
2 F=1.65786*T7-1581
GOTO 4
3 F=1.30089*T7-1331
4 ENERGY=(141*T10 + F)*4.187
RETURN
END

DOUBLE PRECISION FUNCTION XALPH(T)
DOUBLE PRECISION T,CTEMP
CTEMP=(T-273.0D+00)/900.0D+00
XALPH=0.1528D-02-0.8816D-02*CTEMP+0.2450D-01*CTEMP*CTEMP
&-0.2417D-01*CTEMP*CTEMP*CTEMP+
&0.6966D-02*CTEMP*CTEMP*CTEMP*CTEMP
RETURN
END

```